The Provenance and Ages of Glacial Sediments from Long Island, NY

Davies, R. M.[1,2], Jaret, S.[2,3], Nicolas, J. [1], Crowley, J.[4], Kinney, S.[5]

1. Department of Biological Sciences and Geology, Queensborough Community College of the City University of New York, Bayside, NY 11364

2. Department of Earth and Planetary Sciences, American Museum of Natural History, New York, NY 10024

3. Department of Physical Sciences, Kingsborough Community College of the City University of New York, Brooklyn, NY 11235

4. Department of Geoscience, Boise State University, Boise, ID 83725

5. Department of Earth and Planetary Sciences, Rutgers University, New Brunswick, NJ 07102

rdavies@qcc.cuny.edu

During the last glacial maximum, about 24,000-21,000 years before present, the Laurentide ice sheet advanced southward across New York State and terminated where Long Island is today. The glacier left behind ridges of elevated topography trending in an east to west direction across the length of the island and known as the Harbor Hill and Ronkonkoma glacial moraines (Bennington, 2016; Balco and Shaefer, 2006; Balco et al., 2009).

There is debate about the direction the glaciers moved and the provenance of the glacial deposits that make up the Long Island dating back to Fuller (1914). Most workers suggest both the Ronkonkoma and Harbor Hill moraines formed during the last glacial maximum from glaciers moving from a NW-SE to a N-S direction (Sanders & Merguerian, 1994; 1998; Sirkin, 1996; Pacholik and Hansen, 2001; Bennington and Young, 2005; Kundic et al. 2007). In eastern Long Island, evidence of a NE-SW direction for glacier motion also exists (Pachilok, 2014; 2018; Sirkin and Mills, 1975; Kundic et al., 2007; 2012).

Considering the basement rocks of New York and New England are well mapped and age dated, showing a general younging from west to east across Laurentia and Gondwana derived terranes, it should be possible to identify the dominant source of the rocks that make up the moraines of Long Island and to better constrain the direction glaciers moved. The goal of this work is to determine the provenance of the rocks that make up the moraines of Long Island to provide insights into the pathway and travel history of the Laurentide ice sheet.

We measured sand-sized grains from three glacial deposits and one sedimentary unit along an 80-mile west to east transect for (1) ages from U-Pb dating of detrital zircons and (2) provenance using heavy mineral concentrates. 939 detrital zircons from four localities were age dated with LA ICPMS. Overall and for each location age dates have a large range (183 to 2699 Ma) which is to be expected considering the zircons are detrital and represent many populations of source rocks. However, dominant age peaks at each location inform us of the most representative populations.

From western Long Island, glacial sediments at Huntington and Cretaceous sediments from Caumsett State Park have dominant Mesoproterozoic age peaks at 1017 and 1043 Ma respectively. These ages correspond to the Grenville orogenies and likely represent recycled zircons in Laurentian margin metasedimentary rocks from the Manhattan prong (Jaret et al., 2023). Huntington and Caumsett also have a small peak at ~440 Ma, consistent with peak metamorphism during the Taconic orogeny.

The Caumsett Cretaceous sediments also show peaks at 183 and 363 Ma. These ages are discussed below.

Eastern locations at Greenport, on the North Fork, and Hither Hills near Montauk have peaks at ~275, which may correspond to plutonism and pegmatite emplacement throughout New England. Glacial sands from Hither Hills also contain a large peak between 365 and 409, similar to that at Caumsett, which likely represents igneous and metamorphic events related to the Acadian and Neoacadian orogenies. The paucity of Alleghanian age zircons is surprising considering these rocks are well represented in southern New England.

Jurassic ages (~190 Ma) for zircons from Caumsett State Park, Greenport, and Hither Hills are puzzling considering they do not correspond to the ages of igneous or metamorphic events of nearby terranes. We suggest they are derived from igneous rocks of the White Mountain batholith in northern New Hampshire (Kinney et al., 2022) which is north-northeast of Long Island.

Heavy minerals at Huntington are dominated by kyanite, magnetite, tourmaline, rutile, garnet pyroxene, and amphibole with minor staurolite to suggest the sediments are largely derived from metamorphic rocks. At Caumsett State Park heavy minerals are dominated by kyanite with minor sulfides, rutile, and staurolite. At Greenport, heavy minerals mostly contain magnetite, tourmaline, and garnet with minor kyanite, staurolite, rutile, pyroxene, and epidote. Hither Hills contains a wide range on heavy minerals with a dominance of kyanite followed by amphibole, pyroxene, magnetite, tourmaline and small amounts of rutile, garnet, staurolite, and epidote. Staurolite is not common in metamorphic rocks of the Manhattan prong to the northwest (Jaret pers. comm.).

Our data rules out glacial motion from was from a northwest direction and indicates it was from the north to northeast.

References

Balco, G. and Schaefer, J.M., 2006. Cosmogenic-nuclide and varve chronologies for the deglaciation of southern New England.Quaternary Geochronology, 1, pp.15-28. https://doi.org/10.1016/j.quageo.2006.06.014

Balco, G., Briner, J., Finkel, R.C., Rayburn, J.A., Ridge, J.C. and Schaefer, J.M. 2009. Regional beryllium-10 production rate calibration for late-glacial northeastern North America. Quaternary Geochronology. 4, pp. 93–107. https://doi.org/10.1016/j.quageo.2008.09.001

Bennington, B.J., 2016. New observations on the glacial geomorphology of Long Island from a digital elevation model (DEM). https://www.geo.sunysb.edu/lig/Conferences/abstracts-03/bennington/index.pdf

Bennington, B.J. & Young, T., 2005. Determining the Direction of Ice Advance Forming the Roanoke Point Moraine From a Survey of Hartford Basin Erratics. 12th Long Island Geologists Conference on the Geology of Long Island and Metropolitan New York, SUNY Stony Brook.

Fuller, M. L., 1914, The geology of Long Island, New York: U. S. Geological Survey Professional Paper 82, 223 p.

Jaret, S.J., Tailby, N.D., Hammond, K.G., Rasbury, E.T., Wooton, K., Ebel, D.S., Plank, T., DiPadova, E., Yuan, V., Smith, R. and Jaffe, N., 2023. The Manhattan project: Isotope geochemistry and detrital zircon geochronology of schists in New York City, USA. Geological Society of America Bulletin. https://doi.org/10.1130/B37024.1

Kinney, S.T., MacLennan, S.A., Szymanowski, D., Keller, C.B., VanTongeren, J.A., Setera, J.B., Jaret, S.J., Town, C.F., Strauss, J.V., Bradley, D.C. and Olsen, P.E., 2022. Onset of long-lived silicic and alkaline magmatism in eastern North America preceded Central Atlantic Magmatic Province emplacement. Geology, 50, pp.1301-1305.

Kundic, V., Hemming, S. and Hanson, G.N., 2012. Single-grain 40Ar/39Ar ages of detrital muscovite from loess on Long Island, New York. *Geological Society of America Special Paper*, *487*, pp.105-111.

Kundic, V., Zhong, J., Hemming, S., & Hanson, G.N., 2007. Provenance of loess on Long Island using single grain 40Ar/39Ar ages of muscovite: Proceedings of the Conference on the Geology of Long Island and Metropolitan New York, 14th: https://dspace.sunyconnect.suny.edu/bitstream/handle/1951/47833/Kundic-07.pdf?sequence=1.

Pachilok, W., 2018 Long Island Subglacial Drainage Patterns Reveal the Direction of Glacial Flow, Proceedings of the 25th Conference on the Geology of Long Island and Metropolitan New York https://www.stonybrook.edu/commcms/geosciences/about/_LIG-Past-Conference-abstract-pdfs/2015-Abstracts/pacholik.pdf

Pacholik W., 2014. Direction of the ice flow through Long Island during maximum extension of Laurentide Ice Sheet, Proceedings of the 21st Conference on the Geology of Long Island and Metropolitan New York http://www.geo.sunysb.edu/lig/Conferences/abstracts14/Pacholik-edited.pdf

Pacholik, W. Gilbert N. Hanson, G.N. & Hemming, S., 2001. Using erratic boulders to map the basement in Long Island Sound. https://www.geo.sunysb.edu/lig/Conferences/abstracts_02/pacholik/pacholik-abs.pdf

Exploring Climate Change Effects on Sinkhole Formation:
Long-Term Temperature Analysis in Long Island, NY (1948-2024)

Gonzalez, X.[1], Hubbs, D.[1], Dailey, S.[1], Marsellos, A.E.[1], Tsakiri, K.G.[2]

[1]*Department of Geology, Environment and Sustainability, Hofstra University, Hempstead, NY 11549*
[2]*Dept. Information Systems, Analytics, and Supply Chain Management, Rider University, Lawrenceville, NJ 08648*

Abstract

In recent years, there has been an overall increase in sinkhole occurrences in Long Island, NY. Sinkholes typically form when water erodes detrital or evaporite rock beneath the Earth's surface, creating a cavity that eventually collapses. Increased underground water mobility may lead to accelerated sinkhole development, especially upon more frequent warming temperatures due to climate change. We have analyzed historical atmospheric temperature data in Long Island, NY, spanning 76 years (1948-2024) by applying the Kolmogorov-Zurbenko (KZ) filter to investigate the number of prolonged freezing and thawing events per year. We have utilized R language coding (Rstudio) to account for the number of times that the temperature fluctuated at two specific temperature intervals of freezing (-4 to 1°C) and thawing (4 to 10°C). We have found that the number of prolonged thawing events has increased while the number of freezing times has decreased, leading to an increase in water mobility and, ultimately, the exacerbation of underground erosion. Understanding the relationship between temperature changes and water mobility is crucial for assessing the potential impacts of climate change on sinkhole dynamics and for implementing effective mitigation strategies in vulnerable regions of Long Island.

Introduction

The present study investigates the mechanisms of sinkhole formation in Long Island's unique geological setting, which consists primarily of loosely consolidated glacial till. Many scientists have studied climate change over the past few decades, surveying temperature extremes, weather changes, ice core data, etc. While climate change is supported by the vast majority of the scientific community already, its connection to certain geohazards is not. Some of the most commonly studied correlations to climate change are that of hurricanes, volcanic activity, floods, and heat waves as seen by the map provided by (Extreme weather and climate change. Center for Climate and Energy Solutions, (2024),Earthjustice. (2024) the top four years in terms of extreme weather (Tropical storms, Droughts, Severe Storms, etc.) are 2020-2023 which is indicative of climate change. One specific hazard that is undermined within most online databases when discussing climate change is sinkholes, especially in the Eastern United States, as they occur less frequently than in other parts of the country, thus it is not considered as much.

Long Island's surface is mostly composed of loose glacial sediments like sand, clay, and gravel. This separates it from New York City and other parts of New York (Cohen 2014). Long Island has experienced a slight increase in sinkhole frequency over recent years; there are about nine documented events on the official New York NBC database within the last ten years (2013-2023) (NBCNY 2024). While this number seems low, the frequency of sinkholes before this decade is much less. This is understood due to the lack of reports online about any sinkhole occurrences in the past. Within the last ten years, sinkhole reports have been more frequent, and there is limited research on the correlation between climate change/rising temperatures and water mobility that affects sinkholes. The goal of this study is to support the idea that increased temperature fluctuations due to climate change correspond to water mobility as freeze-thaw melting increases, resulting in more erosion and sinkholes on Long Island.

The prevalence of sinkholes relates to climate change since the decreases in freeze-thaw action correspond to increases in temperature values. The lack of freeze-thaw events bridges the connection between climate change and underground water mobility since it is understood that there is more water flow when there is less ice. Sinkholes are a geohazard caused by unsteady grounds and sediment. If there is more water mobility, there is more erosion, leading to those causes. Other factors that play into this are saline concentrations; if they are high, which they are on Long Island, clay particles become flocculated, making them less steady (Palomino and Santamarina, 2005; Lyu et al., 2020). In addition to salinity, researchers consider thermal conductivity to be a factor in freeze-thaw cycles, since ice melting increases in winters. Thirdly, the apparent thermal conductivity of soils increases with increased concentrations of NaCl in a soil solution (Noborio & McInnes 1993). This fact is relevant because it means thermal conductivity is generally higher when there is more NaCl in soil. Further supporting that Long Island soil gets warm easily. In another study, it was found that "thermal conductivity increases linearly with density [of NaCl] from 0.2 to 1 W/(m*K) for densities from 1.1 to 2.3 g/cm^3" (Stacy et al. 2014). This also suggests that Long Island soil may weaken due to increased temperatures, since increased salinity is directly proportional to increased thermal conductivity. Increased thermal conductivity heightens the impacts that climate change has on freeze-thaw fluctuations and the melting that comes from that (Lyu et. al. 2020). This all supports how global heating is increasing water mobility, thus eroding the depths of Long Island, causing more sinkholes to occur in recent years. This research aims to investigate the number of freeze and thaw times per year over the past 76 years and apply it to our data. This offers a proxy for underground erosion and subsequent sinkhole occurrences, which will be analyzed in our results.

Methodology

We used Rstudio to acquire and clean data using the reproducible R language packages GSODR (Sparks A., Hengl T., Nelson A., 2024), KZA (Close B., Zurbenko I., Sun M., 2020), and rNOAA (Chamberlain S., Hocking D., 2023) packages which gathered data directly from different weather stations throughout Long Island and the Tristate area. We cleaned the data and interpolated wherever there were small gaps utilizing *imputeTS* package (Moritz S,

Bartz-Beielstein T 2017). The relevant data was ultimately derived from two stations, located at John F. Kennedy International Airport. We wrote a script in Rstudio to count the number of times per year the atmospheric temperature entered into two specific intervals. The first, called the freezing, is represented by the interval of -4°C to 1°C, and the thawing interval is represented by 4°C to 10°C. A moving average utilizing the KZ filter with a window of 11 years was applied three times for each temperature interval (Fig. 1) to investigate a possible trend. The KZ filter demonstrates a robust performance in the presence of non-stationary data and outliers; there was no signal loss or tail-clipping like a standard moving average may introduce (Zurbenko, 1986; Tsakiri & Zurbenko, 2011). Its iterative process efficiently addresses the impact of abrupt changes or anomalous data points, ensuring a more stable and reliable output. Consequently, the KZ filter strengthens with few iterations the elimination of short-term noise and avoids over-smoothing potential trends.

Results
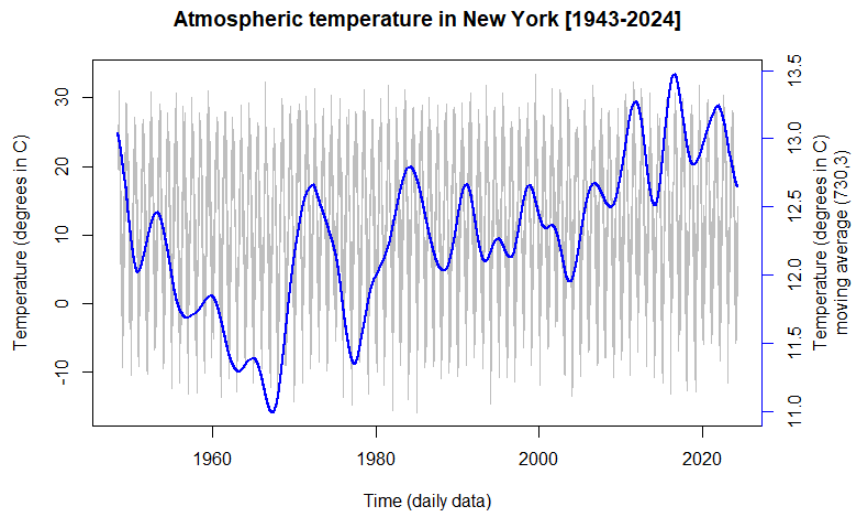
Figure 1: The trend of historical atmospheric temperatures over the past 76 years on Long Island, New York. The graphs portray frequencies of underground temperature values as they occur within the respective temperature ranges (℃). Temperature (℃) averages are represented on the right side axis, aligning with the blue line. The blue line represents the moving average over a window of two years (730 days) applied three times to limit outliers and show more accurate trends.

A negative trend in the total number of times (Figure 1) temperatures crossed the freezing window per year (left) as well as a positive trend in the total number of times temperatures crossed the thawing window per year (right). Figure 2 shows a positive trend in average yearly temperature over the last 74 years.
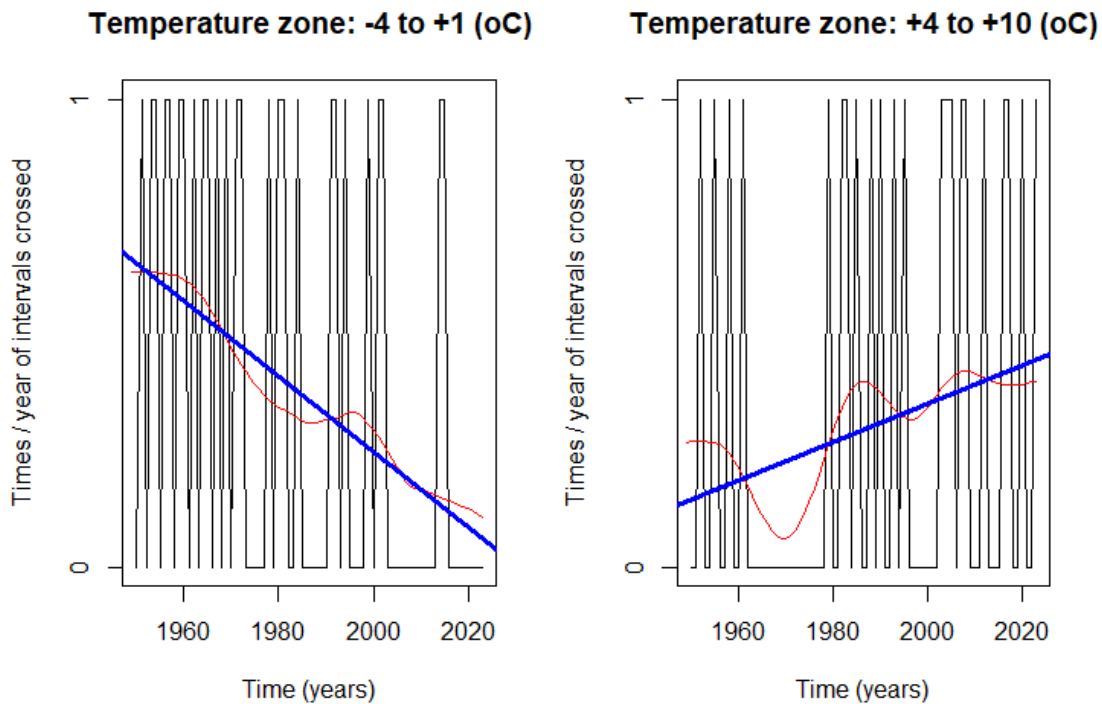
Figure 2: Times per year of intervals crossed at zones of temperature between -4 to +1 ℃ and +4 to 10℃. The blue line follows the trend, analyzing temperature change over that time frame. Red line data excludes the sunspot impact of eleven-year cycle (utilizing a KZ filter with 11 years window applied for an iteration of 3 times), since sunspots are known to affect groundwater temperatures (Tentomas & Marsellos 2022).

Discussion

In conceptualizing this experiment, our aim was to explore a potential correlation between global warming and the occurrence of sinkholes. Specifically, we endeavored to investigate the relationship between the documented increase in global temperature, as elaborated upon in subsequent sections of this paper, and the erosion of glacial sediments precipitated by heightened water mobility and increased rainfall resulting from elevated temperatures. Our data gathering methodology involved using R language (RStudio) to gather historical atmospheric temperature data of daily intervals from selected weather stations operated by NOAA (The National Oceanic and Atmospheric Administration) situated within the immediate tristate area and along Long Island, NY. Subsequently, we compared this data with existing research findings to understand potential correlations between rising global temperatures, amplified water mobility, and the anticipated heightened incidence of sinkholes.

Conclusion

The research we have conducted and the data we have collected both work together to support the concept that increased temperatures due to climate change have a direct impact on sinkhole formations. The way we supported this hypothesis was through research on freeze-thaw, as our data exposed the truth that these freeze-thaw cycles have declined in frequency over time. This suggests that ice is melting and remaining unfrozen underground even in the coldest portion of the year, supporting the development of water mobility within Long Island soil. With the observation of temperatures over the past sixty to eighty years, it is clear that sinkhole formation due to climate change is a recent phenomenon at the northern latitudes that used to experience more prolonged winter times.

Credit Authorship Contribution Statement

Gonzalez,X editing, literature, Rstudio coding, Figure 1, Figure 2, writing- Abstract, Introduction Methodology, Discussion; Hubbs, D: Literature, editing, writing-, Abstract, Introduction Results; Pelletier, A.: references, literature, editing, writing - Introduction, Discussion; Dailey,S.: editing,, writing - introduction, Discussion, Conclusion; Marsellos, A.E.: supervision, Rstudio coding, guidance, editing;

Reference

Chamberlain S, Hocking D (2023). _rnoaa: 'NOAA' Weather Data from R_. R package version 1.4.0, <https://CRAN.R-project.org/package=rnoaa>.

Chao Lyu, & Qiang Sun, & Weiqiang Zhang. (March 2019). Effects of NaCl concentration on thermal conductivity of clay with cooling. Bulletin of Engineering Geology and the Environment (2020) 79:1449–1459. https://link.springer.com/content/pdf/10.1007/s10064-019-01624-w.pdf

Chao Lyu, Qiang Sun, & Weiqiang Zhang. (2020) Effects of NaCl concentration on thermal conductivity of clay with cooling. Bulletin of Engineering Geology and the Environment (2020) 79:1449–1459. https://link.springer.com/content/pdf/10.1007/s10064-019-01624-w.pdf

Close B, Zurbenko I, Sun M (2020). _kza: Kolmogorov-Zurbenko Adaptive Filters_. R package version 4.1.0.1, <https://CRAN.R-project.org/package=kza>.

Cohen, J. (2014). School Climate Policy and Practice Trends: A Paradox. A Commentary. Teachers College Record, Date Published: February 21, 2014 http://www.tcrecord.org

Extreme weather and climate change. Center for Climate and Energy Solutions. (2024, January 29). https://www.c2es.org/content/extreme-weather-and-climate-change/

Georgia Tentomas & Antonios E. Marsellos . (2022). SUNSPOT NUMBER EFFECTS ON EARTH'S CLIMATE CHANGE AND WATER SUSTAINABILITY FOR LONG ISLAND, NY. https://www.stonybrook.edu/commcms/geosciences/about/_LIG-Past-Conference-abstract-pdfs/2022-Abstracts/Tentomas.pdf

How climate change is fueling extreme weather. Earthjustice. (2024, February 28). https://earthjustice.org/feature/how-climate-change-is-fueling-extreme-weather

Moritz S, Bartz-Beielstein T (2017). "imputeTS: Time Series Missing Value Imputation in R." _The R Journal_, *9*(1), 207-218. doi:10.32614/RJ-2017-009 <https://doi.org/10.32614/RJ-2017-009>.

Noborio, K. & McInne, K. J. (1993). Thermal Conductivity of Salt-Affected Soils. Soil Science Society of America Journal. https://acsess.onlinelibrary.wiley.com/doi/abs/10.2136/sssaj1993.03615995005700020007x

Palomino &Santamarina. (2005). Fabric map for kaolinite: effects of pH and ionic concentration on behavior. Clay Miner., 53 (3) (2005), pp. 211-223. https://www.sciencedirect.com/science/article/pii/S1674775522000178?

Sanders, J. E., & Merguerian, C., 1994. The glacial geology of New York City and vicinity, p. 93-200 in A. I. Benimoff, ed., The Geology of Staten Island, New York, Field guide and proceedings, The Geological Association of New Jersey, XI Annual Meeting, 296 p.

Sanders, J. E., and Merguerian, C., 1998. Classification of Pleistocene deposits, New York City and vicinity – Fuller (1914) revived and revised: p. 130-143 in Hanson, G. N., chm., Geology of Long Island and metropolitan New York, 18 April 1998, State University of New York at Stony Brook, NY, Long Island Geologists Program with Abstracts, 161 p.

Sirkin, L. A., & Mills, H. C., 1975. Wisconsinan glacial stratigraphy and structure of northwestern Long Island, Trip B5, p. 299-327 in Wolff, M. P., ed., Guidebook to Field Excursions: New York State Geological Association, Annual Meeting, 47th, Hofstra University, Hempstead, New York: Hempstead, N.Y., Hofstra University, Department of Geology, 327 p.

Sirkin, L., 1996, Western Long Island Geology, history, process, and field trips. The Book and Tackle Shop, p. 179.

Comparing the Effects of Coastal Erosion on Unprotected vs. Protected Shorelines Using GIS and 2011/2014 LiDAR Data

Appel, C., Rahman, M. M., Boddu, D., Marsellos, A.E.
Department of Geology, Environment and Sustainability, Hofstra University, Hempstead, NY 11549 U.S.A

Abstract

Long Beach is a barrier island and one of the many protective barrier islands found in the southern area of Long Island, NY. Barrier islands are crucial to the safety of areas on the mainland as it serves as a shield against erosion for coastlines on multiple cities of Long Island such as Oceanside. Oceanside's shorelines are protected by Long Beach; for the beach often takes the brunt of any coastal erosion without any protection. In recent years, sea-level rise and storm surge have increased enough to make this barrier islands' job progressively harder. These ongoing threats have tested Long Beach's effectiveness as a barrier island and its resilience to erosion. This study employs geospatial analysis methods, specifically Global Mapper and LiDAR data, to compare the effects of coastal erosion on Long Beach (unprotected) and Oceanside (protected) and the conditions of protected shorelines versus unprotected shorelines. Our research shows there is damage to protective barrier islands such as Long Beach, as a result of climate change that was not seen in the protected areas of the island. We found that there was up to 3.1 meters (approximately 10 ft) of erosion in some areas and up to 3 meters (9 ft) of deposition in others. Using GIS to analyze coastal erosion will help to create response plans for the communities of Long Island to combat and adapt to the changes caused by coastal erosion. LiDAR data from USGS surveys for 2011 and 2014 were obtained for geospatial analysis and subtraction comparison. Our results depicted that the coastal changes and storm surges have led to significant erosion of at least 100% decrease in elevation on parts of the shoreline over the span of four years, and it is forecasted to erode even more.

Introduction

Long Island is surrounded by the Atlantic Ocean on all sides, in the southeast corner of New York. Its history extends back to the early years of the Appalachian Mountains and the Atlantic Coastal Plains from 90 million years ago. During this time, the Appalachian Mountains were heavily subjected to weathering and erosion, and its "gravel, sand, and mud flowed down their eastern slope creating a broad apron of deep soils and sediments called the Atlantic Coastal Plain" (Lynch, 2021). As time progressed from the Cretaceous to the Pleistocene periods, glaciers deposited sediments along the coasts of the northeast part of the US. For Long Island, it was during the Pleistocene ice ages when "glaciations scraped the ancient coastal plain sediments off the landscape, depositing much of the sediment as the great regional moraines that

created the coastal surface geology of Long Island" (Lynch, 2021). The ice ages were a turning point for the creation of Long Island's mainland. The glacial activity created its foundation, and the sediments leftover from the episodes created the barrier islands examined in this study. Long Island and its surrounding features formed through erosion and deposition, which makes it just as vulnerable to evolve by the same methods.

The island is naturally known for its tourist attractions and rich biodiversity and is also at the center of wildlife attractions. With the Island witnessing significant tourism and climate change impacts slowly growing, the Island has become prone to floods and, most importantly, erosion. Erosion has been at the forefront of the negative side that Long Island has been facing for a long time. The island's coast is highly dynamic and constantly changing depending on various factors such as wind, ocean patterns, natural hazards, and anthropogenic activities. The presence of plant life on dunes on the south shore of Long Beach that have prevented erosion on Long Beach has also deteriorated in recent years. Long Island particularly faces erosion from the north and south sides as it is surrounded by the Atlantic Ocean on the south and the Reynolds Channel on the north. Beaches tend to get narrower during winter as it is a repetitive cycle in the coastal regions. However, in the case of Long Island, this pattern is different and needs to be followed accordingly (Tanski, 2012). Storm surges can have more impacts on the coastal beaches of Long Island and affect the shorelines in various ways. Depending on the level of the storm surge, it can rapidly erode the shorelines. The increased levels of storm surge are a byproduct of global warming, but sea level rise and ocean currents also play a massive role in the erosion seen on Long Island's coasts. Sea level along the U.S. coastline is projected to rise, on average, 10 - 12 inches, creating a profound shift in coastal flooding over the next 30 years (Sea Level Rise Technical Report, 2022).

Methodology

This study was conducted by using geospatial analysis consisting of ArcGIS and GlobalMapper software usages for the LiDAR data that were extracted from United States Geological Survey (USGS). We downloaded the surveys for the years 2011 and 2014 of LiDAR elevation data from the FTP's (File Transport Protocol) NYC 2021 database (ftp://ftp.gis.ny.gov/elevation/LIDAR/), totaling 22 LAS files and approximately 15.1 million points of data to construct a high-resolution Digital Elevation Model (DEM) (ftp://ftp.gis.ny.gov/elevation/LIDAR/) to make two digital elevation models (DEM-2011, DEM-2014) in particular a bare-earth model for each survey. We created a bare-earth model to avoid artifacts made by trees and other distractions. The differences in elevation shown on this created model for both years were subtracted to determine the magnitude of land change occurring on the coastlines of our two study areas on Long Beach and Oceanside (DEM-DIF). Google Earth Pro was also utilized to capture aerial photographs of the coastlines of our study areas for both 2011 and 2014, to facilitate the identification of changes at the coastline areas as they would appear in real time.

In order to calculate the percent change in elevation for the two years (2014 and 2011), the meters above sea level of the specific area was taken from the 2011 USGS NorthEast LiDAR map. Then, the change in elevation was taken from the digital elevation model that was created by subtracting the differences in elevation from both years. Using this information, the percent change in elevation was calculated by hand using the formula (elevation change from DEM-2011 x 100). For example, in Figure 5, the maximum elevation in the red areas in the channel was 1.5 meters in 2011. According to DEM-2014 it lost 3.1 meters of elevation, which means the percent elevation change was ((3.1/1.5) x 100) = 206.7%.

For Figure 2, the elevation in 2011, right before the dune vegetation, was 3 m, and according to the DEM-2014 it changed by -3m, which makes the percent change in elevation decrease 100%. For the area at the top of the dune with the vegetation, it was 4.3m in 2011 which increased from the previous 3 m, which makes the change in elevation ((3/4.3) x 100)) = 69.8 % increase. For Figure 3, the percent change in elevation for the red areas near the middle of the channel was 206.6% as it was 1.5 m and lost 3.1 meters in elevation. For Figure 4 the middle of the channel in red areas decreased by 91.2 % and in the yellow areas, it decreased by 100% from 2011. For Figure 5, the red area was on average -1.2m deep in DEM-2011 and changed by 2.8 m. That causes a 233.2% decrease in elevation.

Results
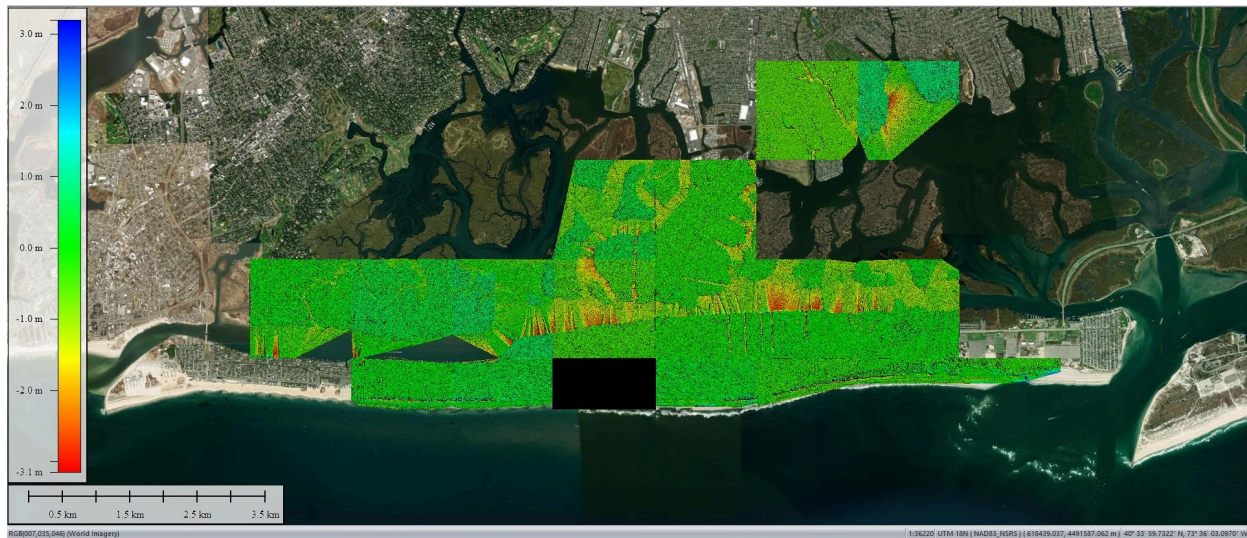
Figure 1: Digital Elevation Model (DEM-DIF) of the difference in meters above sea level in 2011 to 2014 using LiDAR of the study areas in the comparison. The locations are in Long Beach and in Oceanside. The black box is an area that was not used in the study because of missing data. The areas in red represent erosion with the maximum erosion being 3.1m loss of elevation in some areas. The blue represents deposition, which was noted to be up to 3 m in some areas.
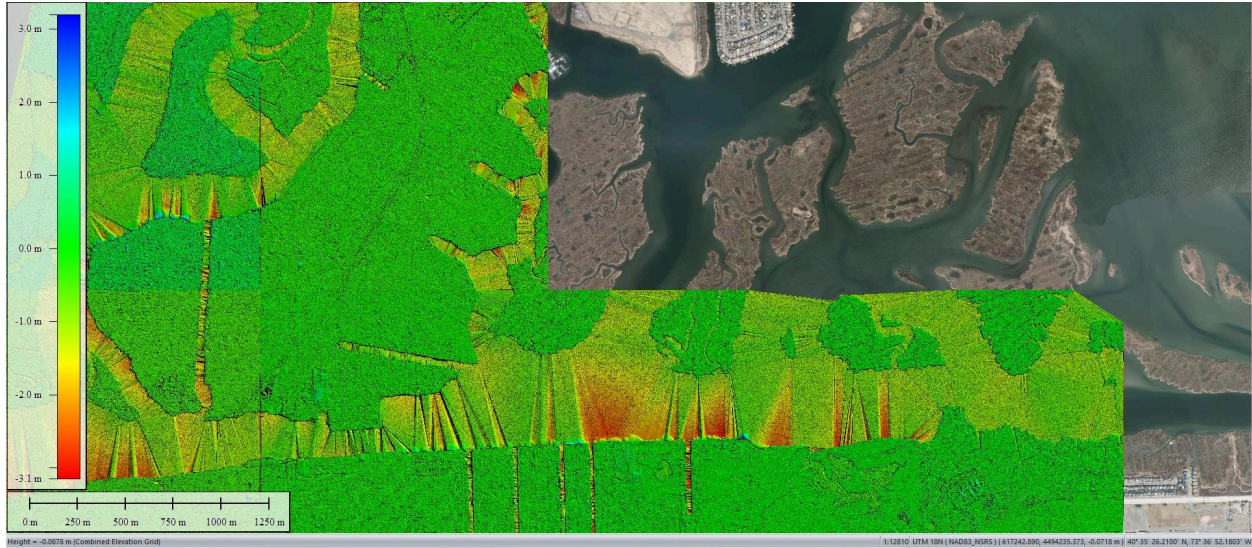
Figure 2: Digital Elevation Model (DEM-DIF) of the difference in meters above sea level in 2011 to 2014 using LiDAR data of a portion of Long Beach coast on the south side of the island. Half of the model was replaced with satellite imagery of the same area for better comparison. The areas in red represent significant land change caused by erosion; the loss in land was around 3.1 meters. The blue represents deposition and was up to 3 meters. The impact of dunes on coastal erosion can also be observed. The areas before the dunes have lost a little more than 2 meters worth of elevation, but the dunes gained 2-3 meters of height where the vegetation is.
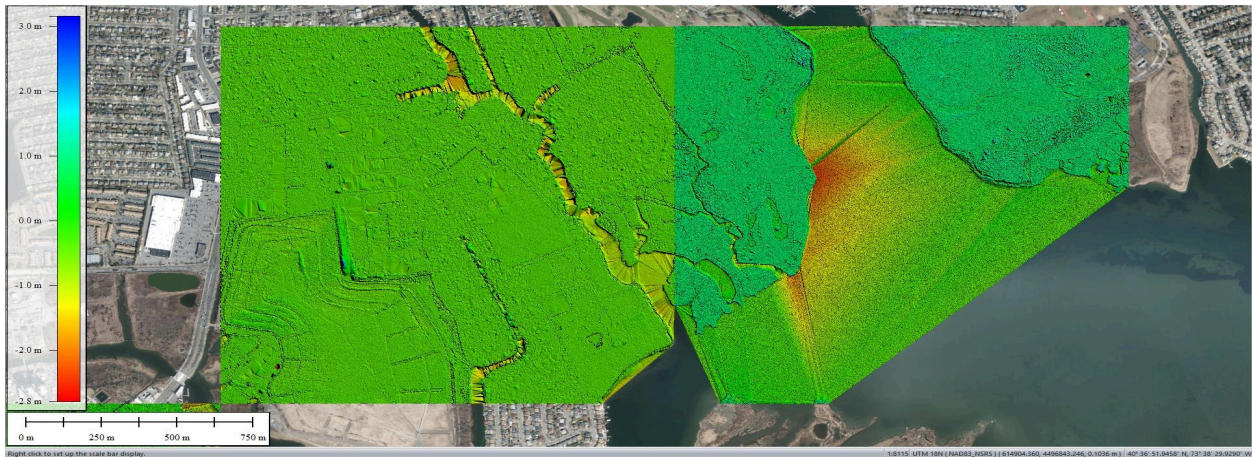

Figure 3: Digital Elevation Model (DEM-DIF) of the difference in meters above sea level in 2011 to 2014 using LiDAR imagery of a portion of Long Beach coast on the north side of the island. Part of the DEM model was replaced with satellite imagery of the same area for better comparison. The areas in red represent erosion with the maximum erosion being 3.1 m loss of elevation in some areas. The blue represents deposition, which was noted to be up to 3 m in some areas.

4

Figure 4: Digital Elevation Model (DEM-DIF) of the difference in meters above sea level from 2011 to 2014 using LiDAR imagery of a portion of Long Beach coast on the north side of the island at a different location from Figure 3. The areas in red represent erosion, with the maximum elevation loss being 3.1 m. The blue represents deposition, which was noted to be up to 3 m in some areas.

Figure 5: Digital Elevation Model (DEM-DIF) of the difference in meters above sea level from 2011 to 2014 using LiDAR data of Oceanside, NY; it is on the south shore of Long Island NY, with a satellite imagery map behind it to give context for its location. The areas in red represent erosion, with the maximum loss of elevation being 3.1m in some areas. The blue represents deposition, which was noted to be up to 3 m in some areas.

Figure 6: Satellite image of Long Beach taken at 4938ft, June 2010. The image, taken from Google Earth, marks previous vegetation and the jettie system present before significant erosion.

Figure 7: Satellite image of Long Beach taken at 4938ft, October 2014. Image taken from Google Earth, marks significant vegetation loss and jettie destruction as the beach recedes. The jetties eventually succumbed to the strengthened natural force of ocean currents, for they are no longer present on Long Beach in Fig. 7. Approximately half of the vegetation that was present on the beach in 2010 was gone in 2014.

Figure 8: Real-time satellite image of Oceanside Park taken at 4938ft, June 2010. Image taken from Google Earth, marks previous vegetation and marsh presence along the coast.

Figure 9: Real-time satellite image of Oceanside Park taken at 4938ft, October 2014. Image taken from Google Earth, marks vegetation and marsh presence after four years. Loss of vegetation cover can be witnessed on the left hand side of the figure, and along the coast of Oceanside Park. The beachline of the far right corner also witnessed a recession of the shoreline and small amount of erosion.

Discussion

Overall, the trends shown in Figure 1 show that the most erosion in Long Beach occurred on the north side and by the coast. The dunes, seen in more detail in Figure 2, likely protect the island from erosion and land loss, as most of the land loss and gain is seen on the south side of the island.

Figure 2 shows a close-up of the beaches on the south side of Long Beach. The impacts of the jetties can be seen in how the land is shaped near the water. Shifting dune height to rest where the vegetation is demonstrates the plant's ability to keep sand and soil trapped in its roots. This is important not only for preventing erosion, but also because the plants act as a buffer against storms and flooding. The land elevation behind the dunes has stayed relatively consistent; this is the same for the land on the north side of the island as well as at Oceanside.

The land cover on the north side of Long Beach is more consistent than the coasts of the south side. However, as seen in Fig. 3, the north side of Long Beach is the Reynolds Channel, and there is more elevation change in its waterways. Fig. 3 shows that there is a decrease in land elevation wherever there is water. With the larger rivers in the channel having a notable portion of the land in the channel, it has lost up to 3.2 meters of elevation. This pattern of more elevation loss in the land near the shore of the channel was expected as the channel has more moving water in a narrower space, which would cause more erosion. This pattern can be seen in Figure 4 as well.

The biggest difference between the northern and southern sides of Long Beach is that even though there is more erosion in the waters (because of the channel), the land is more consistent than the shoreline. The entire south shore of Long Beach shows the same pattern seen in Figures 1 and 2, which is that there is consistent erosion and elevation loss along the coast, but the coast is protected from further erosion by the dunes. On the north side of the island and in Oceanside, there are no signs of erosion along the coasts, only in bodies of water already there.

Like the northern coast of Long Beach, the southern coast has also displayed significant evidence of erosion. Comparisons of Fig. 6 and Fig. 7 show multiple indicators of this, such as the total degradation of the jetties put in place along the beach before 2010. Jetties are known as blocks put in place along a beach to protect it from water-related damage. They are typically made of wood, concrete, or stone, as in the case of Long Beach. Unfortunately, a major part of the erosion seen in Long Beach was caused by the jettie system put in place there. The intended purpose of the jetties was to protect the beach from coastal erosion, but it only brought more erosion to the beach through ocean currents and sand pileup.

In addition to the Jettie destruction, the large amounts of disappearing dune vegetation are quite noticeable. Native vegetation and its roots act as an anchor that keeps the land below it in place, making it difficult for weathering and erosion to displace it. When that vegetation is no

longer present, the ground is weakened and more prone to be impacted and shifted by natural surface processes. For beaches, recession inland is one of the main consequences, and the sand-dominated parts of the beach spread further inland, eventually risking damage to nearby property that cannot move with the shore. This is the exact situation shown on the southern coast of Long Beach.

The evidence for coastal erosion is expected to become more prominent for Long Beach, an unprotected shoreline facing natural coastal erosion caused by sea level rise and storm surge, in addition to the failure of human innovation. These combined forces led to the receded beachline's visibility in the 2014 photos, and will most likely be seen clearer in more recent documentation.

The location of Oceanside has witnessed erosion over the years as well, but the rate of erosion is pretty low compared to Long Beach. Based on geographical location and patterns of wind, the erosion level can change. The north side of Long Beach has the most erosion closest to the shore for Figure 9, likely due to the movement of the water from the ocean currents. In Oceanside, this pattern is seen with the channel cutting through Oceanside Park, where erosion is likely from the movement of water, but in the delta, there is only one large area of erosion while the rest of the land mass seems stable. That one spot may be where currents converge, which could contribute to the large spot of land that eroded.

The reason why Oceanside displays fewer effects of erosion than Long Beach can be attributed to the location of the study area, which falls under the protection of Long Beach. Since Long Beach is the barrier island on the outskirts absorbing most of the impacts of erosion, areas such as Oceanside that fall behind it will experience less devastation. If Oceanside was an unprotected shoreline like Long Beach, the currents of the Atlantic ocean would exacerbate the existing erosion patterns of the bodies of water surrounding Oceanside.

Oceanside's existence as an area under protection by other land masses is the main reason barrier islands such as Long Beach are important. The relationship between Long Beach and Oceanside can be seen throughout Long Island with multiple other cities and beaches. This study is simply one case of the many that make up this corner of New York State.

More research is needed as the most recent LiDAR data we found was a decade old and missing part of the island. We were able to complete the analysis without the missing data, but the experiment bears repeating because the changing climate makes it important to monitor changes. The erosion and coastal changes we found spanned over the course of four years, and storm surges and damage have been getting worse since then. This presents the possibility that the erosion we found could have increased significantly since the creation of this study, which is another reason why it needs to be repeated after the collection of more recent data.

Conclusion

While more erosion was expected to be seen on the south shore, the fact that the erosion seen on the dunes of the north side of Long Beach and Oceanside showed no coastal elevation change, furthers the hypothesis that Long Beach is a barrier island that is a source of protection against land loss and erosion for Oceanside and many other areas on Long Island. In addition, dunes and other native vegetation are an important environmental defense as it protects against erosion and acts as a buffer to storm damage as well. This is increasingly important as the severity and frequency of storms and erosion have increased. The numbers and costs of disasters have been increasing for several decades as well due to increases in exposure (more people moving into harm's way and increases in the values of property and infrastructure at risk), vulnerability of people and infrastructure, and climate change.

Credit Authorship Contribution Statement
Abstract: Appel, C., Rahman, M. M., Boddu, D., Marsellos, A.E. (*Supervision*). *Introduction*: Rahman, M. M., Boddu, D. A.E. *Figures*: Appel, C., Boddu, D., *Methods*: Appel, C., Rahman, M. M., Boddu, A.E. *Results*: Appel C., Rahman, M. M., Boddu, D., *Discussion:* Appel, C., Rahman, M. M., Boddu, D., *Conclusion:* Appel, C., Rahman, M. M., Boddu, D.

References

Tanski, J. (2012). *Long Island South Shore Dynamics Study*. Long Island South Shore Estuary
Reserve. https://www.seagrant.sunysb.edu/cprocesses/pdfs/lidynamicsouthshore.pdf

Lynch, P. J. (2021). *Geology of Beaches and Barrier Islands*. Yale University Press.
https://yalebooks.yale.edu/2021/07/23/geology-of-beaches-and-barrier-islands/#:~:text=N
orth%20of%20New%20York%20Harbor%20the%20Pleistocene%20glaciations,Block%
20Island%2C%20Martha's%20Vineyard%2C%20Cape%20Cod%2C%20and%20Nantuc
ket.

Sweet, W.V., B.D. Hamlington, R.E. Kopp, C.P. Weaver, P.L. Barnard, D. Bekaert, W. Brooks,
M. Craghan, G. Dusek, T. Frederikse, G. Garner, A.S. Genz, J.P. Krasting, E. Larour, D.
Marcy, J.J. Marra, J. Obeysekera, M. Osler, M. Pendleton, D. Roman, L. Schmied, W.
Veatch, K.D. White, and C. Zuzak, (2022). *Global and Regional Sea Level Rise
Scenarios for the United States*. National Oceanic and Atmospheric Administration.
https://aambpublicoceanservice.blob.core.windows.net/oceanserviceprod/hazards/sealeve
lrise/noaa-nos-techrpt01-global-regional-SLR-scenarios-US.pdf

Stratigraphy, Structure and Tectonic Implications of the New York Botanical Garden, Bronx, NY

Merguerian, Charles[1] and Merguerian, J. Mickey[2]
[1]Duke Geological Laboratory, 55 Spongia Road, Stone Ridge, NY 12484
[2]DukelabsDSC, 16 Middle Lane, Westbury, NY 11590
CharlesM@Dukelabs.com
Mickey@DukelabsDSC.com

Introduction

This extended abstract reports on our compiled field mapping, structural analysis and petrography of bedrock at the New York Botanical Garden (NYBG) in Bronx, NY. Starting with our dear late colleague Dr. John E. Sanders, our analysis began with research in support of our On-The-Rocks field trip program of the NY Academy of Science of post-Woodfordian Bronx River diversion (Merguerian and Sanders 1993a, 1996a), mapping and petrography of a NYBG building site (Pfizer Building) then under construction in the NW corner of the Garden (Merguerian and Sanders 1998) and adjacent Bronx parks (Fuller, Short and Merguerian 1999). Research continued in 2011 with outcrop mapping of the entire grounds and a recent guidebook and field trip (Merguerian and Merguerian, 2024a). Here we compile the results of these NYBG studies and offers two preliminary geological maps and a location map (Plates 1, 2, 3 at end of extended abstract) and our findings on the structural geology and tectonic setting of the NYBG.

NYBG Location

The NYBG is located in the central Bronx, NY just north of E. Fordham Road and east of Fordham University (Figure 1).

Figure 1 – Location map of the NY Botanical Garden which is bounded on the east by the Bronx River Parkway, on the south by East Fordham Road, on the west by Southern Boulevard and on the north by the Mosholu Parkway. Outline of Plate 1, 2 and 3 maps of the NYBG shown as a red rectangle. (Hagstrom).

GEOLOGIC BACKGROUND

The NYBG is situated within the southerly terminus of the Manhattan Prong (Figure 2), a region of low rolling ridges and valleys underlain by a northeast-trending, deeply eroded crystalline sequence of Proterozoic- to Lower Paleozoic metamorphic rocks. South of NYC, the crystalline rocks of the Manhattan Prong plunge southwestward and disappear beneath a gently inclined covering of Cretaceous coastal-plain sedimentary strata and an overlying blanket of Pleistocene (glacial) drift.

Figure 2 – Physiographic diagram showing the major geological provinces in southern New York, northern New Jersey, and adjoining states. The NYBG is within the Manhattan Prong. (From Bennington and Merguerian, 2007.)

BEDROCK UNITS

Under this section we briefly describe the history of local bedrock investigations to provide an overview of the geology of the region and the specifics of the stratigraphy-, geologic structure-, and metamorphic geology of the NYBG.

Although the rocks underlying the Bronx were first studied by naturalists in the 1700's, and by geologists and mineral collectors from the NY Mineralogical Club in the 1800's and 1900's, detailed geologic mapping began in the mid- to late 1800s to earliest 1900s by W. W.

Mather (1843) and F. J. H. Merrill et al (1902). The rich history of NYC geologic investigations is covered elsewhere (Merguerian and Sanders 1991b). Suffice to say that in 1890 (p. 390), Merrill named the Manhattan Schist to include all of the micaceous metamorphic rocks found on Manhattan Island and suggested, following the views of Professors W. W. Mather (1843) and J. D. Dana (1880), that they represent metamorphosed equivalents of the Paleozoic strata of southern Dutchess County, New York. Merrill (1890) states that *"the name Manhattan Group was proposed by R. P. Stevens, Esq., to include the rocks of New York Island"*.

F. J. H. Merrill (1890, 1902), in concert with other geologists published the first comprehensive geologic map of New York City in the United States Geological Survey New York City Folio 83. In this compilation Merrill outlined the basic stratigraphic- and structural framework that modern geologists would test and refine (Figure 3). Merrill's major contribution was subdivision of Mather's Primitive Series into mappable units. He first defined the correct relative chronology of the basal Proterozoic Fordham Gneiss (fgn), the overlying Cambrian to Silurian (sic) Stockbridge dolomite (Є Ss) and the Silurian (sic) Hudson Schist (Sh) – now known as Ordovician and older Manhattan Schist and associated Lower Paleozoic schistose rocks).
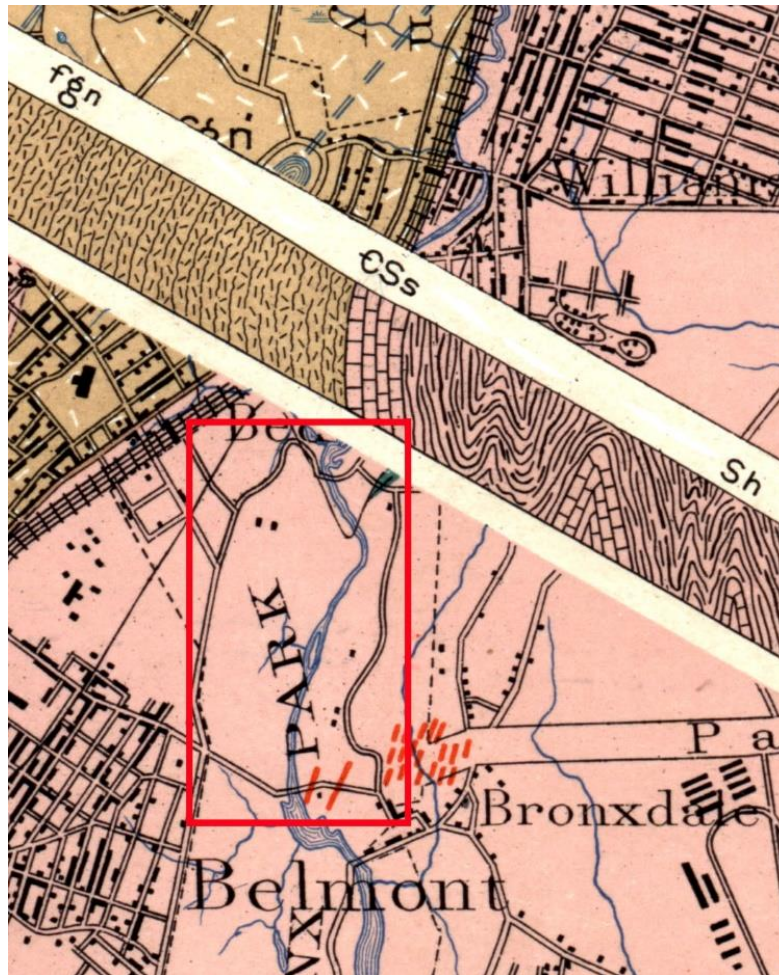
Figure 3 – Map and diagonal section of Merrill et al (1902) USGS folio map of the region of the Bronx that includes the NYBG (red rectangle) and shows a simplified view of the folded structure of NYC bedrock. The area of the NYBG shown in Plates 1, 2 and 3 is shown as a red rectangle.

Following our revisions in the stratigraphy and structure of NYC (Merguerian 1981a, 1983a; Merguerian, Baskerville and Okulewicz, 1982; Baskerville and Merguerian, 1982, 1983; Mose and Merguerian, 1985, and Merguerian and Sanders 1991b), Baskerville's (1992) USGS map of the Bronx showed a more complex geological interpretation of NYC that embraced <u>some</u> of the stratigraphic and structural ideas proposed by many in the 1980s. A portion of his map of the region surrounding the NYBG is reproduced below as Figure 4.
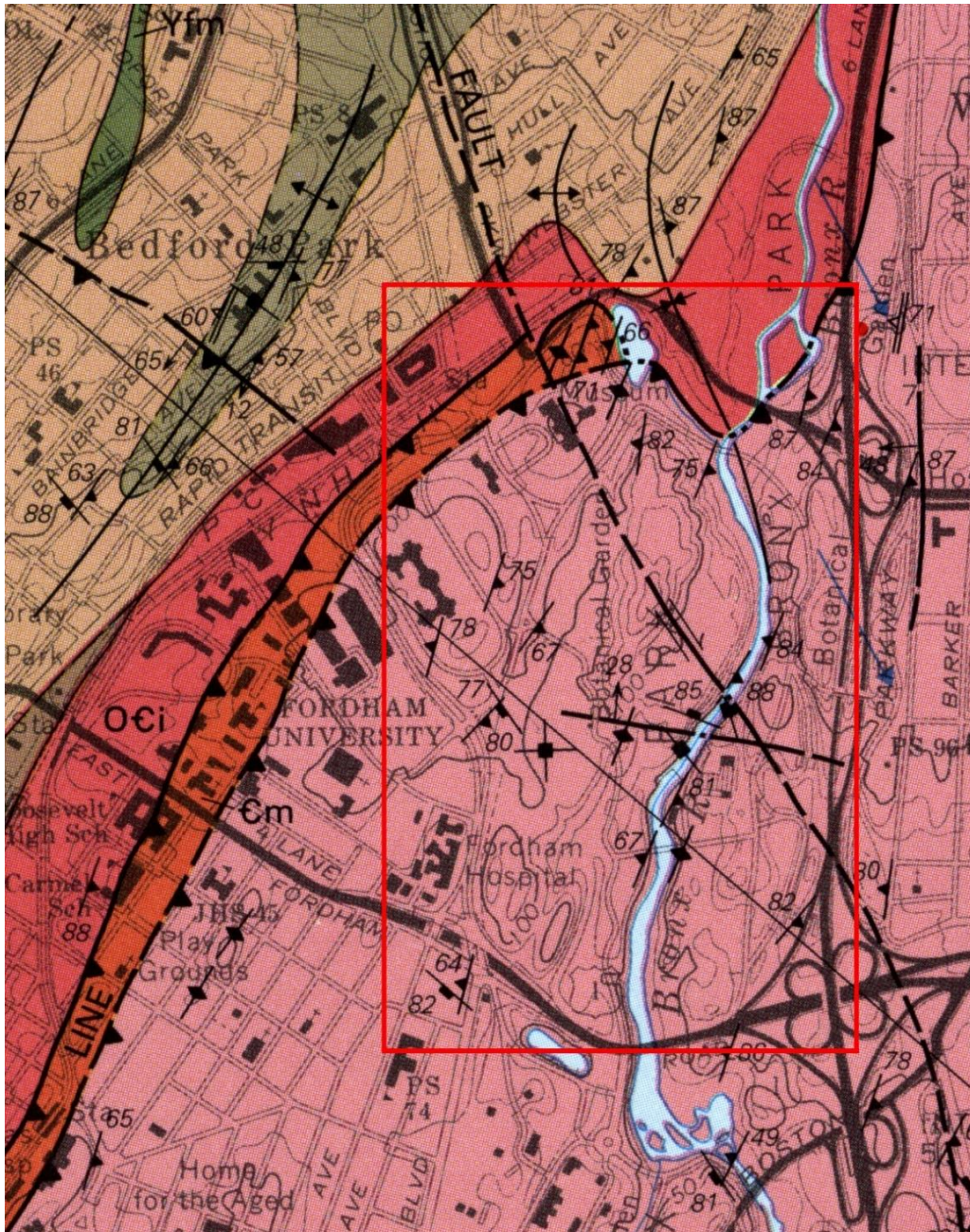
Figure 4 – Geological map of the NYBG showing the position of Fordham Gneiss (Yfd and Yfm - brown and green units, the Inwood Marble (OЄi – reddish unit), Manhattan Schist (Єm – red-brown unit), and the Hartland Formation (OЄh - pink unit) and the trace of the right-lateral Mosholu fault and Cameron's Line. The area of our new NYBG geological map (See Plates 1, 2, 3 below) shown in red rectangle. (Adapted from Baskerville 1992).

4

Our field- and laboratory investigations of the bedrock geology in the NYC area over the past 40 years have drawn heavily from earlier- and contemporary studies and suggest that the Manhattan Schist exposed in Manhattan and the Bronx is a lithically variable sequence consisting of three, structurally complex, roughly coeval, tectonostratigraphic units. The major findings from this period have been presented elsewhere (Merguerian 1983b, 1984, 1994a, 1996c, 2002b, 2015b; Merguerian and Baskerville 1987; Merguerian and Merguerian 2004, 2012, 2014a, b, 2016a, b; and Merguerian and Moss 2005, 2006a, 2007, 2015).

Our investigations agree, in part, with designations proposed by Hall (1976, 1980), but indicate the presence of a hitherto-not-recognized, structurally higher schistose unit that is a lithostratigraphic correlative of the Hartland Formation of western Connecticut and we thus carry the name into NYC. CM's renegade interpretations on the stratigraphy and subdivision of the Manhattan Schist were presented during a lecture at the New York Academy of Sciences on the evening of 17 December 1984 entitled *"Will the Real Manhattan Schist Please Stand Up!"*

Bedrock Stratigraphy of New York City and the Bronx

The following section outlines our new views on the stratigraphy and ductile- and brittle structure of New York City which includes the Garden grounds. Two basic subdivisions of NYC crystalline bedrock (Figure 5) include:

1) Paleozoic Cover Rocks. Schist, granofels, marble, amphibolite and associated lithotypes, and
2) Proterozoic Y Basement Rocks. Granulite facies gneiss and cross-cutting igneous rocks.

Both rock sequences were internally folded and sheared during extended Paleozoic orogenesis and cut by younger brittle fractures (fault- and joint discontinuities). They are distinguishable in the field using the following field- and petrographic criteria:

Hartland Formation (Є-Oh). Gray weathering, fine- to coarse-textured, typically well-layered muscovite-quartz-biotite-plagioclase± kyanite±garnet schist, gneiss, and migmatite with cm- and m-scale layers of gray quartzose granofels and greenish amphibolite± biotite± garnet. Known for relatively easy excavation because of pervasive weakness parallel to layering, the unit has been encountered in the Central and Riverside parks, East Side Access, Second Avenue Subway, Manhattan Water Tunnel, #7 Line IRT Extension and Con Edison Steam Tunnel projects and crops out mostly east of the Bronx River near the NYBG. It is considered a southernly, more metamorphosed correlative of the slates and interlayered lithic sandstones (graywackes) of the Taconic allochthon (Merguerian and Sanders 1996b). Hartland rocks are exposed in a vertically plunging structure involving Cameron's Line and the Saint Nicholas thrust in the east part of the NYBG but mostly occurs east and south of the park. (See Table 1; Plates 1-3.)

Manhattan Formation (Є-Om). Massive rusty- to maroon-weathering, medium- to coarse-textured, biotite-muscovite-plagioclase-quartz±garnet±kyanite±sillimanite±magnetite ±tourmaline gneiss, migmatite, and schist. Characterized by the lack of internal layering except for kyanite± sillimanite+quartz+magnetite interlayers and lenses up to 10 cm thick, cm- to m-scale layers of blackish amphibolite and lesser quartzose granofels, it forms the bulk of exposed Paleozoic metamorphic rocks of northern Manhattan, Central Park and the Bronx including most
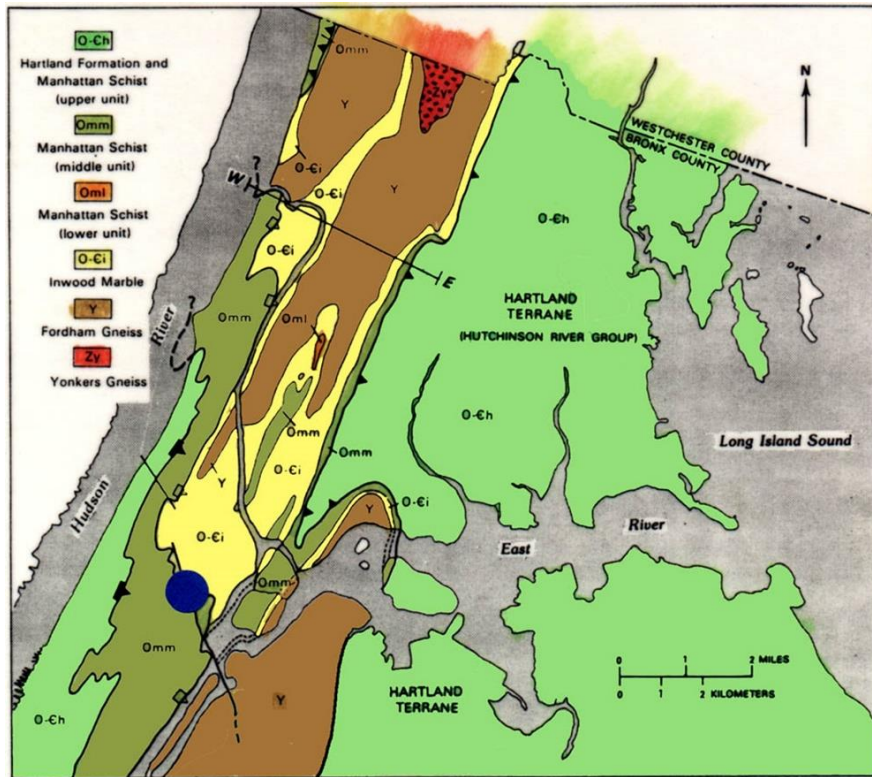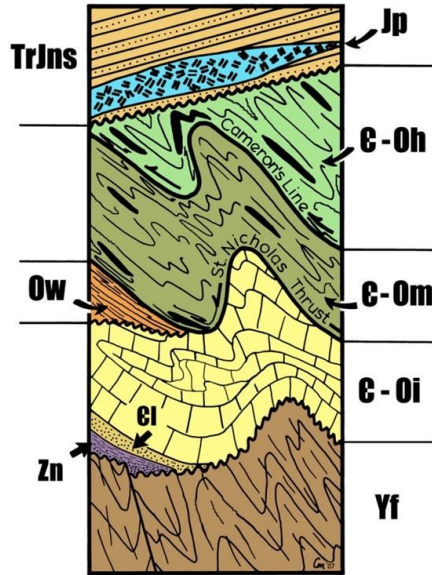
Figure 5 – Bedrock stratigraphy of New York City. The polydeformed bedrock units are in NYC are nonconformably overlain by west-dipping Triassic and younger strata (TrJns) and the Palisades intrusive sheet (Jp) west of the Hudson River. Triangles show the dip of Cameron's Line (solid) and the Saint Nicholas thrust (open) and the flagged triangles indicate overturned thrusts. The map depicts the F₃ folding of Cameron's Line and the Saint Nicholas thrust and shows major cross-cutting brittle faults. Blue dot shows earthquake epicenter of magnitude 2.4 (21 January 2001) whose focus projects above the NW-SE trace of the Manhattanville fault. Note that the unit Omm is equivalent to Є-Om in this paper. (Adapted from Merguerian and Baskerville 1987.)

of the central NYBG exposures. From the NYBG they extend southwestward in the Bronx cropping out in the east half of Boro Hall Park and also along the central portion of Crotona Park. These allochthonous rocks are interpreted as a transitional, "proximal to craton" part of the Taconic Sequence deposited on the former slope-rise. (See Table 1; Plates 1-3.)

Walloomsac Formation (Ow). Unit composed of fissile brown- to rusty-weathering, fine- to medium-textured, biotite-muscovite-quartz-plagioclase±kyanite± sillimanite±garnet±pyrite ±graphite schist, granofels and migmatite containing interlayers centimeters to meters thick of plagioclase-quartz-muscovite granofels, layers of diopside±tremolite±phlogopite calcite- and dolomitic marble, calc-schist and greenish calc-silicate rock. Amphibolite is absent although green amphibole-bearing rocks are locally found. Diagnostic mineralogical features of the former pelitic portions of the formation include strongly pleochroic reddish biotite, pinkish garnet as scattered concentrations of small crystals and as porphyroblasts (up to 1 cm), graphite and pyrite. The lack of amphibolite and the presence of graphitic schist and quartz-feldspar granofels invites the interpretation that this unit is metamorphosed middle Ordovician carbonaceous shale + greywacke strata of the autochthonous Annsville, Normanskill and Austin Glen formations of SE New York and the correlative Martinsburg Formation farther southwest. Ow is exposed in the SE and NW edges of the NYBG and extends southward through the Bronx Zoo onto the west edge of Boro Hall Park and on both edges of Crotona Park.

Inwood Marble (C-Oi). Occurring always west of the NYBG, the Inwood is white to bluish-gray fine- to coarse-textured dolomitic and lesser calcitic marble locally with siliceous interlayers containing diopside, tremolite, phlogopite, muscovite (white mica), and quartz together with accessory graphite, pyrite, tourmaline (dravite), chlorite and zoisite (Merguerian, Merguerian and Cherukupalli 2011). Layers of fine-textured gray quartzite with a cherty appearance and mica-quartz calc-schist are locally present. Inwood Marble is exposed mostly in the Inwood section of Manhattan, the shoreline along the NW edge of Inwood Park and Mt. Morris Park of Manhattan. Exposures on I-95 (Cross Bronx Expressway) and beneath the Webster Avenue valley are known in the Bronx. The Inwood is correlative with the Cambro-Ordovician carbonate platform or "Sauk" Sequence of the Appalachians.

Fordham - Queens Tunnel Gneiss (Yf). The oldest rocks in NYC are a complex assemblage of Proterozoic Y orthogneiss, metasedimentary, metavolcanic, dike and granitoid rocks. Based on detailed studies and U-Pb age dating in the Queens and Brooklyn portions of NYC Water Tunnel #3 (Merguerian, 1999a, 2000a; Brock, Brock, and Merguerian 2001) the Fordham correlative we mapped are there known as the Queens Tunnel Complex (QTC) which consists of predominately massive mesocratic, melanocratic and leucocratic, orthogneiss with subordinate schist, granofels, and calc-silicate rocks. Grenvillian high pressure granulite facies metamorphism produced a tough, anhydrous interlocking texture consisting of clino- and orthopyroxene, plagioclase, and garnet that has resisted hornblende and biotite grade Paleozoic retrograde regional metamorphism. No Fordham rocks are found in the Garden in situ though a few scattered glacial erratics are scattered about the grounds. In situ Fordham underlies the Fordham Ridge in an antiformal structure immediately west of the park where Fordham University is in session.

Paleozoic Orogenesis

The venerable Manhattan Schist of NYC is exposed in Manhattan and Bronx and consists of three separable map units including the Hartland, Manhattan, and Walloomsac formations. These subdivisions agree, in part, with designations proposed by Hall (1968a, b, c) but recognize a structurally higher unit that is a direct correlative of the Hartland Formation of western Connecticut (Merguerian 1981a, 1983b and 1987). The three schistose tectonostratigraphic units are imbricated along regional ductile faults known as the Saint Nicholas thrust and Cameron's Line (Merguerian 1981a, 1983a, 1994a, 1996c).

Now metamorphosed to amphibolite facies grade, the exposed Paleozoic metamorphic cover rocks of NYC were originally deposited on the proto–North American shelf edge as sediment and intercalated volcanic and volcaniclastic materials, though in vastly different depositional environments (Figure 6). Protoliths of the Hartland were originally deposited in a deep ocean basin fringed by offshore volcanic islands. Protoliths of the Manhattan originated along the shelf edge of the Laurentian continental margin as slope-rise strata including thick clay-rich sediment with occasional sand interlayers and mafic dikes or flows.
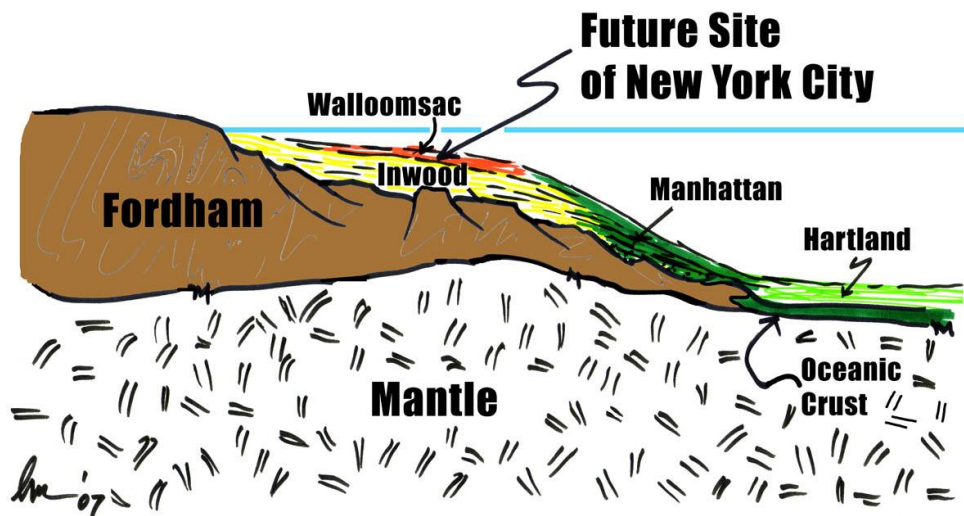
Figure 6 – Reconstruction snapshot cartoon of proposed depositional realms at Laurentian margin of protoliths of the Inwood, Walloomsac, Manhattan and Hartland strata before the Taconian arc-continent collision deformed them in mid-Ordovician time (~450 Ma). (CM drawing.)

Formed in the back-arc environment and being closed off from open-ocean conditions with the encroachment of the Taconic arc and subduction complex, protoliths of the Walloomsac became compositionally unique since they originated under restricted oceanic conditions (a reducing environment) which fostered thick accumulations of carbonaceous and sulphidic clay-rich sediment with occasional sandy and calcareous interlayers in a rapidly subsiding intracontinental foreland basin. Loading of the continental shelf edge by the Taconic arc may have been the agent that triggered the subsidence of the Walloomsac foreland basin and allowed for thick accumulations of black shale and turbidites on shelf-sequence carbonates of the Sauk sequence as seen in the Hudson Valley (Annsville, Normanskill, Austin Glen and correlatives).

In our view, underthrusting within the accretionary prism associated with the Taconian arc-continent collision produced the internal shearing, imbrication, deep-seated deformation, and amphibolite facies regional metamorphism of the Paleozoic cover rocks with some basement involvement and the coeval development of Cameron's Line and the Saint Nicholas thrust zones. The Taconian arc-continent collision is depicted in a series of time slices in Figure 7.
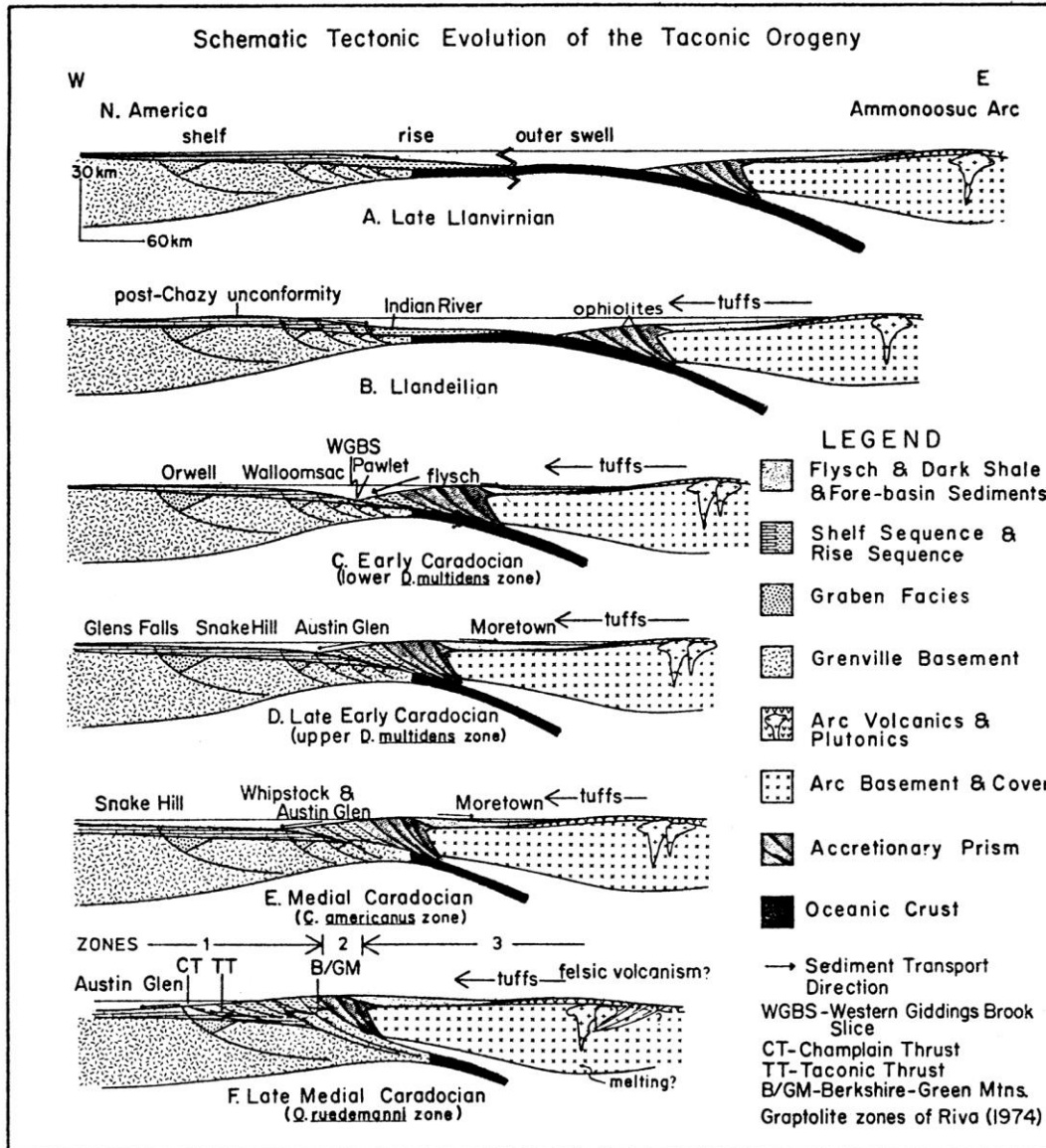
Figure 7 - Sequential tectonic cross sections for the Taconic orogeny in New England that show from the top downward the development of the Taconic suture zone. From Rowley and Kidd (1981).

In summary, the three distinctive mappable units of the "Manhattan Schist" represent essentially coeval shelf- (Ow), transitional slope/rise- (Є-Om), and deep-water (Є-Oh) lithotopes that were juxtaposed during telescoping of the ancestral North American shelf edge in response to closure of the proto-Atlantic (Iapetus) ocean during the Taconic orogeny. (See Figure 7.)

Arc-Trench Tectonics

The development of plate tectonic theories to better explain the mountain building process has been strengthened by remapping of former geologic terrains and also by studying modern convergent margins. One such study that stands out was an investigation of deep sea drilling and study of extracted core from the Nankai Trough area of the Shikoku subduction zone in southwestern Japan (Moore and Karig 1976).

Two figures from their paper are combined below as Figure 8 that demonstrate the shallow level isoclinal folding and imbrication of strata detected in the upper levels of thrust sheets within the upper plate subduction complex. Our model of the Taconic orogeny (Figure 9) takes into account the attenuation of strata during deep-seated convergent tectonics and how complex the original starting strata may have been before the obscurities produced by metamorphism. As such, traditional formational mapping in uplifted mobile belts produced in arc-continent or arc-arc convergent margin settings may be best understood by abandoning layer-cake stratigraphic models and entertaining the idea that shear zones and thrust faults may be more pervasive than outcrop mapping may indicate – even away from major shear zones. The card-carrying field geologist in deeply eroded core zones of mountain belts may inquire "are there shear zones around every outcrop"? We have seen many examples of confusion in the field trying to determine which formation is which but we should be open to imbrication (mixed zones) and intimate shearing of strata at the small scales as they descend to the deeper levels of a subduction zone, especially in light of the fold-thrust complexities of starting materials within the developing subduction complex. (See Figure 8.)
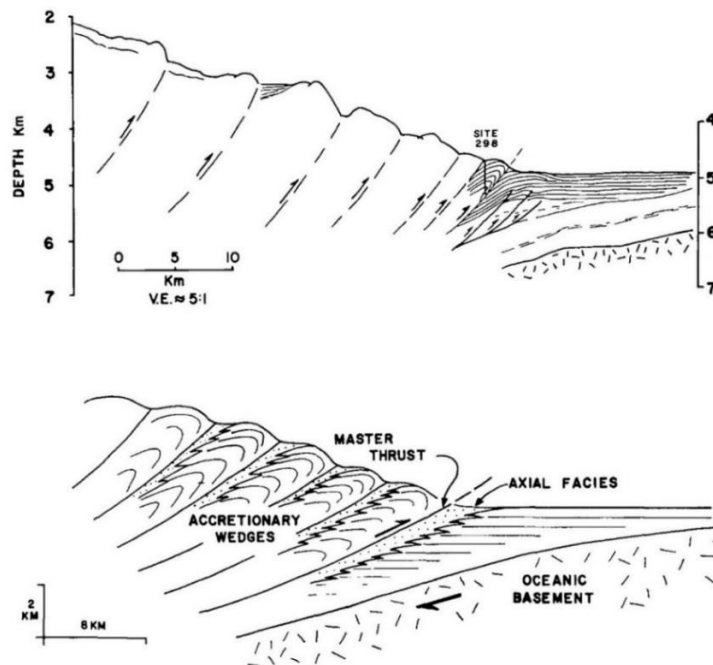
Figure 8 – Two views of internal structure of the trench wall of accretionary wedge associated with modern subduction in the Shikoku subduction zone of the Japanese trench based on drilling (Sites 297, 298). Their study of bedding-cleavage relationships demonstrated that isoclinal folding and imbrication of subducted strata took place in concert with thrust faulting in the upper plate at high crustal levels. (From Moore and Karig, 1976, figs 11, 12.)

10
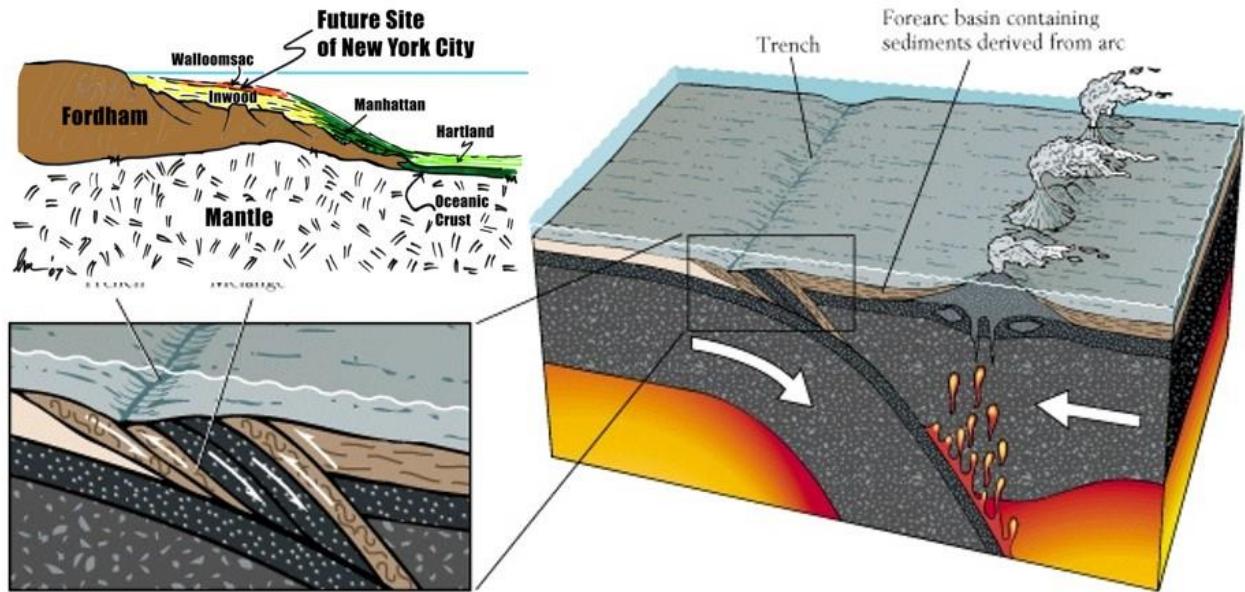
Figure 9 – Composite diagram showing the subduction zone imbrication and deeper area of deformation, metamorphism and imbrication along ductile faults of former sedimentary strata that would produce the Inwood, Walloomsac, Manhattan and Hartland Formations. These rocks and structures developed at the deep levels of a mid-Ordovician arc-continent collision zone of the ~450 Ma Taconic orogeny. In our view, the development of the Saint Nicholas Thrust and Cameron's Line involved the juxtaposition of disparate former sedimentological realms of the Laurentian shelf, slope and rise, and abyssal regions formerly adjacent to the continental margin.

Structural Geology of New York City

All Paleozoic strata in the Bronx have shared a complex structural history which involved three superposed phases of deep-seated Taconian deformation (D_1, D_2, D_3) followed by three or more episodes of open- to crenulate folds (D_4, D_5, D_6) in mid- to late Paleozoic or younger time. Synmetamorphic juxtaposition of the bedrock units along ductile thrusts (Saint Nicholas Thrust and Cameron's Line) occurred very early in their structural history, culminating during D_2 and deformed during D_3 based upon field relationships. The three Paleozoic orogenies (Taconian, Acadian, and Alleghenian) developed prograde (D_1, D_2, D_3) and later retrograde (D_4, D_5, D_6) effects in the Inwood, Walloomsac, Manhattan, and Hartland rocks. Only Taconian structures of D_1, D_2, D_3 are shown plotted on Plates 1 and 2.

The obvious map scale F_3 folds in NYC are those with steep NNE- to NE-trending axial surfaces (S_3) and variable but typically shallow plunges toward the S and SW. (See Figure 5.) The F_3 folds are typically overturned to the NW with a steep SE-dipping foliation. Shearing in fold limbs and along S_3 axial surfaces typically creates a transposition foliation that combines S_1, S_2, and S_3 that is commonly invaded by granitoids to produce migmatite during both the D_2 and subsequent D_3 events. These third-generation structures deform two earlier penetrative structural fabrics (S_1 and S_2). Regionally, the older penetrative fabrics are detected as enveloping surfaces that trend roughly N50°W and dip gently toward the SW except along the limbs of F_3 folds. We suspect that all of these structures (D_1, D_2, and D_3) are all products of protracted Taconian orogenesis.

11

D$_1$ to D$_3$ folds and crosscutting fabrics that formed during the Taconic orogeny are overprinted by two- and possibly three- fold phases that, based on their style and general lack of attendant foliation, undoubtedly took place at much-higher crustal levels than did the three Taconian fabrics. Presumably, the younger fold phases D$_4$ to D$_6$ record the effects of the Acadian- and terminal-stage Appalachian orogenies.

During D$_2$, the rocks acquired a penetrative S$_2$ foliation consisting of oriented mica and intergrown sillimanite and kyanite with flattened quartz together with staurolite and garnet porphyroblasts. Distinctive layers and lenses of kyanite + quartz + magnetite developed in the Manhattan Formation and very locally in the Hartland during D$_2$. Near ductile fault contacts the S$_2$ fabric is highly laminated with frayed and rotated mica and feldspar porphyroclasts, ribboned and locally polygonized quartz, lit-par-lit granitization, and quartz veins all developed parallel to the axial surfaces of F$_2$ folds. The D$_3$ folding event, a period of L-tectonism, smeared the previously flattened kyanite + quartz layers and lenses into elongate shapes parallel to F$_3$ axes in schistose rocks. Large porphyroblasts of tremolite pseudomorphic after diopside also show alignment parallel to F$_3$ hingelines in the Inwood Marble of northern Manhattan. Metamorphism associated with D$_3$ annealed and recrystallized the older D$_2$ mylonites in NYC (Merguerian 1988; Merguerian and Sanders 1998).

Preliminary Geological Map of the New York Botanical Garden

Found at the end of this paper in tabloid format Plates 1, 2 and 3 (two geological maps and a stop location and sample map) display our current view on the bedrock geology of the NYBG although we need a couple of more visits to finalize the maps. The maps show folded thrust slices of Manhattan (C-Om), Hartland (C-Oh), and Walloomsac (Ow) rocks in a complex pattern of steep to vertically inclined ductile faults which imbricate metamorphic rocks of identical steep to vertical orientation. The Manhattan is thrust against the Walloomsac (Ow) along the Saint. Nicholas thrust in the NW and W part of the park. Baskerville (1992) showed a thin belt of Manhattan against Inwood along an unnamed thrust did not recognize the belt of Walloomsac (where he mapped Manhattan) in the NW and W part of the park. (See Figure 4.) He also showed a broad belt of Hartland rocks thrust against Manhattan along Cameron's Line in the same area we place the Saint Nicholas thrust.

Hartland rocks (OCh in pink) are simply not where Baskerville shows them in the bulk of the park. Rather, based on our mapping the overall structure of the NYBG is synformal with Manhattan Schist at the center SW-plunging asymmetrical F$_3$ synform with gentle plunge but steep to vertical limbs overturned to the NW. The SE-limb of the synform is truncated by Cameron's Line (CL) near the course of the Bronx River where Hartland rocks were first detected by us in the Garden. They terminate to the SW in a vertical F$_2$ fold with NNE-trending subvertical axial surface. This structure is cut by the Saint Nicholas thrust toward the SE. The two shear zones are marked by imbricated lithologies and broad zones of mylonite ± migmatite and foliated granitoid (g). The granitoid in the SE portion of the park shows the effects of late syn-tectonic shearing at the juncture of the regional shears (SNT and CL) and shows brittle offset by NW-trending faults. Indeed, all of the bedrock units and ductile faults are cut by the NW-trending, right-lateral Mosholu fault and various splays showing minor left- and right lateral offset.

Brittle Faults in NYC

NYC Paleozoic cover rocks are cut by two main sets of brittle faults trending ~N30°E [paralleling the long axis of Manhattan] and those ranging from N20°W to N50°W with steep dips toward the SW [diagonally across Manhattan]. Proterozoic basement rocks show a more complex brittle fault history (Merguerian 2002b, 2004a). The NE-trending faults, which locally reactivate annealed ductile fault zones (Cameron's Line and the Saint Nicholas thrust), are steep-to vertical and show dominantly dip-slip slickenlines. The NW-trending faults are steep to moderate in dip (toward SW) and show complex movement dominated by strike-slip offset followed by dip-slip or oblique-slip reactivation. The NW-trending faults have produced map-scale offset and geomorphic evidence in the NYBG suggesting post-glacial ground effects.

North of NYC, contemporary seismicity along the NW-trending Dobbs Ferry fault in late October 1985 included two small (~4.0) tremors and many aftershocks. As shown in Figure 10, more robust earthquakes in and around the vicinity of NYC were recorded in 1884, 1783, and 1737. Unequivocal post-glacial ground rupture is difficult to demonstrate in NYC where most bedrock faults are (especially by seismologists) deemed to have formed at depth and then later elevated to the surface. Yet, the Bronx River, which formerly flowed SSW in an open valley underlain by the Inwood Marble belt shows diversion away from its "pirated" marble valley along the NW-trending right-lateral Mosholu fault, suggesting neotectonic displacement.

Merguerian and Sanders (1997) did not prove that the surface displacement of the bedrock near the East 204th Street bulge accompanied an earthquake generated by sudden slippage along the reactivated Mosholu fault nor did they prove that surface rupture took place. However, in many seismically active zones, surface displacement, such as the bedrock contour bulging mentioned above adjacent to the Mosholu fault, typically is associated with energetic earthquakes (e.g. – the Palmdale Bulge along the San Andreas fault in California).
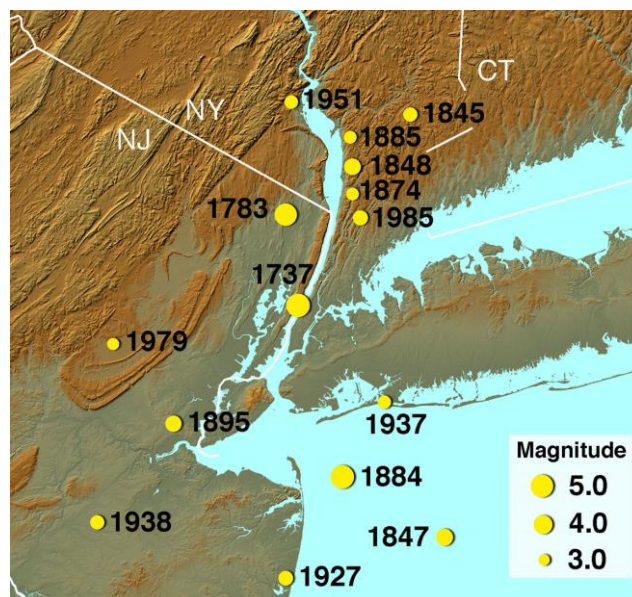

Figure 10 – Map showing historic seismic activity in the vicinity of New York City showing a diffuse zone of seismicity and the position of M3 and greater events before 1986. (From Bennington and Merguerian 2007.)

No observed surface rupture of crustal rocks has been previously reported in connection with any of NYC's strongest earthquakes of 1737 (~M5.2), 1783 (~M4.9), and 1884 (~M5.2). Yet, the August 1884 earthquake produced 4 m long by 3 m deep soil openings, cracked buildings and chimneys in Brooklyn and was felt over a hundred miles from the epicenter, which was located in the New York Bight. No historic earthquake has caused surface rupture of a fault anywhere along the east coast seismic zone. Equivalent shaking in NYC today would likely cause failure of older masonry walls, shatter glass windows in skyscrapers and rupture water and gas mains as soils liquefy and ground shaking ensues.

Because the contemporary stress regime in the lithosphere is oriented N60°E (Sykes et al. 2008), left-lateral offset might be expected in W- to NW-trending faults but NNW-trending faults might exhibit contemporary right-lateral offset. Given the modern stress regime, the presence of NNW- and NW-trending faults in the NYC area portend seismic risk. Knowing the history of time-separated moderate intensity seismic activity in New York City, the potential that a damaging earthquake may affect this densely populated area should not be ruled out. Because earthquakes **have** happened here, **can** happen here, and **will** happen here, effective pre-emptive planning to mitigate seismic hazards is an urban necessity.

Arm waving aside, the NW-trending fractures may be the result of Atlantic ocean ridge push with transcurrent and transform fracture propagation into the edge of the continental crust (Figure 11). This ridge-push model, proposed over twenty years ago at a GSA meeting while the audience snoozed and visited the rest rooms, is still suggested by us as a possible mechanism for neotectonic reactivation of these younger NW-trending brittle discontinuities.
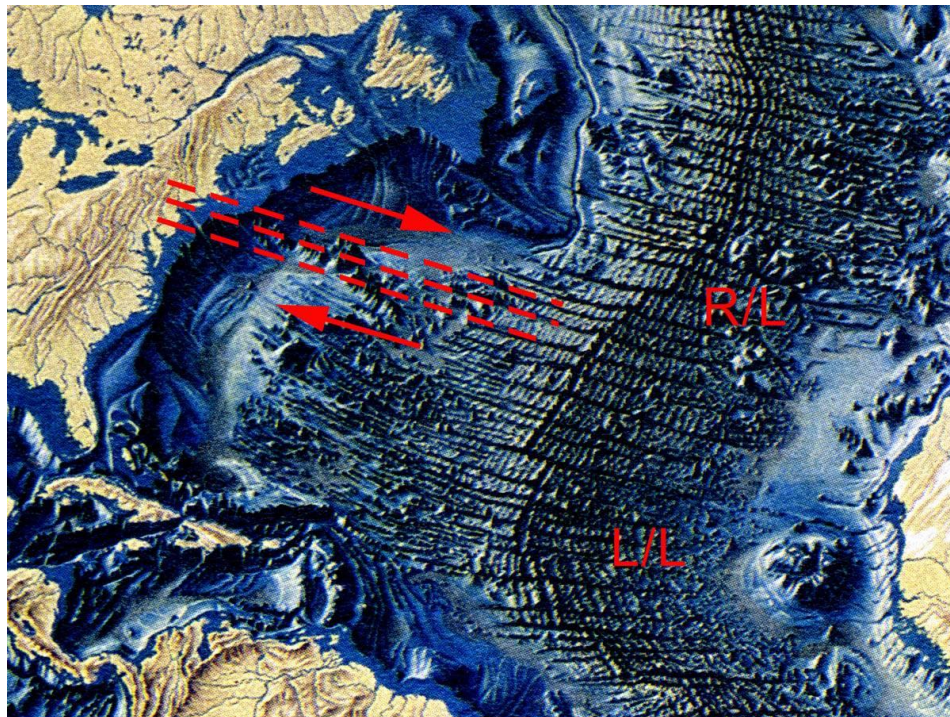
Figure 11 - Contemporary NYC seismicity seems to be localized along NW-trending brittle faults. As diagrammed above, the right-lateral and left-lateral offset sense of active NYC faults may be caused by offset along transcurrent faults that segment to mid-ocean ridge of the Atlantic Ocean basin. (Basemap from Heezen and Tharp, 1968.)

14

Acknowledgements

References Cited

Baskerville, C. A., 1992, Bedrock and engineering geological maps of Bronx County and parts of New York and Queens counties, New York: United States Geological Survey Miscellaneous Investigations Map I-2003, scale 1:24,000.

Baskerville, C. A.; and Merguerian, Charles, 1982, Tectonic history of the New York Metropolitan area (abs.): Empire State Geogram, Albany, N.Y., v. 18, p. 19, 43.

Baskerville, C. A.; and Merguerian, Charles, 1983, Stratigraphic differentiation in the Manhattan Schist, New York City (abs.): Geological Society of America Abstracts with Programs, v. 15, no. 3, p. 169.

Bennington, J Bret, and Merguerian, Charles, 2007, Geology of New York and New Jersey: Physical Geology Textbook Supplement: Thomson Brooks/Cole Company, 24 p.

Brock, Pamela Chase; Brock, Patrick W. G.; and Merguerian, Charles, 2001, The Queens Tunnel Complex: a newly discovered granulite facies Fordham orthogneiss complex that dominates the subsurface of western Queens: p. 1-8 *in* Hanson, G. N., *chm*., Eighth Annual Conference on Geology of Long Island and Metropolitan New York, 21 April 2001, State University of New York at Stony Brook, NY, Long Island Geologists Program with Abstracts, 128 p.

Dana, J. D., 1880, On the geological relations (sic) of the limestone belts of Westchester County, New York: American Journal of Science, 3rd series, v. 20, p. 21-32, 194-220, 359-375, 450-456; v. 21, p. 425-443; 1881, v. 22, p. 103-119, 313-315, 327-335.

Fuller, Tyrand; Short, Lesley; and Merguerian, Charles, 1999, Tracing the St. Nicholas thrust and Cameron's Line through The Bronx, NYC, p. 16-23 *in* Hanson, G. N., *chm*., Sixth Annual Conference on Geology of Long Island and Metropolitan New York, 24 April 1999, State University of New York at Stony Brook, NY, Long Island Geologists Program with Abstracts, 143 p.

Hall, L. M., 1968a, Times of origin and deformation of bedrock in the Manhattan Prong, p. 117-127 in Zen, Ean; White, W. S.; Hadley, J. B.; and Thompson, J. B., Jr., eds., Studies of Appalachian geology, northern and maritime: New York, Wiley-Interscience Publishers, 475 p.

Hall, L. M., 1968b, Geology in the Glenville area, southwesternmost Connecticut and southeastern New York, Section D-6, p. 1-12 in Orville, P. M., ed., Guidebook for field trips in Connecticut: New England Intercollegiate Geological Conference, Annual Meeting, 60th, New Haven, Connecticut, October 1968: Connecticut Geological and Natural History Survey Guidebook 2, not consecutively paginated.

Hall, L. M., 1968c, Trip A: Bedrock geology in the vicinity of White Plains, New York, p. 7-31 in Finks, R. M., ed., Guidebook to Field Excursions: New York State Geological Association Annual Meeting, 40th, Queens College, Flushing, New York, October 1968: Flushing, NY, Queens College Department of Geology, 253 p.

Hall, L. M., 1976, Preliminary correlation of rocks in southwestern Connecticut, p. 337-349 in Page, L. R., ed., Contributions to the stratigraphy of New England: Boulder, CO, Geological Society of America Memoir 148, 445 p.

Hall, L. M., 1980, Basement-cover relations (sic) in western Connecticut and southeastern New York, p. 299-306 in Wones, D. R., ed., International Geological Correlation Project, Proceedings, Project 27: The Caledonides in the U. S. A.: Blacksburg, VA, Virginia Polytechnic Institute and State University Department of Geological Sciences, Memoir 2, 329 p.

Mather, W. W., 1843, Geology of New York. Part I. Comprising (sic) the geology of the First Geological District: Albany, Carroll & Cook, Printers to the Assembly, 653 p., 46 pl. (Includes report of Prof. L. D. Gale on New York Island based on survey of 1828 and 1829.)

Merguerian, Charles, 1981a, Tectonic history of the New York City area (abstract): Empire State Geogram, v. 17, p. 28 (only).

Merguerian, Charles, 1983a, The structural geology of Manhattan Island, New York City (NYC), New York (abstract): Geological Society of America Abstracts with Programs, v. 15, p. 169 (only).

Merguerian, Charles, 1983b, Tectonic significance of Cameron's Line in the vicinity of the Hodges Complex--an imbricate thrust (sic) model for Western Connecticut: American Journal of Science, v. 283, p. 341-368.

Merguerian, Charles, 1984, Revised stratigraphy of the Manhattan Schist, New York City (abstract): Empire State Geogram, v. 20, p. 28-29.

Merguerian, Charles, 1994a, Stratigraphy, structural geology, and ductile- and brittle faults of the New York City area, p. 49-56 in Hanson, G. N., *chm.*, Geology of Long Island and metropolitan New York, 23 April 1994, State University of New York at Stony Brook, NY, Long Island Geologists Program with Abstracts, 165 p.

Merguerian, Charles, 1996c, Stratigraphy, structural geology, and ductile- and brittle faults of New York City, p. 53-77 in Benimoff, A. I. and Ohan A. A., *chm.*, The Geology of New York City and Vicinity, Field guide and Proceedings, New York State Geological Association, 68th Annual Meeting, Staten Island, NY, 178 p.

Merguerian, Charles, 1999a, Techniques of TBM tunnel mapping - the Queens Tunnel, NYC, p. 8-12 in Hanson, G. N., *chm.*, Sixth Annual Conference on Geology of Long Island and Metropolitan New York, 24 April 1999, State University of New York at Stony Brook, NY, Long Island Geologists Program with Abstracts, 143 p.

Merguerian, Charles, 2000a ms., Rock mass properties of the Queens Tunnel Complex: Duke Geological Laboratory Report QT0010, 257 p. + Geological Field Map Album, Scale 1"=10' (Stations 3+65 to 254+00).

Merguerian, Charles, 2002b, Brittle Faults of the Queens Tunnel Complex, NYC Water Tunnel #3: p. 63-73 in Hanson, G. N., *chm.*, Ninth Annual Conference on Geology of Long Island and metropolitan New York, 20 April 2002, State University of New York at Stony Brook, NY, Long Island Geologists Program with Abstracts, 116 p.

Merguerian, Charles, 2004a, Brittle fault chronology of New York City (NYC): Geological Society of America Abstracts with Programs, v. 36, no. 2, p. 73.

Merguerian, Charles, 2015b, Review of New York City bedrock with a focus on brittle structures; *p. 17-67 in Herman, G. C. and Macaoay Ferguson, S., eds.*, Geological Association of New Jersey Guidebook, Neotectonics of the New York Recess, 32nd Annual Conference and Field Trip, Lafayette College, Easton, PA, 214 p.

Merguerian, Charles; and Baskerville, C. A., 1987, The geology of Manhattan Island and the Bronx, New York City, New York, p. 137-140 in Roy, D. C., ed., Northeastern Section of the Geological Society of America, Centennial Fieldguide, v. 5, 481 p.

Merguerian, Charles; Baskerville, C. A.; and Okulewicz, S., 1982, Cameron's Line in the vicinity of New York City (abs.): Geological Society of America Abstracts with Programs, v. 14, p. 65.

Merguerian, Charles; and Merguerian, Mickey, 2004, Geology of Central Park – From rocks to ice: *in* Hanson, G. N., *chm.*, Eleventh Annual Conference on Geology of Long Island and Metropolitan New York, 17 April 2004, State University of New York at Stony Brook, NY, Long Island Geologists Program with Abstracts, 24 p.

Merguerian, Charles; and Merguerian, J. Mickey, 2012, Structural geology and metamorphism of the Inwood Marble, NYC, NY: Geological Society of America Abstract # 199974, Abstracts with Programs, v. 44, no. 2, p. 73.

Merguerian, Charles; and Merguerian, J. Mickey, 2014a, Stratigraphy, structural geology and rock mass properties of the Hartland Formation, Second Avenue Subway, NYC, NY: Geological Society of America Abstract # 235972, Abstracts with Programs, v. 46, no. 2, p. 90.

Merguerian, Charles; and Merguerian, J. Mickey; 2016a, Stratigraphy, structure and tectonics of New York City as viewed through its parks: p. 142-162 in Alexander A. Gates and J Bret Bennington, *eds.*, Geologic diversity in the New York metropolitan area, New York State Geological Association, 88th Field Conference, 30 September - 02 October 2016; 446 p.

Merguerian, Charles; and Merguerian, J. Mickey; 2016b, Trip A-5 - Field guide to Isham, Inwood, and Central parks, NYC, NY: p. 163-189 in Alexander A. Gates and J Bret Bennington, *eds.*, New York State Geological Association, 88th Field Conference, 30 September - 02 October 2016; 446 p.

Merguerian, Charles and Merguerian, J. Mickey, 2024a, From Rocks to Ice: Geology of the NY Botanical Garden, Bronx, NY; Guidebook for Long Island Association of Professional Geologists Field Trip, 06 April 2024, 50 p.

Merguerian, Charles; Merguerian, J. Mickey; and Cherukupalli, Nehru, E., 2011, Stratigraphy, structural geology and metamorphism of the Inwood Marble Formation, northern Manhattan, NYC, NY: *in* Hanson, G. N., *chm.*, Eighteenth Annual Conference on Geology of Long Island and Metropolitan New York, 09 April 2011, State University of New York at Stony Brook, NY, Long Island Geologists Program with Abstracts, 19 p.

Merguerian, Charles; and Moss, C. J., 2005, Newly discovered ophiolite scrap in the Hartland Formation of midtown Manhattan: *in* Hanson, G. N., *chm.*, Twelfth Annual Conference on Geology of Long Island and Metropolitan New York, 16 April 2005, State University of New York at Stony Brook, NY, Long Island Geologists Program with Abstracts, 8 p.

Merguerian, Charles; and Moss, C. J., 2006a**,** Structural implications of Walloomsac and Hartland rocks displayed by borings in southern Manhattan: *in* Hanson, G. N., *chm.*, Thirteenth Annual Conference on Geology of Long Island and Metropolitan New York, 22 April 2006, State University of New York at Stony Brook, NY, Long Island Geologists Program with Abstracts, 12 p.

Merguerian, Charles; and Moss, C. J., 2007, Newly discovered serpentinite bodies associated with the St. Nicholas thrust zone in northern Manhattan: *in* Hanson, G. N., *chm.*, Fourteenth Annual Conference on Geology of Long Island and Metropolitan New York, 14 April 2007, State University of New York at Stony Brook, NY, Long Island Geologists Program with Abstracts, 13 p.

Merguerian, Charles and Moss, C. J., 2015, Structural geology and metamorphism of the World Trade Center Site: *in* Hanson, G. N., *chm.*, Twenty-second Annual Conference on Geology of Long Island and Metropolitan New York, 11 April 2015, State University of New York at Stony Brook, NY, Long Island Geologists Program with Abstracts, 12 p.

Merguerian, Charles; and Sanders, J. E., 1991b, Trip 16: Geology of Manhattan and the Bronx, 21 April 1991: New York Academy of Sciences Section of Geological Sciences Trips on the Rocks Guidebook, 141 p.

Merguerian, Charles; and Sanders, J. E., 1993a, Geology of Cameron's Line and the Bronx Parks: Guidebook for On-The-Rocks 1993 Fieldtrip Series, Trip 26, 08 May 1993, Section of Geological Sciences, New York Academy of Sciences, 103 p.

Merguerian, Charles; and Sanders, J. E., 1996a, Diversion of the Bronx River in New York City - evidence for postglacial surface faulting?, p. 131-145 *in* Hanson, G. N., *chm*., Geology of Long Island and metropolitan New York, 20 April 1996, State University of New York at Stony Brook, NY, Long Island Geologists Program with Abstracts, 177 p.

Merguerian, Charles; and Sanders, J. E., 1996b, Contrasting styles of the Taconic orogeny in New York: deep- vs. shallow thrusts, p. 116-130 *in* Hanson, G. N., *chm*., Geology of Long Island and metropolitan New York, 20 April 1996, State University of New York at Stony Brook, NY, Long Island Geologists Program with Abstracts, 177 p.

Merguerian, Charles; and Sanders, J. E., 1997, Bronx River diversion: neotectonic implications (abs.): Paper No. 198, p. 710 *in* Hudson, J. A. and Kim, Kunsoo, *eds.*, International Journal of Rock Mechanics and Mining Sciences, Special Issue, 36th U.S. Rock Mechanics Symposium, Columbia University, New York, June 29-July 02, 1997, v. 34, no. 3/4, 714 p. Full version on CD-ROM, 10 p.

Merguerian, Charles; and Sanders, John E., 1998, Annealed mylonites of the Saint Nicholas thrust (SNT) from a new excavation at the New York Botanical Gardens, The Bronx, New York: p. 71-82 *in* Hanson, G. N., *chm*., Geology of Long Island and metropolitan New York, 18 April 1998, State University of New York at Stony Brook, NY, Long Island Geologists Program with Abstracts, 161 p.

Merrill, F. J. H., 1890, On the metamorphic strata of southeastern New York: American Journal of Science, 3rd series, v. 39, p. 383-392.

Merrill, F. J. H.; Darton, N. H.; Hollick, Arthur; Salisbury, R. D.; Dodge, R. E.; Willis, Bailey; and Pressey, H. A., 1902, Description of the New York City district: United States Geological Survey Geologic Atlas of the United States, New York City Folio, No. 83, 19 p. (Includes colored geologic map on a scale of l:62,500).

Moore, J. C. and Karig, D.E., Sedimentology, structural geology, and tectonics of the Shikoku subduction zone, southwestern Japan: Geological Society of America Bulletin, v. 87, p. 1259-1268.

Mose, D. G.; and Merguerian, Charles, 1985, Rb-Sr whole-rock age determination on parts of the Manhattan Schist and its bearing on allochthony in the Manhattan Prong, southeastern New York: Northeastern Geology, v. 7, no. 1, p. 20-27.

Rowley, D. B., and Kidd, W. S. F., 1981, Stratigraphic relationships and detrital composition of the Medial (sic) Ordovician flysch of western New England: Implications for the tectonic evolution of the Taconic orogeny: Journal of Geology, v. 89, p. 199-218.

To Cite this extended abstract:
Merguerian, Charles and Merguerian, J. Mickey, 2024b, Stratigraphy, structure and tectonic implications of the New York Botanical Garden, Bronx, NY: *in* Jaret, S. L., *chm*., Thirty-first Annual Conference on Geology of Long Island and Metropolitan New York, 13-14 April 2024, State University of New York at Stony Brook, NY, Long Island Geologists Program with Abstracts, 22 p.

Petrography New York Botanical Garden

N0910	NYBG Stop 17	COm	Myl pg bio qtz musc kf gt gneiss	massive; flaser
N0911	NYBG Stop 21	g	Pg qtz bio musc foliated granitoid	small sample
N0912	NYBG Stop 33	COma	Hbl pg qtz op amphibolite	blackish, dense; tr bio, trem
N0913	NYBG Stop 42	COm	Mig pg qtz bio musc kf gt gneiss	dissem kf; late idio musc
N0914	NYBG Stop 45	COm	Mig pg qtz bio musc kf gt gneiss	mixed w/ Ow?; some rb-bio; kf in mig sweats
N0915	NYBG Stop 49	COm	Myl pg bio qtz gt kf gneiss	
N0916	NYBG Stop 50	COm	Pg qtz bio musc gt gneiss	
N0917	NYBG Stop 58	COm	Mig pg qtz bio gt gneiss	
N0918	NYBG Stop 57	Ow	Pg bio qtz gt ky py grph tour granofels	rb-bio; pale pink gt; fissile; v. fine textured
N0919	NYBG Stop 61	COma	Hbl (75) pg op qtz amphibolite	Blackish, dense
N0920	NYBG Stop 64	COm	Myl pg bio qtz musc ky gt apa gneiss	tr kf, chl; late idioblastic musc and bio; frayed musc
N0921	NYBG Stop 66	COm	Pg bio qtz musc gt gneiss	
N0922	NYBG Stop 70	OCh?	Bio musc pg qtz gt schist	1 cm musc pseudos after ky
N0923	NYBG Stop 78	Ow	Pg qtz bio py grph tour granofels	rb-bio; abundant py; zoned tour; fine textured
N0924A	NYBG Stop 79	Com	Pg bio qtz musc gt gneiss	fine textured; late idioblastic musc and bio
N0924B	NYBG Stop 79	COm	Pg qtz bio musc gt gneiss	gt porphs; ky? or sill?
N0924C	NYBG Stop 79	g/s	Sillimanite nodule near granitoid	in OZm
N0925	NYBG Stop 82	OCh	Pg qtz bio ky gt sill musc gneiss	lustrous; ky clusters w/ bio
N0926	NYBG Stop 83	OCh	Qtz pg bio musc gt granofels	foliated
N0927	NYBG Stop 86	COm	Myl bio qtz musc pg ky gt tour gneiss	
N0928	NYBG Stop 89	COm	Mig pg qtz bio musc gt schist	some kf in sweats
N0929	NYBG Stop 97	Ow	Pg bio qtz kf musc grph gt granofels	rusty weath; pale pink gt; rb-bio; mosaic texture
N0930A	NYBG Stop 28	Ow	Bio pg qtz musc grph gt schist	rusty weath; pale pink gt; rb-bio
N0930B	NYBG Stop 28	Ow	Pg qtz musc bio gt grph granofels	rusty weath; pale pink gt; rb-bio
N0931	NYBG Stop 74	COm	Qtz pg bio musc gt gneiss	red gt; khaki br bio; massive
N0932	NYBG Stop 100	COm	Myl pg qtz bio musc gt gneiss	red gt; musc porphs
N0933A	NYBG Stop 102	OCh	Pg qtz bio musc granofels	foliated granitoid layer?
N0933B	NYBG Stop 102	OCh	Mig musc pg qtz bio gt schist	red gt
N0934	NYBG Stop 103	Ow	Myl pg bio qtz musc gt py grph granofels	rusty weath; pale pink gt; rb-bio; fine textured; op rich
N0935	NYBG Stop 105	Ow	Mig musc bio qtz pg gt schist (OCh?)	rb-bio layers w/ gts; little opaques; no grph
N0936	NYBG Stop 109	Ow	Myl pg qtz bio musc gt py grph granofels	rusty weath; pale pink gt; rb-bio

TABLE 1
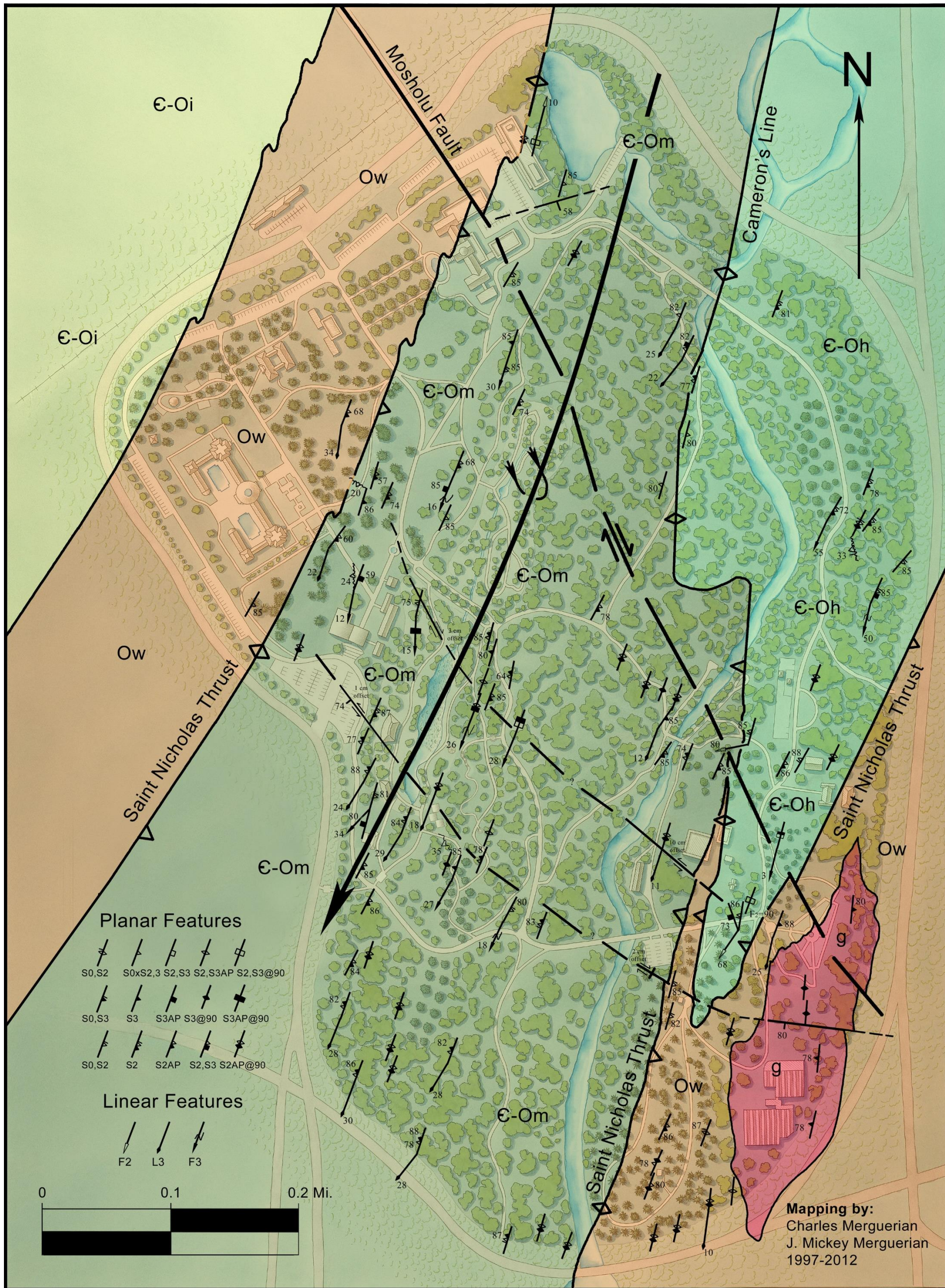
Plate 1 – Preliminary geological map of the New York Botanical Garden showing the ductile faults (Cameron's Line and Saint Nicholas thrust) and brittle faults including the Mosholu fault, associated splays and other mapped brittle faults. Units – Є-Oi = Inwood Marble, Ow = Walloomsac Formation, Є-Om = Manhattan Formation, Є-Oh = Hartland Formation, g = foliated late syn-tectonic granitoid. Foliation and bedding (planar features) and fold axes and lineations (linear features) symbols explained in legend with dip and plunge values plotted. Map scale synformal NW-vergent F_3 axial surface trace shown. See Plate 2 for structural contacts and field data plotted on non-colored park trail map and Plate 3 for sample and stop locations on park trail map. Basemap courtesy NYBG.

N

Mosholu Fault

Cameron's Line

Saint Nicholas Thrust

Saint Nicholas Thrust

Є-Oi

Ow

Є-Oi

Ow

Ow

Є-Om

Є-Om

Є-Om

Є-Om

Є-Oh

Є-Oh

Є-Oh

Ow

g

g

Planar Features

S0,S2	S0xS2,3	S2,S3	S2,S3AP	S2,S3@90

S0,S3	S3	S3AP	S3@90	S3AP@90

S0,S2	S2	S2AP	S2,S3	S2AP@90

Linear Features

F2	L3	F3

0   0.1   0.2 Mi.

Mapping by:
Charles Merguerian
J. Mickey Merguerian
1997-2012

Plate 2 – Uncolored preliminary geological map of the New York Botanical Garden showing the ductile faults (Cameron's Line and Saint Nicholas thrust) and brittle faults including the Mosholu fault, associated splays and other mapped brittle faults. Units - Є-Oi = Inwood Marble, Ow = Walloomsac Formation, Є-Om = Manhattan Formation, Є-Oh = Hartland Formation, g = foliated late syn-tectonic granitoid. Foliation and bedding (planar features) and fold axes and lineations (linear features) symbols explained in legend with dip and plunge values plotted. Map scale synformal NW-vergent F3 axial surface trace shown. See Plate 3 for sample and stop locations plotted on park trail map. Basemap courtesy NYBG.

21

Plate 3 – NYBG trail map showing sample locations and stop localities used in production of the geological maps. (See Plates 1 and 2.) Basemap courtesy NYBG.

Title: BeachCam monitoring of shoreline dynamics.

Authors: Anna Crouse[1], Kathleen Fallon[2] and Henry Bokuniewicz[1]
[1] School of Marine and Atmospheric Science
Stony Brook NY
[2] New York Sea Grant Institute
Stony Brook New York

Abstract: Long-term periodic monitoring on New York's ocean shoreline showed that, despite waxing and waning in the course of any year, beaches have maintained a stable average width between about 200 and 300 feet. To examine the shorter-term patterns of change in the beach width, a camera was used to monitor a location along the New York Ocean shoreline. Images were calibrated to allow beach widths to be determined. Beach widths measured at low tide varied between less than 60 feet to more than 175 feet between January and August,2023. A pattern of modulation showed a quasi-cyclical behavior with periods between 5 and 15 days. This seems consistent with the classic synoptic periods of between two and seven days for the passage of mesoscale weather systems. Large variations seem to coincide with high low wave activity monitored 30 nautical miles south of Long Island (NOAA station 44025) as represented by a "profile parameter"[1] taking into account wave height, period and sediment settling speed. Conversely, beach widths increased at a rate of about 2.5 feet per week as wave activity decreased over the summer.

[1] Dalrymple R.A., 1992. Prediction of storm/normal Journal of Waterway, Port, Coastal, and Ocean Engineering 118: 193-200.

Point of contact: henry.bokuniewicz@stonybrook.edu

Greenhouse Phase Implications To Non-Indigenous Marine Life: Migrations In The New York Bight And Hudson River

Epstein, S.,[1] Epstein, P., and Sassen R.
Geoval Consultants LLC, Sassen Geocatalysts

Epstein.samuel58@gmail.com

Over the past 60 years' modern sedimentary depositional environments have been extensively studied in order to interpret the ancient rock record. Conversely, ancient reconstructed paleo-environments are studied in respect to climate in order to help model current and future climate changes.

In 2006 the authors published a paper (2006) on the observance of a spot-fin butterfly fish indigenous to Florida and Caribbean situated in the N.Y. Bight shallow shelf of Rockaway Beach, Queens. The spot-fin was part of eddies offshoots from the Gulf Stream, 150 miles to the east

Over the past 7 years a noticeable migration of warm water non-indigenous animal life is occurring in the same Queens waters, including spinner and reef sharks, turtles, pods of dolphins, humpback whales (spotting went from 5 to 250 per season). Additionally, the spot-fin butterfly fish now occurs further inland in Jamaica Bay, between the Rockaway Peninsula and the open Atlantic Ocean. The migration of marine animal life can be primarily attributed to New York State banning the harvesting of Menhaden, an oil rich bait fish 13 inches long. Large bait balls occur in the NY harbor well as large schools off Rockaway Beach. Additional factors may include over a 25-year period (1973-1998) increase in dissolved oxygen and the reduction of coliform bacteria in the lower Hudson River estuary, New York Harbor. Phytoplankton and zooplankton are primary food for the Menhaden for the large predatory marine life and birds.

An Identified threat to the marine and bird life of Rockaway Beach and further to the east on Southern Long Island (Long Beach, Atlantic Beach etc.,), is the occurrence of a significant dumpsite `12 miles from the Rockaway Beach and 6 miles from Sandy Hook New Jersey. High levels of total organic carbon, various organic compounds hydrocarbon derived along with low pH and high Eh levels, along with hydrogen sulfide, suggest an oxygen reducing environment. Recent sub-bottom photographs over 4 years (1998-2002) suggest repopulation of epifauna and benthonic fauna.

Sub-bottom floatation studies along with shear velocity lift capabilities suggest the dump site located in 20 m of water is within an area of high probability (80%) of resuspension during storms, and offer a threat to the shallow waters and coastal beaches.

 The predicted temperature increase to 2100 of 4 degrees (f) may alter the annual summer-winter thermocline positioning of upwelling cycles.

The effects of the resuspension of the chemical and organic waste would probably effect the animal life for a relative short duration due to the efficient annual cool pool circulation patterns on the shelf.

Crocodilians genus demonstrate maximum numbers during the Triassic, Late Cretaceous, Miocene, and Eocene. The question remains are we approaching a cycle maximum in biodiversity(Genera) during the Phanerozoic preceding a major (5 in past), or minor (5 in past) extinction event.

Shedding light on Long Island's glacial history: A luminescence dating approach aimed to involve undergraduate students in field- and laboratory-based research.

Grandfield, T.[1], and Frouin, M.[1,2].
[1] Stony Brook University, Department of Geosciences
[2] Turkana Basin Institute
Taylor.grandfield@stonybrook.edu

The upper portion of Long Island's, geological layers formed during the Wisconsin Glacial Episode (from ~95 to 11,000 years ago) as the Laurentide Ice Sheet retreated. The Ronkonkoma moraine lies at the south shore of LI and is thought to have been the terminus of the ice sheet deposited ~20,000 years ago [1]. Northwards, the Harbor Hills moraine is assumed to have formed later during glacial retreat. Cosmogenic nuclide dating of boulders suggests that the Harbor Hills moraine was deposited after 18 ka [2-3]. However, based on recent measurements of till directions and bedrock orientation [4], it is possible that the HH moraine was deposited as early as 20,000 years ago. Previously research on the glacial history of Long Island have primarily focused on the nature and structure of the deposits. Yet, little work has been done to directly date the moraines and constrain the timing of formation across Long Island.

The luminescence dating technique is a robust tool for late quaternary deposits. It measures the amount of time since sediments were last exposed to light [5]. Our project aims to directly date glacial sediment deposits using the luminescence dating technique and provide the first comprehensive chronology of glacial deposition across Long Island, NY.

The location of the Luminescence dating research laboratory at Stony Brook University provides unique research opportunities to undergraduate students from field surveys to age determination.

During the presentation, the principle of the luminescence dating will be presented, preliminary luminescence dating results will be discussed, and we will describe our efforts to involve undergraduate students in research projects.

[1] Sirkin, L., 1982, Wisconsinan glaciation of Long Island, New York to Block Island, Rhode Island, in Larson, G.J., Stone, B.D., eds. Late Wisconsinan glaciation of New England: Kendall/Hunt.

[2] Das, S., Origin and Evolution of Dry Valleys South of Ronkonkoma Moraine, M.S. Thesis, Stony Brook University, 2007.

[3] McCabe, M., Kelly, M. A., Schaefer, J. M., Schwartz, R., Hanson, G. N., and Benimoff, A. I., 2006, Dating glacial features in New York's Lower Hudson Valley - The last deglaciation of the Eastern Laurentide Ice Sheet: Geological Society of America Abstracts with Programs, 38, no. 7, p. 72.

[4] Sanders, J. E., and Merguerian, Charles, 1994b, The glacial geology of New York City and vicinity, p. 93-200 in A. I. Benimoff, ed., The Geology of Staten Island, New York, Field guide and proceedings, The Geological Association of New Jersey, XI Annual Meeting, 296 p.

[5] Aitken, M.J., 1998. An introduction to optical dating -The dating of quaternary sediments by the use of photon-stimulated luminescence. Oxf. Univ. Press 266.

High-Frequency of Groundwater Level Fluctuations, Underground Erosion, Potential Sinkhole Occurrences Across Long Island, NY

Hope, J. H.[1], Marsellos, A. E.[1], and Tsakiri, K. G.[2]

[1]*Dept. Geology, Environment, and Sustainability, Hofstra University, Hempstead, NY*
[2]*Dept. Information Systems, Analytics, and Supply Chain Management, Rider University, Lawrenceville, NJ*
*jhope3@pride.hofstra.edu*

Abstract

Sinkhole formations pose significant hazards to infrastructure and safety, with Long Island, NY experiencing a recent surge in such occurrences. This paper investigates the potential correlation between high-frequency groundwater level (GWL) fluctuations and accelerated underground erosion, leading to sinkhole formation. Utilizing statistical analyses of GWL data from USGS monitoring stations, we identify locations exhibiting various GWL fluctuations across Long Island. While the results do not indicate a strong correlation between high-frequency GWL fluctuations and sinkhole occurrences on an individual basis, regions characterized by predominantly high-frequency GWL oscillations tend to have a higher incidence of sinkhole formations. This study provides insights into the factors contributing to sinkhole occurrences on Long Island and underscores the importance of further research in understanding and predicting such phenomena related to oncoming warmer temperatures and underground water mobility upon intensive climate change.

Introduction

Groundwater is defined as water which is located underground in between sediment particles and the zones of porous sediments are called aquifers. Subsequently, most of Long Island's freshwater supply comes from pumping these underground aquifers. The groundwater level (GWL) fluctuations occur naturally due to various factors including seasonal changes, precipitation levels, and also human activity (Tamiru et al. 2018).

Underground erosion occurs when groundwater is able to break down sediment particles, which creates fractures and leads to further erosion. When there is an abundance of underground erosion, fractures will expand until the groundwater reaches a non-porous layer of sediments. Sinkholes form where the sediment layers below the surface undergo chemical weathering, or dissolution, due to groundwater movement from surface water or precipitation. (Matthew, 2018). Typically, rocks such as limestone are naturally dissolved by underground water circulation. Eventually, the surface above the underground eroded area becomes destabilized and collapses inwards, creating a sinkhole.

New York's Long Island landscape was formed from the outwash of glacial sediments, specifically quartz, clay, silt, sand and gravel deposits. The Upper Glacial Aquifer on Long Island is the closest aquifer to the surface and is composed of porous sands and pebble sediments. (Monti, J. et al. 2006) The water table is found within the top of the Upper Glacial Aquifer (Figure 1).
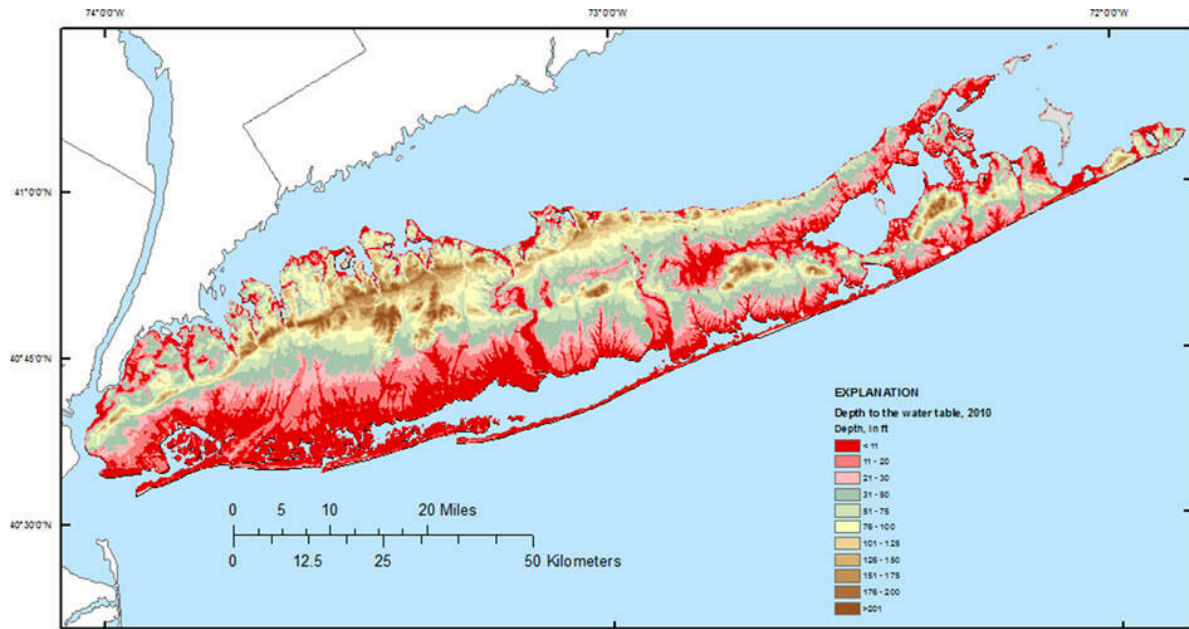
Figure 1. USGS map of the depth to the water table in feet on Long Island, NY 2010 (Como et al. 2013).

Figure 2. A Google Earth map showing the locations of sinkhole formations from 2013-2023 on Long Island, NY. Location data was sourced from local news reports.

Several local news outlets have recorded multiple sinkhole occurrences on Long Island in the past 10 years, most reports within the last year (Figure 2). Some of these formations were recorded to be as much as 20 ft deep (Table 1). Sinkholes often cause the destruction of highways, roads, public and privately owned properties, and are hazardous to be around. As such, the cost of repairing damages from sinkhole formations is very high.

Table 1. Sinkhole formations on Long Island 2013-2023 and their respective locations and depths.

Sinkhole	Longitude	Latitude	Year	Depth (ft)
1) Huntington Station	-73.411268°	40.853503°	2023	6
2) Bay Ridge	-74.018219°	40.633155°	2024	20
3) Islip	-73.235022°	40.740219°	2014	12
4) Elmont	-73.712909°	40.700940°	2023	9
5) West Hempstead	-73.650142°	40.704847°	2023	6
6) Baldwin	-73.610711°	40.671756°	2023	n/a
7) Oceanside	-73.633872°	40.645077°	2023	20
8) Lido Beach	-73.629828°	40.587992°	2023	20

Not a lot of previous research has been conducted on the occurrences of sinkholes on Long Island specifically. Most of the sediment on Long Island is mostly Cretaceous sands, gravels and clay (Cohen, 2014). Usually, sinkholes are associated with karst topography and soluble rock types such as limestone or marble. Previous research focusing on GWL oscillations to identify underground erosion and sinkhole formations has also not been widely studied. A study done in 1997 concluded that groundwater oscillations are one of the main causes of sinkholes in karst (Roje-Bonacci, 1997) but this study does not investigate observations of high GWL oscillations promoting underground erosion.

In this investigation, we introduce a new hypothesis stating that groundwater stations exhibiting high frequencies of GWL oscillations is an identifier of accelerated underground erosion, and thus an area prone to occurrences of sinkhole formations across Long Island, New York.

Methods

To analyze groundwater level (GWL) oscillation frequencies, we utilized advanced statistical analysis techniques using the R programming language. The GWL data from the United States Geological Survey (USGS) was downloaded from 58 USGS monitoring stations at various distances from the previous sinkhole occurrences across Long Island, New York (Figure 3). A map showing the locations of sinkhole occurrences on Long Island, New York during the past 10 years was created in Google Earth Pro by using local news reports/sightings of sinkholes to specify location (Figure 2).

A moving average is a statistical calculation which creates a series of averages within different subsets of a whole dataset. This calculation is used to smooth short-term fluctuations and highlight long-term data trends. We also subtracted the moving average from the raw GWL dataset, specifically using a window of 27 days applied three times (27, 3) to filter out moon-tide related cycles and other noise, and focus on short-term data trends.

The Kolmogorov-Zurbenko (KZ) filter, known as the running mean filter, is a smoothing statistical technique that filters time-series data. It is particularly useful for smoothing noise from data while simultaneously preserving the tails of data distributions. We used the KZ filter from the kza package in R (Close et al. 2020) to remove noise and smooth our GWL data without altering the original dataset. This also allowed a more precise analysis of the high-frequency GWL oscillations.

A periodogram time-series analysis (TSA) is a statistical tool used to identify the dominant frequencies in a dataset. It can be helpful in situations when trying to identify dominant cyclical patterns within a noisy dataset. We used this analysis technique in R to identify the high-frequency GWL oscillation from the USGS groundwater stations on Long Island by plotting $\frac{1}{frequency}$ to show periods. The maximum period of GWL fluctuations observed on each of the USGS stations was detected. Projection of the maximum periods at all monitoring stations created a GIS map (Figure 3) with red being the wells showing high-frequency fluctuations and blue dots for those of low-frequency groundwater level fluctuations. The GIS map was composed in R utilizing the packages sf (Pebesma & Bivand, 2023) and ggspatial (Dunnington, 2023) to input and process shapefiles, ggplot2 (Wickham, 2016) to plot the GIS map, and celestial (Robotham, 2018) to retrieve latitude and longitude of the stations.

Results:

Based on the media reports and news about sinkhole occurrences, we have gathered a list of recent sinkholes (Table 1) that occurred mostly at the southern Long Island with few exceptions. Time series analysis of the groundwater stations has detected high-frequency (red dots) and low-frequency (blue dots) GWL oscillations across Long Island (Figure 3). We observe a moderate spatial correlation between stations showing high-frequency GWL oscillations and the occurrence of sinkhole formations mapped in Figure 2 and 3.
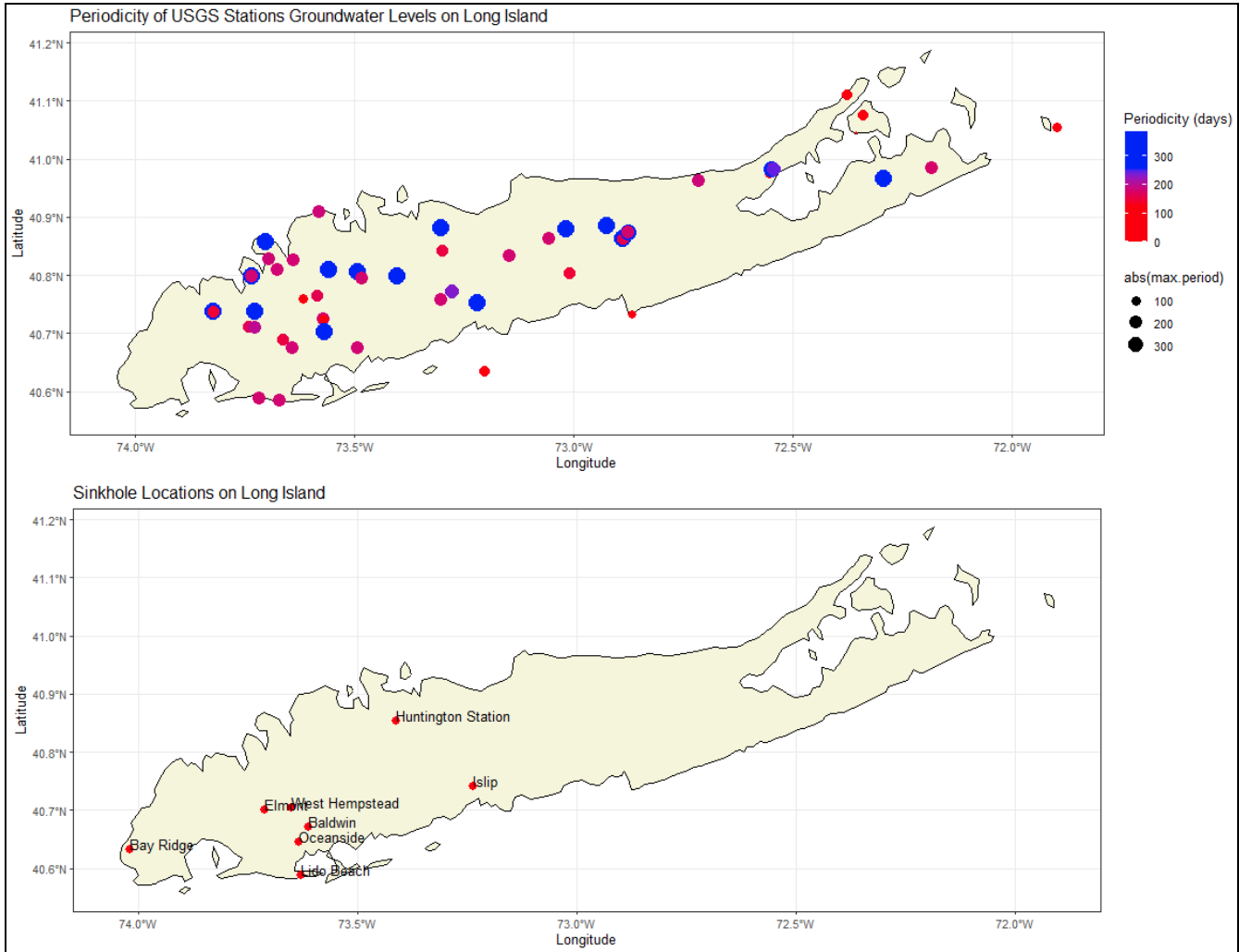
Figure 3. (Top) A GIS map showing the periodicity in days of USGS stations GWL across Long Island, NY. Higher frequency of GWL oscillations indicate lower periodicity (red dots). (Bottom) A map of the sinkhole locations from Table 1 across Long Island, NY.

Discussion

Observing the depth to the water table on Long Island (Figure 1) and the map of sinkhole formations (Figure 2 and 3) we can see that most of the sinkholes that were formed occurred in areas where the depth to the water table was less than 30 ft below the surface. A low depth to water table surface is more likely to be vulnerable to contamination from salt water intrusions or flooding due to high precipitation. Due to these natural factors that influence fluctuations of

GWL, we can relate the occurrences of sinkhole formation to areas where the depth to the water table is shallow on Long Island.

We observe a slight linear pattern among the sinkhole formations mapped in Nassau County between 2013-2023 (Figure 2). The reason for this is not quite clear. When looking for any structural formations which could influence the occurrence of sinkholes like fault lines, none appeared in any previous record. The two moraines on Long Island, Ronkonkoma and Harbor Hill, form east to west across the northern portion of Long Island's landscape, not in the southern part. The pattern of sinkholes occurring in north-south lineation may suggest more anthropogenic influenced formation.

Comparing depth to the water table (Figure 1) and the periodicity of the GWL from the USGS stations (Figure 3) we observed that at lower depths we find lower periodicity of GWL. This would suggest that the higher frequency GWL fluctuations are located at more shallow depths from the surface to the Upper Glacial aquifer. We can also use this relationship to identify a higher rate of underground erosion at these shallow depth, low periodicity stations. These areas should be marked for further study due to any climatic conditions influencing GWL fluctuations to prevent flooding or sinkhole hazards.

Looking at the formation of sinkholes across Long Island and the USGS groundwater stations exhibiting low periodicity of GWL (Figure 3) we observed that the locations of sinkholes from 2013-2023 are slightly related to the locations of low periodicity GWL stations, particularly near the Elmont and West Hempstead sinkholes. This would support our hypothesis that the formation of sinkholes are related to high frequency GWL oscillations. The oscillation describes the number of days in which the GWL fluctuates. A higher periodicity indicates GWL fluctuations are less frequent and more gradual in a given time. A lower periodicity indicates GWL fluctuations are more frequent in a given time. This also indicates a higher frequency of oscillation. From our results, we observed that the occurrence of sinkhole formation across Long Island slightly relates to the location of high frequency GWL oscillations.

Conclusion

Long Island's sinkhole occurrences have not been sufficiently investigated in recent years. The influence of anthropogenic activity on the occurrence of sinkhole formations is still a topic needing further investigations. We can conclude there is a distinct relationship between the depth to the water table and sinkhole formations from 2013-2023 across Long Island with most of the sinkhole formations occuring where water table is closer to the surface that is at the south area of Long Island with few exceptions. We can also conclude that high-frequency oscillations of GWL occur at shallower depths of the water table on Long Island. This supports our hypothesis on identifying accelerated underground erosion. Lastly, we can confirm that the occurrence of sinkhole formations are somewhat related to the USGS groundwater stations exhibiting high frequency GWL oscillations. From our results, we can predict the relative location of future sinkhole formations by looking at the USGS stations showing high frequency GWL oscillations. Future investigations into other areas with sinkhole formations would provide a more coherent result for our hypothesis.

Credit Authorship Contribution Statement:

Hope, J.H: writing – Introduction, Methods, Results, Discussion & Conclusion. Data analysis and R-coding practicing, reference citations, cartography, editing, formatting. Marsellos, A.E: writing – Abstract. Supervision, editing, GIS mapping, R-coding guidance. Tsakiri, K.G: R-code/providing additional insights to KZ filter for data processing.

References

Close B., Zurbenko I., Sun M. (2020). kza: Kolmogorov-Zurbenko Adaptive
     Filters_. R package version 4.1.0.1, https://CRAN.R-project.org/package=kza
Cohen, Phoebe. (2014) "Geological History of Long Island |." *Williams Sites*, 15 March 2014,
     https://sites.williams.edu/geos101/mid-atlantic/geological-history-of-long-island/
Como, M.D. et al. (2013). "Water-table and Potentiometric-surface altitudes in the Upper
     Glacial, Magothy, and Lloyd aquifers beneath Long Island, New York, April-May 2010"
     New York Water Science Center, 10.3133/sim3270
Dunnington D. (2023). _ggspatial: Spatial Data Framework for ggplot2_. R package
     version 1.1.9, https://CRAN.R-project.org/package=ggspatial
Kennedy, Sean. "Three sinkholes emerge in two months | Herald Community Newspapers."
     LIHerald, 7 August 2023,
     https://www.liherald.com/stories/three-sinkholes-emerge-in-two-months,187898.
     Accessed 2 March 2024.
Krauth, Dan. "Repairs underway after broken sewer line causes 20-foot-deep sinkhole in Bay
     Ridge, Brooklyn." *ABC7 New York*, 2 January 2024,
     https://abc7ny.com/20-foot-sinkhole-bay-ridge-brooklyn-broken-sewer/14260368/.
     Accessed 29 March 2024.
Matthew C.D, Adam M. M.(2018), "Sinkhole formation mechanisms and geostatistical-based
     prediction analysis in a mantled karst terrain", CATENA, Volume 165, 2018, Pages
     333-344, ISSN 0341-8162, https://doi.org/10.1016/j.catena.2018.02.010
Monti, J. et al. (2006) "Water Table and Potentiometric Surface Altitudes in the Upper Glacial,
     Magothy, and Lloyd Aquifers beneath Long Island, New York, March-April 2006." *New
     York Water Science Center*,
     https://ny.water.usgs.gov/archived_files/projects/gisunit/Long_Island_SIM3066_Handout
     .pdf.
NBC New York. "Long Island Recovers After Storm Dumps Record-Setting Rain, Causes
     Flooding." 14 August 2014,
     https://www.nbcnewyork.com/news/local/storm-cleanup-islip-record-rainfall-long-island-
     bay-shore-suffolk-nassau-ny/. Accessed 2 March 2024.
News 12. "New sinkhole brings traffic to a halt on Oceanside roadway." *News 12 - Long Island*,
     30 July 2023,
     https://longisland.news12.com/new-sinkhole-brings-traffic-to-a-halt-on-oceanside-roadw
     ay. Accessed 29 March 2024.
Pebesma, E., Bivand, R. (2023). Spatial Data Science: With Applications in R.
     Chapman and Hall/CRC. https://doi.org/10.1201/9780429459016
Robotham, A. (2018). "celestial: Collection of Common Astronomical Conversion Routines and

Functions." R package version 1.4.6, https://CRAN.R-project.org/package=celestial.

Roje-Bonacci, T. (1997). "Influence of the fluctuation of groundwater levels upon the formation of sinkholes." In *Engineering, Geology and the Environment*, Marinos PG (ed.). Proceedings of the International Symposium on Engineering Geology and the Environment 23-27 June, Athens, Greece. A. A Balkema: Rotterdam 997-1002

Seelig, Jenn. "'I was so scared.' Mother and daughter wake up to massive sinkhole in West Hempstead yard." *News 12 - Long Island*, 28 September 2023, https://longisland.news12.com/i-was-so-scared-mother-and-daughter-wake-up-to-massive-sinkhole-in-west-hempstead-yard. Accessed 2 March 2024.

Tamiru A., Khuliso M., Haile M., Molla D. (2018) "Understanding the groundwater-level fluctuations for better management of groundwater resource: A case in the Johannesburg region, Groundwater for Sustainable Development", Volume 7, 2018, Pages 1-7, ISSN 2352-801X, https://doi.org/10.1016/j.gsd.2018.02.004.

Thorn, Kristen. "3 rescued from sinkhole outside home in Huntington Station, Long Island - ABC7 New York." *abc7NY*, 26 January 2023, https://abc7ny.com/sinkhole-rescue-huntington-station-long-island/12738556/. Accessed 29 March 2024.

Wickham, H. (2016) ggplot2: Elegant Graphics for Data Analysis. Springer-Verlag New York, 2016. https://ggplot2.tidyverse.org

Geochemistry and Geochronology of the Ravenswood Granodiorite, Long Island City

Jaret, S. J.[1,2], Tailby, N. D.,[3], and Crowley, J.[4]

1. Department of Physical Sciences, Kingsborough Community College of the City University of New York, Brooklyn, NY 11235

2. Department of Earth and Planetary Sciences, American Museum of Natural History, New York, NY 10024

3. University of New England, Armidale, NSW Australia

4. Department of Geoscience, Boise State University, Boise, ID 83725

The Ravenswood Granodiorite is a known, mappable unit that occurs in New York City primarily in western Queens near the 59th St, Queensborough Bridge. This unit is a coarse grained slightly metamorphosed granitoid, consisting of a plagioclase-quartz-garnet-biotite mineral assemblage, with rare mafic enclaves. Although this rock is mapped on both the USGS 7.5 minute quadrangle maps (Baskerville, 1992, 1994) and the State Geology Map (southern section) very little is known about this unit. The only published study of the Ravenswood is Zeigler, 1912. However, modern maps have attempted to correlate this unit with other broadly Paleozoic granitoids in the region, specifically the Harrison Gneiss in CT or the Yonkers Gneiss in Westchester NY.

Here we present new whole-rock geochemistry and zircon U-Pb ages for the Ravenswood and the Yonkers Gneiss for comparison. The mean zircon age for the Ravenswood is 583.4 +/- 4.3 Ma. The mean zircon age for the Yonkers is 575.4 +/-3 Ma. Zircon morphology and CL patterns are distinct between the two samples. Rare earth element patterns for both the Ravenswood and the Yonkers are similar: both show a negatively sloping REE pattern with slightly depleted heavy REE compared to the light REE. However, the Yonkers is slightly enriched overall in REEs and shows a dramatic Eu anomaly not seen in the Ravenswood. This suggests, that while these units are broadly similar, they may not be derived from the exact same source, suggesting a broader melting event ~580 Ma. Importantly, the age of the Ravenswood and the Yonkers is not consistent with the Harrison Gneiss in CT, which is younger, 453±3 Ma (Sevigny and Hanson) and more similar to arc volcanics of the Bronson Hill Belt.

Assessing Future Flood Risks: A GIS Simulation of Brooklyn's September 2023 Event with LiDAR Data

Lawlor, J., Jones, W., Tecusan, K., Marsellos, A.E.

Department of Geology, Environment and Sustainability, Hofstra University, Hempstead, NY 11549 U.S.A

Abstract

Brooklyn, one of the five boroughs of New York City, is situated only 67 meters above sea level, with small, yet noticeable elevation changes throughout it. This uneven surface, coupled with its low elevation and proximity to the water, makes Brooklyn very susceptible to flooding, as was the case on September 29th, 2023. With 2023 being the hottest year in recorded history and the trend of global warming having no end in sight, extreme weather events, including major, flood-producing rain storms like the one seen in September will become commonplace. Brooklyn will likely experience another flooding event in the foreseeable future. By reconstructing and simulating this flood using GIS programs such as GlobalMapper and Google Earth, and combining it with the use of the high-resolution LiDAR elevation data to map out which areas are most vulnerable- with special attention given to emergency services- Brooklyn residents and community leaders alike will be better prepared for future floods. Using the information collected, along with proposed alleviation measures like sewage cleanup and emergency services, can remain active and efficient during major future flooding events.

Introduction

In the last 250 years, carbon emissions from human activities have increased the concentration of CO_2 in the atmosphere by 50%, ushering in an era of rapid global warming, the likes of which have never been seen before in the entire geological history of the planet (EPA, 2022). This rapid warming is fraught with dangerous consequences- including sea ice loss, rising sea level, more frequent and intense heat waves and wildfires, and a sharp increase in major storms. Only in the last five decades have we begun to attempt to curb this activity, but it is the opinion of most experts that it is too little, too late- with the most optimistic predictions showing a minimum 1.5°C (2.7°F) increase in global temperature by 2050 (NOAA, 2001). The increase in major storms due to climate change means an uptick in urban flooding events, the damage of which is difficult to overstate. Floods from excessive rainfall in urban settings cause structural and property damage, electrical outages, road closures, and the suspension of public transportation. In extreme cases, flooding can overwhelm city sewage systems, causing contamination in the water supply. Cleanup efforts and emergency relief funds can reach

1

hundreds of millions of dollars, and there is even the possibility of loss of life. One such case of urban flooding occurred in September 2023, when torrential rain caused flooding in major metropolitan areas of New York, New Jersey, and Connecticut, with the New York City borough. Brooklyn was hit particularly hard.

Photos of the event show mass confusion and panic as entire streets became inaccessible. It took a full day for the water to subside after the rain ended, and damages totaled at $100 million (Camacho-Suarez, 2023). This event is likely indicative of a trend. Global warming will increase both the frequency and severity of flooding, and based on the aftermath of a flood with a mean depth of only 4 inches (though in some areas this number was up to nearly 10 inches) (Lauren, 2023). Based on climate change models, future flooding is inevitable, so while it is likely impossible to prevent it, mitigating the impact that those floods have on Brooklyn may be possible. Our goals are to help prepare Brooklyn residents for future flooding events by predicting what areas will be most affected by reconstructing the flood in a GIS program so that community leaders can prioritize sewage cleanup and map out what emergency response services will be affected.

Methodology

We first collected a series of images of the event compiled in an article from the weather channel and determined the geographic location of 9 images (Bonaccorso, 2023). By marking these points on Google Earth, we could then download them as .kmz files and upload them to GlobalMapper (version 24.1), the main GIS software we used for the data. The points we collected came from a 24-square-kilometer area in northern Brooklyn where the flooding was especially significant, so this roughly triangular-shaped polygon (Fig. 1) served as our "study area". We downloaded LiDAR elevation data from the FTP's (File Transport Protocol) NYC 2021 database (ftp://ftp.gis.ny.gov/elevation/LIDAR/), totaling 83 LAS files and approximately 66.4 million points of data to construct a high-resolution Bare-Earth Digital Elevation Model (DEM). A Bare Earth model renders only the "last of many" points and includes no vegetation or structures, which were both subtracted to avoid artifacts (structures rendered on a GIS that do not exist, ie. a tree that is rendered as a building). The DEM gave us an understanding of how and where the water would accumulate. We color-coded the study area so that areas of low elevation were green and areas of high elevation were red (Fig. 2). We followed a previously discussed methodology of flood simulation and reconstruction of damaged areas (Mead, et. al, 2023; Tabarus, et. al, 2020; Mahoney, et. al, 2018). The flooding tool in GlobalMapper allowed us to

2

simulate water flow in our study area to measure the impact of major rainfall events without needing one to actually occur. We determined which areas would flood first and what emergency services would be affected. All distance and elevation were measured in metric units.
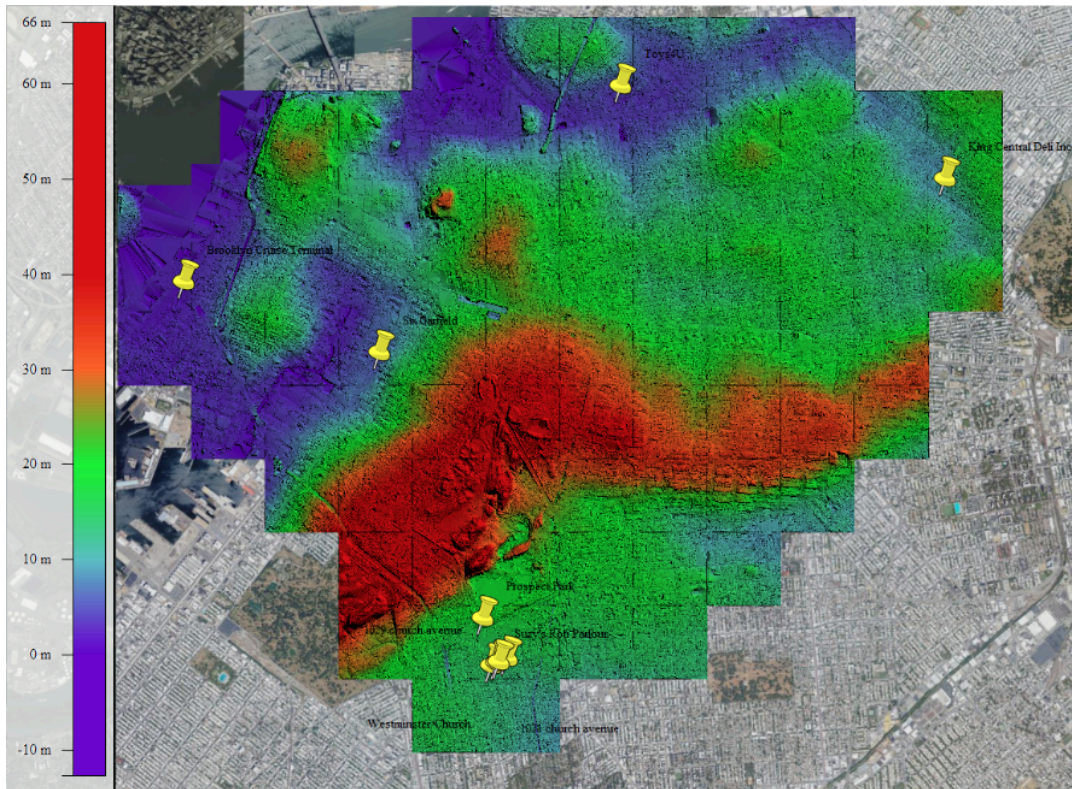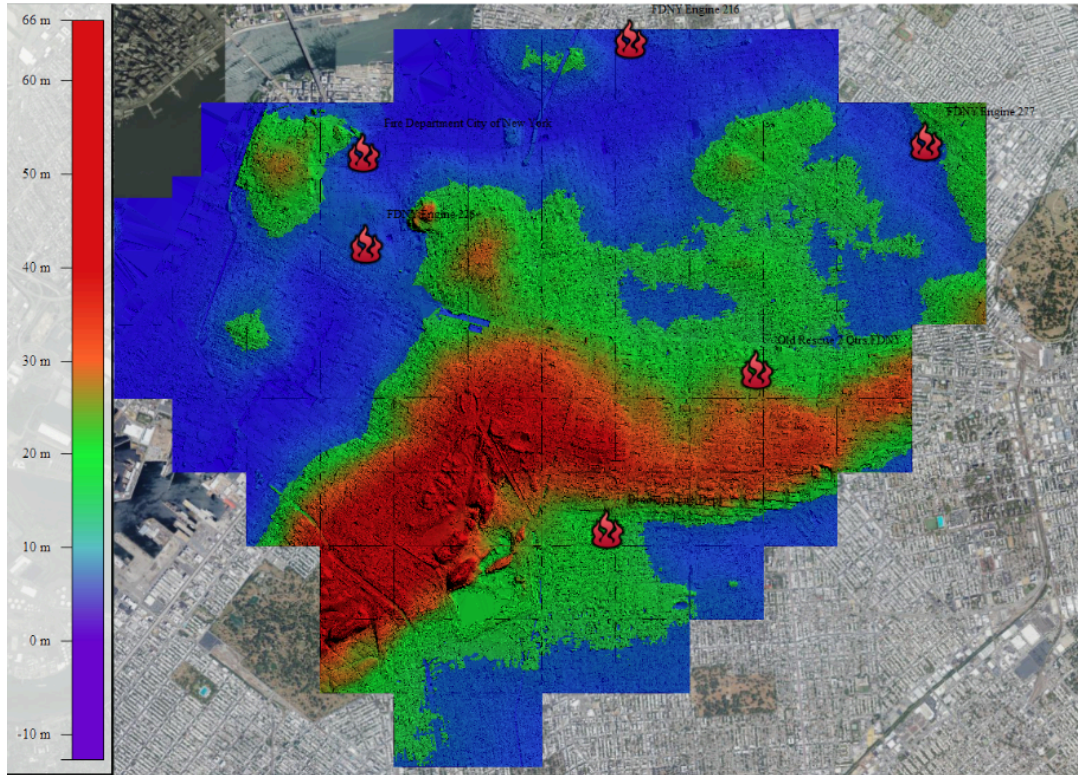

Figure 1: A Global Mapper elevation grid of our study area with 9 labeled points (yellow pins) where floods were reported and LiDAR data displayed. The elevation ranges from 0 meters (blue) to 66 meters (red).
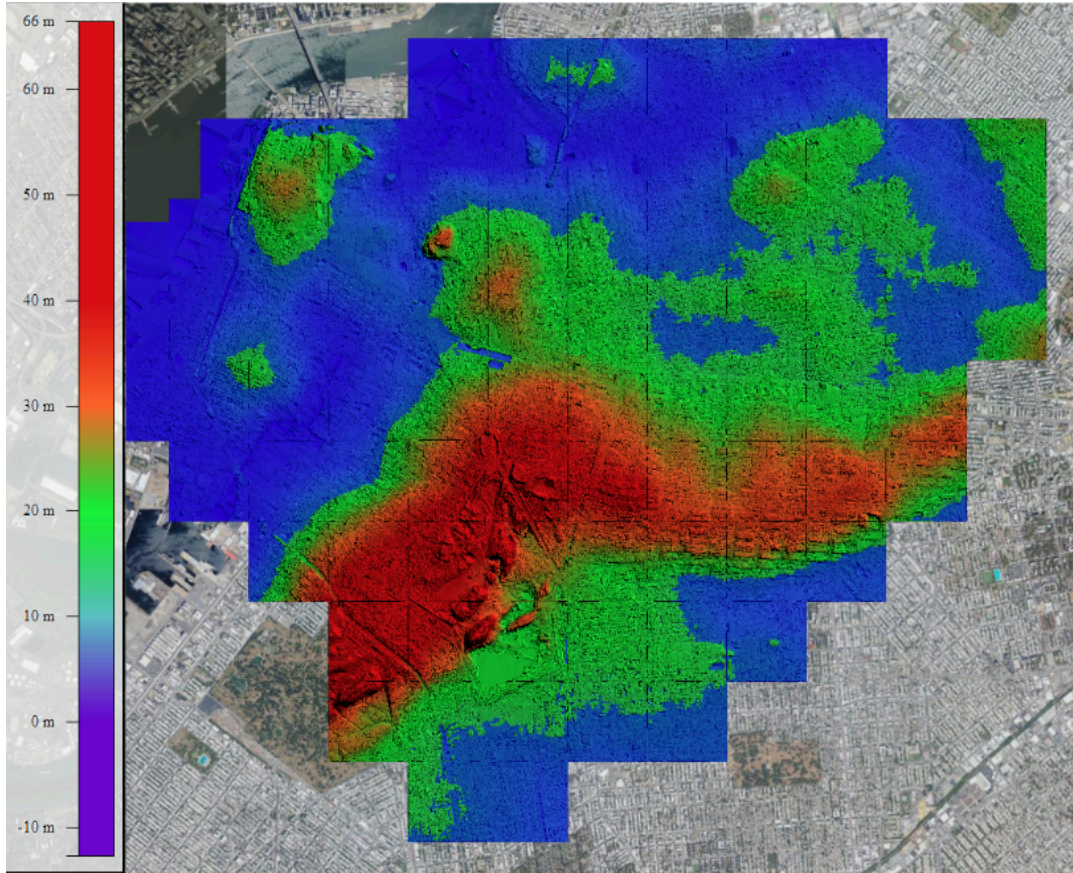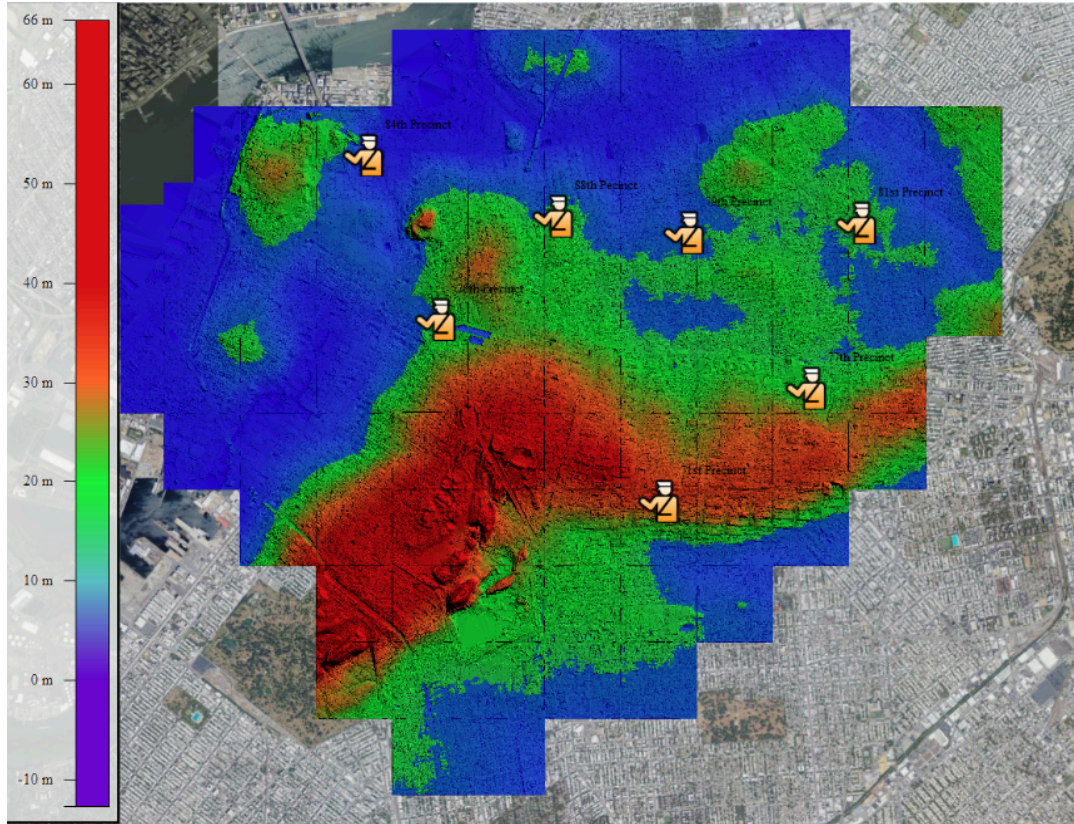
Figure 2: A Global Mapper elevation grid of our study area flood simulated (blue region) with LiDAR data displayed. The elevation ranges from 0 meters (blue) to 66 meters (red).

Figure 3: A Global Mapper elevation grid of our study area with flood simulation (blue region), 6 fire stations labeled (red fire pins), and LiDAR data displayed. The elevation ranges from 0 meters (blue) to 66 meters (red). Yellow pins show the reported floods by the media.

5

Figure 4: A Global Mapper elevation grid of our study area with flood simulation (blue region), 7 police precincts labeled (orange police officer pins), and LiDAR data displayed. The elevation ranges from 0 meters (blue) to 66 meters (red). Yellow pins show the reported floods by the media.
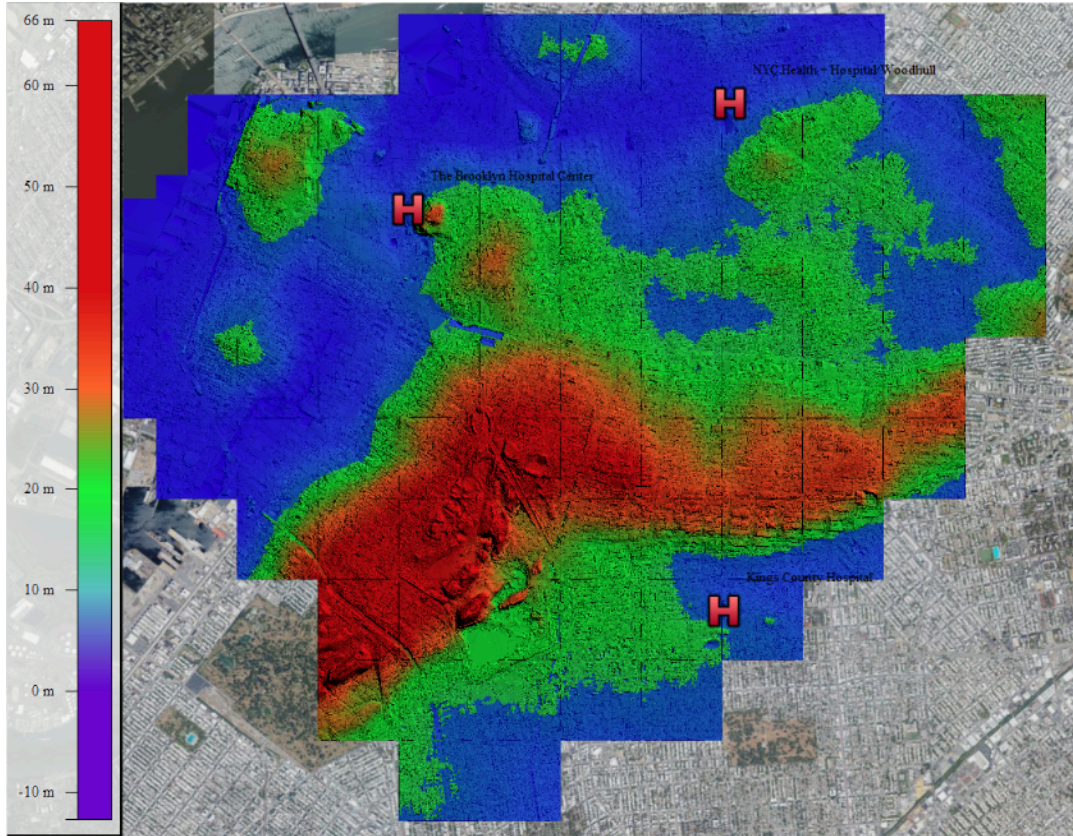
Figure 5: A Global Mapper elevation grid of our study area with flood simulation (blue region), 3 hospitals labeled (red H pins), and LiDAR data displayed. The elevation ranges from 0 meters (blue) to 66 meters (red). Yellow pins show the reported floods by the media.

7
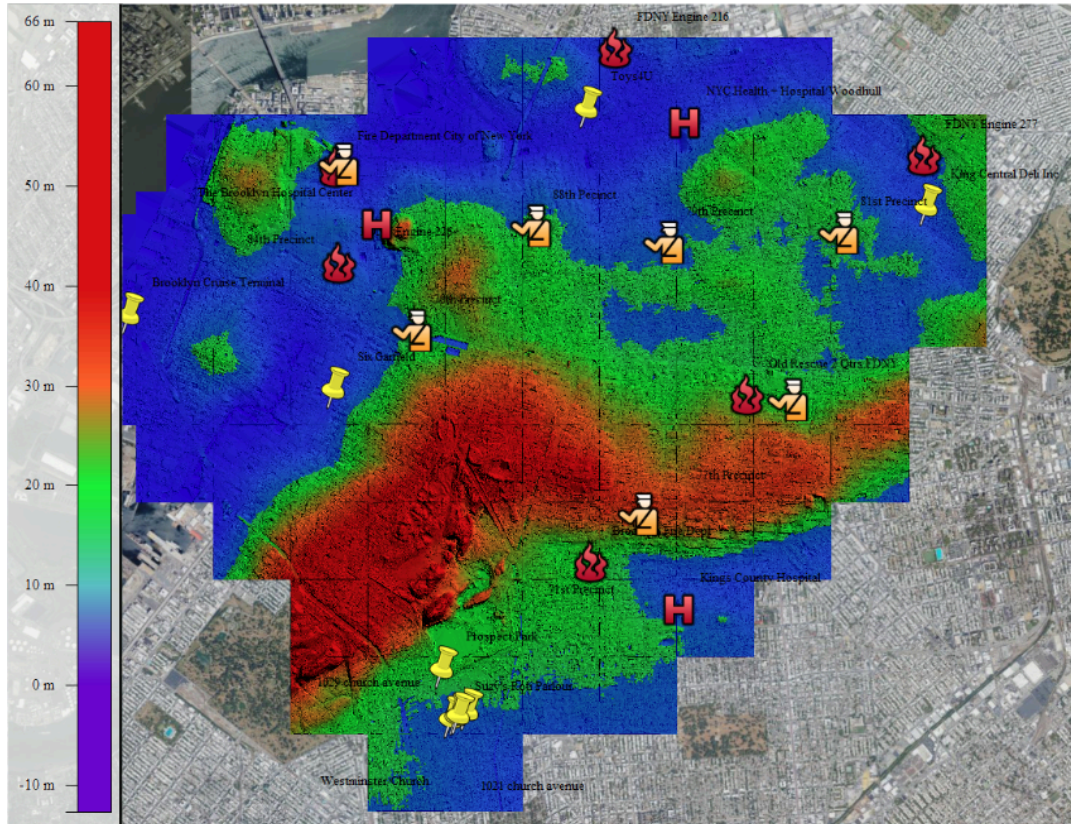
Figure 6: A Global Mapper elevation grid of our study area with flood simulation (blue region), all major rapid response authorities labeled and their vicinity to most affected places, and LiDAR data displayed. The affected roads are also contained within the defined area. The elevation ranges from 0 meters (blue) to 66 meters (red).

Results

The results of simulating the flood in our study area showed us that many of Brooklyn's emergency services, along with many of the borough's roads, will be affected by future flooding. Seven of the thirteen emergency services including FDNY 226, Fire Department City of New York, FDNY 216, FDNY 277 (Fig. 3), and the 71st, 77th, 78th, 79th, 81st, 84th, and 88th Police Precincts (Fig. 4), and all three of the hospitals (Fig. 5) located inside our study area experienced simulated flooding. A major highway, the Brooklyn-Queens Expressway I-278, became completely inoperable. Every road in our study area west of 5th Avenue was flooded (Fig. 6). The highest elevation point is the center of our study area, which encompasses Prospect Park. The flooding formed a circle around the park. In the areas south and west of Prospect Park, intersections experienced more flooding due to slight dips in elevation. Based on the elevation

8

data we gathered in our project, The flooding would accumulate first in the western part of our study area, followed by the northern and southern sections.

Discussion

Climate change and global warming will increase the frequency and severity of extreme weather events that cause flooding, meaning that areas like Brooklyn that are prone to flooding will experience infrastructural and property damage with socio-economic impact in the coming decades. To alleviate some issues, places with lower elevations should be prioritized for sewage cleaning to prevent water contamination (Fig. 1), and Emergency services should be prepared for increased requests for assistance. Communities nearby the flooded area should also prepare to divert some of their emergency services to the affected area. Our data definitively shows that large portions of our study area are prone to flooding from excess rainfall, so it is reasonable to extrapolate the data and assume that Brooklyn and the nearby metropolitan areas of New York, New Jersey, and Connecticut could easily experience extreme weather as well, especially when taking into account the flooding of September 29th, 2023 that affected all of the aforementioned areas. There are also thousands of coastal settlements on Earth with varying levels of preparedness, so this issue is not isolated to the Northeastern United States. In addition, with frequent flooding, insurance costs in these areas may drastically increase, raising living costs for residents who may already be struggling. Our methodology can be applied by the authorities to prepare the regions so that when flooding does occur, the risks of damage to property, infrastructure, and water supplies could be substantially reduced.

Conclusion

As climate change and its accompanying extreme weather events become more widespread, residents in urban areas like Brooklyn must be prepared for recurrent floods. Our study highlights the need for preventative actions to mitigate the impacts these floods have on communities. While our simulation alone cannot resolve the climate crisis, it offers a tool for preparedness and response efforts. The potential damage done to emergency services and critical infrastructure revealed by our GIS simulation demonstrates Brooklyn's vulnerability to future flooding events. By identifying low-elevation areas that are at a high risk of flooding and outlining the potential impact on vital services- namely infrastructure damage, property damage, and water contamination- our study provides the information necessary for community leaders to allocate resources and funds in such a way that the damage is alleviated. Prioritizing sewage cleanup in vulnerable zones and readying emergency response teams are imperative steps towards resilience against flooding. Our findings apply to cities beyond New York: coastal cities and settlements face the same risk of flooding as Brooklyn, so while this specific study and related methodology only applies to the defined area of Brooklyn, preemptive measures guided

by GIS mapping and LiDAR data can empower other communities to navigate and adapt to the changing world and respond to climate-induced flooding.

Credit Authorship Contribution Statement

Lawlor, J.: GIS processing, editing, writing - Abstract, Introduction, Methodology, Discussion, Conclusion, References; Jones, W.: Figures, GIS Processing, editing, writing - Abstract, Introduction, Methodology, Results, References; Tecusan, K.: GIS processing, writing - References; Marsellos, A.E.: Supervision, GIS processing, guidance, editing

Acknowledgements

References

Bonaccorso, Nicole. "Photos of Flooding New York City." *The Weather Channel*, 29 Sep. 2023, https://weather.com/photos/news/2023-09-29-new-york-new-jersey-flood-images

"Brooklyn Topographic Map, Elevation, Terrain." *Topographic Maps*, en-gb.topographic-map.com/map-4dsqnh/Brooklyn/?center=40.6446%2C-73.95526&zoom=15&popup=40.65125%2C-73.97075.

Camacho-Suarez, Vivian. "Flood Event Review - New York City, September 2023."*Previsico* 26 Oct. 2023, previsico.com/2023/10/26/flood-event-review-new-york-city-september-2023/

"Carbon Dioxide Concentration." *NASA*, NASA, 15 Aug. 2023, climate.nasa.gov/vital-signs/carbon-dioxide/.

"Climate Change Indicators: Atmospheric Concentrations of Greenhouse Gases." *EPA*, Environmental Protection Agency, July 2022, www.epa.gov/climate-indicators/climate-change-indicators-atmospheric-concentrations-greenhouse-gases#:~:text=Carbon%20dioxide%20concentrations%20have%20increased,is%20due%20to%20human%20activities.

"Lidar." *Gis*, gis.ny.gov/lidar.

Mahoney, L.*, Roscoe, S.L.*, Marsellos, A.E., 2018.
https://www.stonybrook.edu/commcms/geosciences/about/_LIG-Past-Conference-abstract-pdfs/2019-Abstracts/Rienzo%20et%20al%202019%20LIG.pdf

Mead, N., Bourgeois, J., Pelletier, A., Badger, T., Marsellos, A.E., 2023.
https://www.stonybrook.edu/commcms/geosciences/about/_LIG-Past-Conference-abstract-pdfs/2023-Abstracts/Mead.pdf

"NYC Road Closures and Subway Outages to Know for Your Commute amid Ongoing Flooding." *CBS News*, CBS Interactive, www.cbsnews.com/amp/newyork/news/mta-deploys-crews-equipment-to-flood-prone-stations-to-limit-storms-impact-on-service/.

Q3 Global Catastrophe Recap, www.aon.com/getmedia/7107985e-43d8-412b-a674-7722112cc2b0/20231018-q3-2023-catastrophe-recap.pdf.

Tabarus, N.*, Tran, J.*, Achek, M.*, Marsellos, A.E., 2020.
https://www.geo.sunysb.edu/lig/Conferences/abstracts20/Abstracts%2020/Tabarus%20flood%20rate.pdf

"The Intergovernmental Panel on Climate Change." *IPCC*, 2024.
www.ipcc.ch/

Webmaster, CPC. "NOAA's Climate Prediction Center." *Climate Prediction Center*, 1 Jan. 2001, www.cpc.ncep.noaa.gov/.

Characterizing Boron Isotope Variation in Wetland Plants from Setauket Pond

Iorga, A.[1], Rasbury, E. T.[1,2], Twiss, K.C.[1,3]., Wooton, K.M.[2], and Wright, C.C.[2] [1]Interdepartmental Doctoral Program in Anthropological Sciences, Stony Brook University
[2] Facility for Isotope Research and Student Training, Department of Geosciences, Stony Brook University, Stony Brook, NY
[3] Department of Anthropology, Stony Brook University, Stony Brook, NY
anastasia.iorga@stonybrook.edu

In North America, most major cities can be found in coastal zones at risk from rising sea level (RSL) and increased storm intensity. Coastal wetlands provide protection from RSL and storm surge, but wetland acreage is significantly decreasing across the continent. This loss is exacerbated by RSL and decrease in sediment deposition. In this process, wetlands, and surrounding groundwater, undergo increased salinity and easily flooded low marsh zones expand. Understanding how Long Island wetlands respond to RSL is increasingly important, particularly if increased salinization of wetlands and surrounding groundwater is a possibility. Boron isotopes may be one way to investigate both how plants behave in a wetland and how a wetland responds to increased salinization and RSL. We report boron isotope data from Setauket Pond and Conscience Bay in comparison with boron isotope data from Plum Island (MA). These data show the extent to which seawater can influence boron isotopes in a wetland system, e.g., the water, soil, and plants. Further, boron isotope analyses on *Phragmites* spp., an invasive plant that thrives in all kinds of wetland ecosystems, point towards a complex boron uptake mechanism in its plant physiology that may complicate its use in isotope investigations of wetland economies and land use.

Introducing WhatRocksOnYourBlock: a virtual tour of building stones in NYC

Melzer, L.,[1], Jaret, S. J[2.3]., Hopkins, M. J.,[2] and Taber, K.[2].
[1]New York City Department of Education, Manhattan International High School
[2]American Museum of Natural History
[3]Kingsborough Community College, City University of New York
lmelzer@mihsnyc.org, sjaret@amnh.org

Populated urban areas aren't the first place you think of when geology is mentioned. Aside from some scattered designated areas reserved for nature and relaxation, geological sightings in a city setting are often difficult to come by. Despite that, there are still a wide variety of terrific examples of geology in which the everyday person can observe, simply by looking at the buildings and structures around them.

After several years of running in-person field trips centered on building stones and facades in New York City, we have developed a series of walking tours that are designed to get students of all ages engaged with both geology and their local neighborhoods. Rocks used in buildings you pass every day are an excellent starting point to engage students and to introduce them to geology.

To expand the use of building stones as education tools, we have created a digital version of two building stone field trips in New York City: along 5th Avenue and Midtown East. Thus, we are introducing What Rocks on Your Block?; a space dedicated to showcasing local, urban geology that is accessible to people of all ages and education levels. Using the Esri StoryMaps platform, we have created a way for people to share and experience short walking tours in which a variety of geological examples can be observed and analyzed. Educators will enjoy the curriculum connections and activities that are available with each tour as well. With the goal of bringing more people into the field of geology and the Earth sciences, we're hoping that What Rocks on Your Block fosters a new wave of curiosity and interest amongst people who would otherwise just walk past the stones on an old building.

What Rocks on Your Block walking tours will be hosted on the American Museum of Natural History's website along with materials for teachers and students who want to use them in their classrooms. We hope these tours serve as inspiration for the creation of walking tours in your own neighborhoods.

INVESTIGATING GROUNDWATER AND LANDSLIDES RELATIONSHIP USING R: A STUDY ON LONG ISLAND'S NORTH SHORE

Badger, T.[1] , Parag, A.[1] , Pelletier, A.[1] , DeRocchis, S.[1] , Marsellos, A.E.[1], Tsakiri, K.G.[2]

[1]*Department of Geology, Environment and Sustainability, Hofstra University, Hempstead, NY 11549*
[2]*Dept. Information Systems, Analytics, and Supply Chain Management, Rider University, Lawrenceville, NJ 08648*

Abstract

The north shore, Long Island's coastline, has been experiencing a series of landslides and mudslides since 2010. Most landslides occur on the north shore of Long Island, an area with higher elevation. This research investigates the relationship between groundwater fluctuations and landslide occurrences. The methods employed in this research encompassed the construction of a digital elevation model of Long Island using GIS software (Global Mapper v.24.1) to delineate affected areas, plotting landslide occurrences reported by the media on a map of Long Island's north shore, and utilizing the USGS (United States Geological Survey) database of monitoring wells to analyze groundwater level for identifying areas of high- and low-groundwater fluctuations. Additionally, spectral analysis aimed to test the hypothesis that high-frequency groundwater level fluctuations might exacerbate underground erosion. At the same time, lower frequencies, such as those occurring annually, have a comparatively lesser impact on landslide formation.

Based on the results, fluctuations in groundwater level located along the outer shore of Long Island may trigger groundwater "vibrational" long-term movements causing accelerated erosion underground, leading to potential landslides. With the climate showing warmer temperature fluctuations, particularly in regions with higher latitudes, the risks of landslides grow more severe, notably due to increased underground water mobility during periods previously characterized by prolonged winter cold temperatures and water mobility pauses. Therefore, focusing on areas prone to landslides can prevent the loss of life, damage to roads and structures, and environmental decay.

Introduction

This study aims to provide crucial information about which areas of Long Island in New York are most prone to landslides to prevent future damage to roads and other structures. Due to climate change, there has been an increase in the severity and frequency of storms, which has led to an increase in groundwater. Since 1901, New York's annual precipitation has increased from 10% to 20%, and it is expected to keep increasing to 17% by the end of the century (New York

State Climate Impact Assessment 2024). One of the areas of Long Island most affected by these storms is the north shore. Long Island's north shore was predominantly formed from headland erosion, creating steep bluffs of sandy and glacial till. With an increase in groundwater, the sand and till loosens, increasing the risk of landslides or debris flows. As temperatures freeze, the groundwater becomes stuck in the bluffs and expands, resulting in cracks. These cracks separate the bluffs into large chunks of sediments, which slide down the face, resulting in damages to not only private property but also public beaches (Fallon 2018).

In 2014, a landslide occurred in Sea Cliff, NY, causing two retaining sea walls on private property to collapse. Since the property was on the verge of collapsing into Hempstead Harbor, it was left vacant by the homeowners. When a series of storms hit the town again in 2018, more of the property collapsed, exposing the foundation of the home (Seidman 2018). Landslides endanger the people living in these homes on the north shore but also put anyone walking along the beach at risk as the cliff keeps receding. Leading the north shore at an average rate of one to two feet a year. Bare or sparsely vegetated bluffs erode the fastest as wind and water can easily remove the unconsolidated material. To control further erosion, more vegetation has been planted because the roots can keep soil in place while taking in excess water in the bluffs (Fallon 2018).

Groundwater level fluctuations observed at the monitoring stations administered by the USGS exhibit various periodicities, ranging from high-frequency oscillations to longer-term cycles, such as annual cycles (Rienzo et al., 2019). The aim of this paper is to assess the data of North Shore groundwater wells being monitored by the United States Geological Survey (USGS) in order to determine the connection between groundwater fluctuations and landslides. The rapid fluctuation of groundwater can loosen the sediment on a slope allowing it to slide down and gather other sediment along the way. Since there has been limited research done on this topic previously, we have explored periodicities of the monitoring wells water level fluctuations. This research emphasizes the importance of more groundwater monitoring data as it can show which areas are most vulnerable in the future as precipitation increases. By having this information it can not only preserve infrastructure but also prevent further damage to the environment.

Methods

The areas in Long Island where landslides occur were collected by outlining the map of Long Island in the Google Earth program. Pinpoints of the landslide occurrence areas and site areas, near the occurrences, were also placed in Google Earth. Site areas used in this research were collected from the USGS National Water Information System. This data was then extracted into Global Mapper to create a path profile of the elevation of Long Island. The path profile proved that sites of landslide occurrences had higher elevations. Site areas of landslide occurrence as well as the outline of Long Island were extracted into Global Mapper and enhanced for better viewing. The groundwater data site locations were labeled on the map as well as the landslide occurrences.

Using the USGS National Water Information System, groundwater level data from eleven sites of landslide activity near the north shore of Long Island was analyzed. The measurements were taken in accordance with the National Geodetic Vertical Datum of 1929 (NGVD). This standard measures groundwater fluctuation from the elevation of a point above and depression below mean sea level (MSL). This data was then extrapolated using R language (RStudio), cleaned, and processed including any missing data in the original data found in the USGS National Water Information System.

Underground water level data were obtained from 11 USGS monitoring stations located in the adjacent region affected by landslides, accessed through the USGS National Water Information System (NWIS) (https://waterdata.usgs.gov/nwis/). Utilizing the "data.table" (Barrett et al., 2024) package in R, the time series of groundwater, along with corresponding dates for each station, were extracted and organized. Subsequently, the groundwater level data underwent cleaning and processing procedures. Missing data or gaps within the time series were interpolated using the "imputeTS" package (Moritz et al., 2017), employing the function na_interpolation(). Date manipulations were performed using the "lubridate" package. Moving averages were applied to utilize the Kolmogorov-Zurbenko filter to smooth the data and reduce noise, which was implemented through the "kza" package (Close et al., 2020). Periodograms were constructed to analyze the frequency components of the groundwater fluctuations using the "TSA" package (Chan et al., 2022), with the function periodogram(). To facilitate comparison across different sites, all periodograms were normalized using the "BBmisc" package (Bischl et al., 2022) and the function normalize().

Furthermore, to enhance the visibility of short-term fluctuations and highlight higher frequencies present in the groundwater data, a trend was subtracted from the raw data. This trend was derived from a moving average computed using the Kolmogorov-Zurbenko filter with a window size of 29 days, applied three times consecutively (kz(29,3)). By subtracting this trend from the groundwater levels, the resultant data set more effectively captured short-term variations and revealed the presence of higher frequencies where they existed. Additionally, to mitigate spectral leakage in the periodogram analysis, the zero tapering method was employed. Furthermore, the dataset was replicated ten times to enhance spectral detection in the low periodicities, following a method described in previous literature (Tsakiri & Marsellos, 2024). This preprocessing step aimed to provide greater insights into the dynamics of groundwater fluctuations and their potential relationship with landslide occurrences.

From the graphs created in RStudio, (Figure 3), the moving average was applied to subtract the low frequencies to study the presence of any hidden higher frequencies. The occurrence of these higher frequencies of water was detected using the periodogram method, where station 9 displayed a very high period (low frequency of mostly annual periodicity), and station 11 displayed a very low period (high frequency of mostly monthly or weekly periodicity). Stations 9 and 11 were selected to show the contrast between high- and low-frequency water level fluctuation. Those stations are depicted on the map (Figure 1) to determine the relationship between landslide occurrences and frequencies.

3

31ˢᵗ Conference on the Geology of Long Island and Metropolitan New York, April 2024

Results

The study uncovered a partial correlation between the frequency of groundwater oscillations at certain monitoring wells and the proximity of landslide events. Sites with elevated groundwater frequency fluctuations coincided with areas of frequent landslide activity, underscoring the impact of groundwater dynamics on slope stability and landslide susceptibility. With the exception of missing data from some of the studied sites, most landslide occurrence points displayed a roughly annual fluctuation in groundwater level (spike occurring roughly every 365 days). The sites that experienced the most fluctuations throughout the year are at the greatest risk for landslide occurrences. The periodograms show the frequency of the groundwater fluctuations (Figure 5). As rainfall in New York significantly increases on an annual basis there are rapid movements in groundwater going from above sea level to below sea level.

Based on the result, the lower frequencies occur at station 9 which is located in the inland area of Long Island and the higher frequencies occur at station 11 which is located on the outer shoreline of Long Island. Stations 3, 10, and 11 have more frequent changes. Along the coastline, groundwater has more frequent fluctuations and doesn't follow the annual recharge cycle. Station 7 and others like it are exceptions to this.
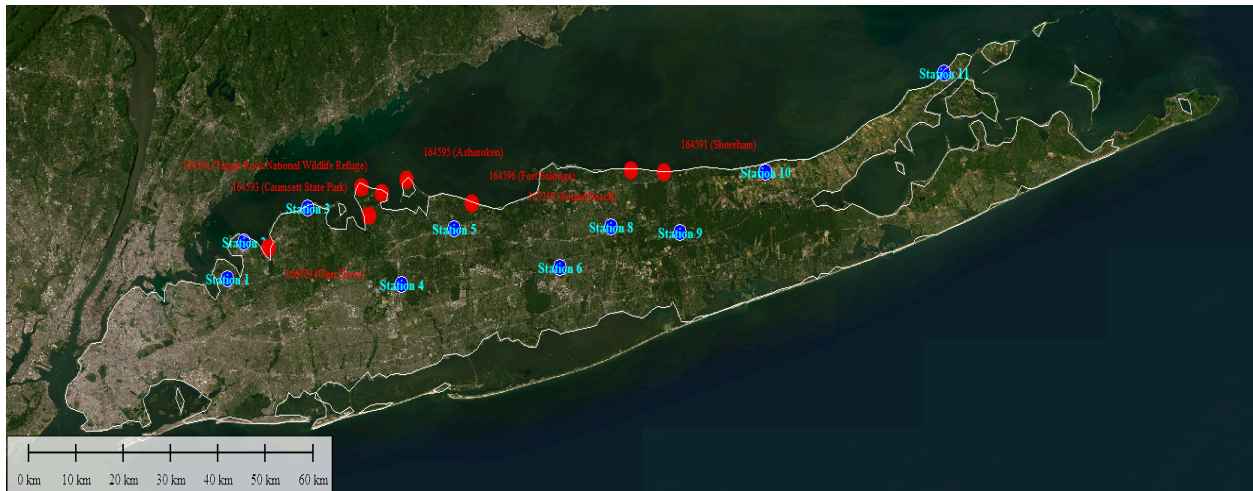
Figure 1: Map of Long Island's recorded landslide occurrences (red dots) and groundwater monitoring stations by USGS (blue dots). Blue dots represent the stations used to gather groundwater data. Stations 6 and 7 are located at the same point. These sites are located in areas of higher elevation.
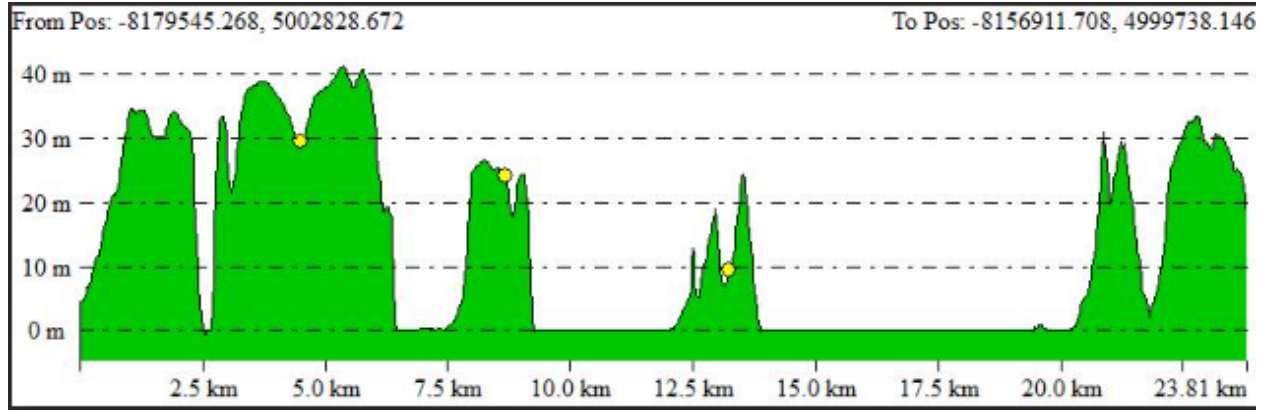
**Figure 2**: Path profile of Long Island's north shore created in Global Mapper.

```
filtered ground water = groundwater - moving_average(groundwater, window(27),iterations(3))
```

Figure 3: The groundwater equation is used to process raw groundwater data with a 27-day moving average filter with an iteration of three times. This period corresponds to the lunar cycle, highlighting its potential impact on groundwater levels.
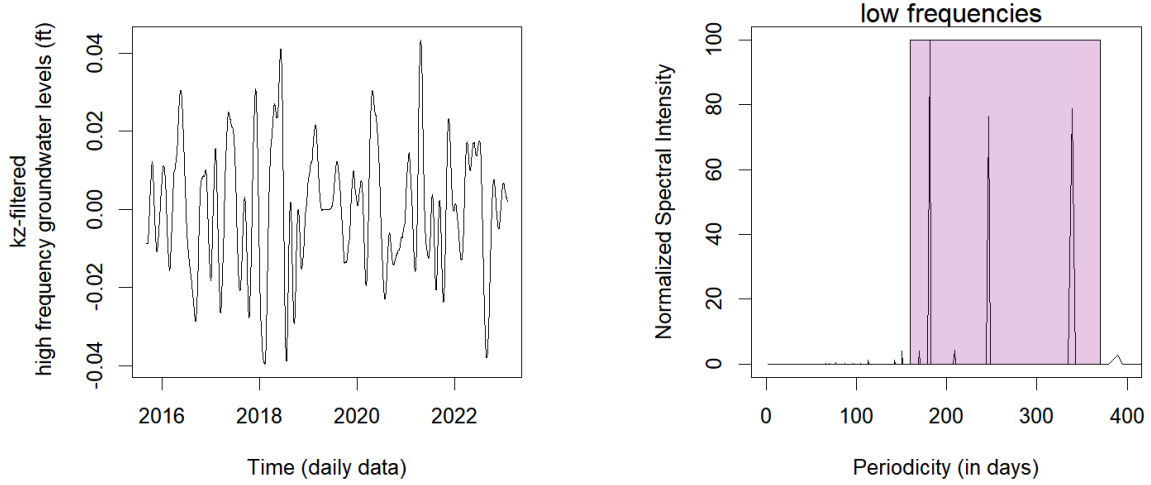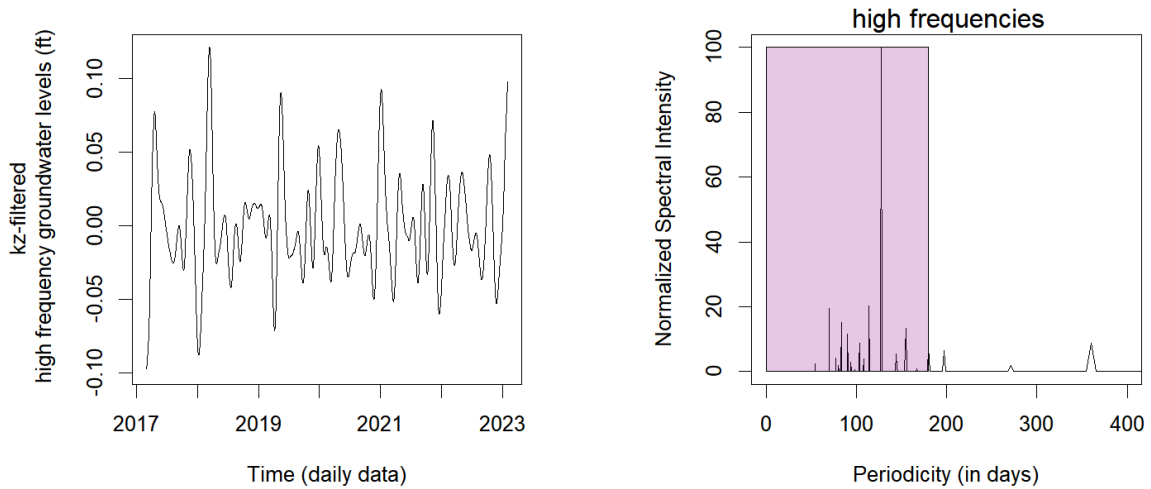
Figure 4: Groundwater Fluctuations and Frequency Levels at Sites 9 and 11. The main peaks in frequency are highlighted in purple.
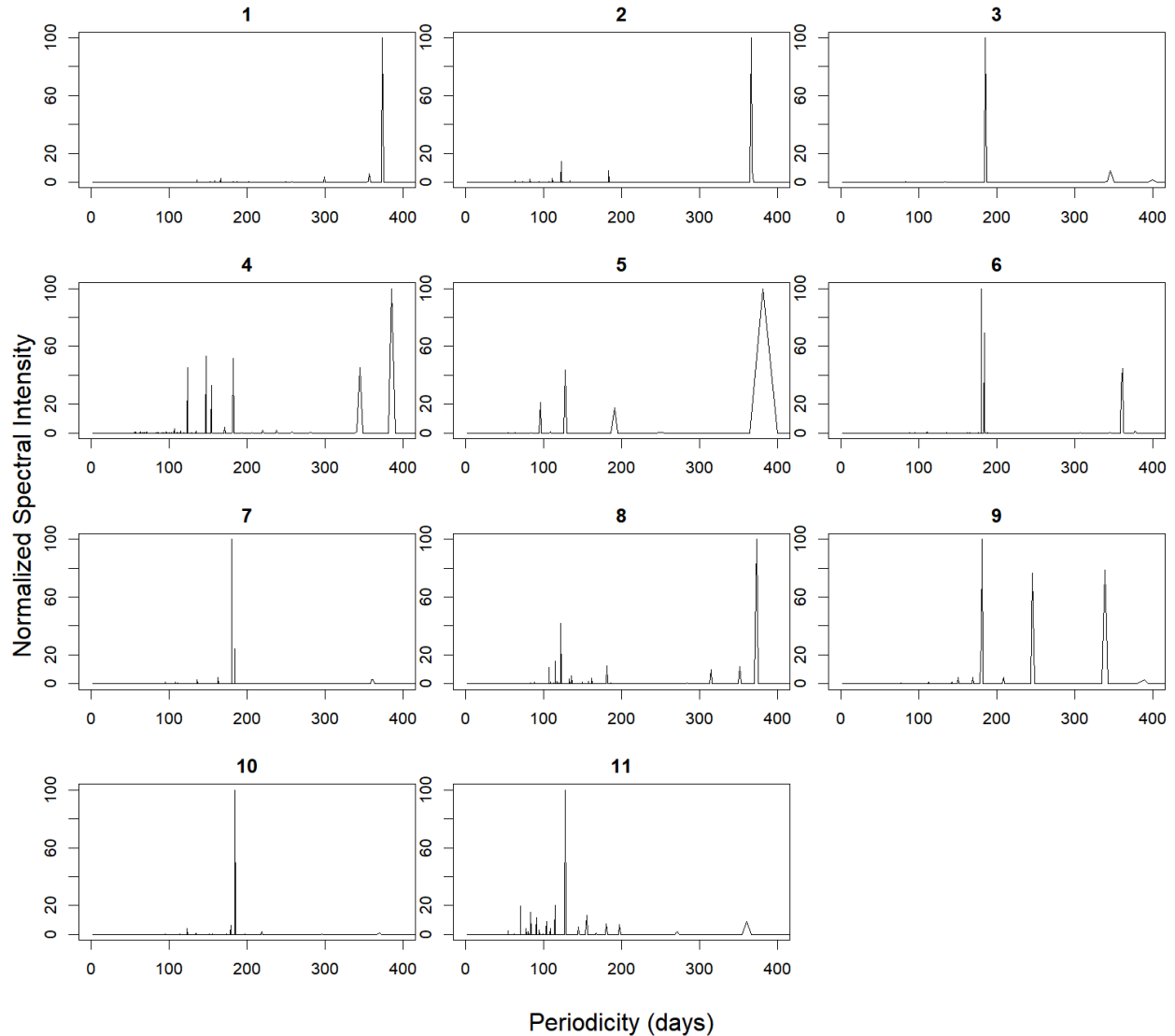
Figure 5: Spectral analysis (periodograms) of groundwater frequencies at stations 1 through 11. Spectral analysis of the frequency of groundwater fluctuations in 11 USGS sites across Long Island, NY at the frequency domain of 1-400 days.

Discussion

As we know, the sites that experience a spike in groundwater annually are at an increased risk of a landslide occurring. Long Island's north shore is known for high property value and beaches which are now vulnerable to erosion due to increased precipitation from climate change. The results from Figure 1 display the closest possible active sites for groundwater data near Long Island's north shore since the sites directly within the region of landslide occurrences provided no available data or with very large time-gaps. Landslides commonly occur along the north shore of Long Island where there are steeper elevations of land. The path profile shown in Figure 2 is a

7

graphical representation of the terrain along a specified line. The line was drawn from west to east, along Long Island's north shore using Global Mapper. This path profile confirmed that the elevation of the north shore varies, and in places with steep slopes, comprising both low and high terrain. Higher terrain present on the north shore are prime sites for landslides because the elevations are formed by loose glacial till which is highly susceptible to erosion as well as changes to groundwater level fluctuation.

The formula presented in Figure 3 shows that the moving average of the groundwater being subtracted from the raw groundwater to remove noise from low-frequency annual cycles. A moving average window of 27 days is chosen because it represents the moon cycles and was performed for a total of 3 times. The subtraction of periodicities higher than 27 days, such as moon cycles or other monthly or annual cycles, does not entirely eliminate them from the raw data; rather, it enables the revelation of higher frequencies that may be obscured by long-term trends. High-frequency water fluctuations can lead to more underground erosion. The formula was used to lessen the noise seen within the datasets. The rapid movements of these fluctuations then allow the sediment to become loose and based on the steepness and high level of elevation the sediments are stationed at, it will begin to slide down the hill pushing other small pieces of sediment along with it, thus forming landslides.

The groundwater fluctuations and frequencies (Fig. 4) emphasize on the lowest and highest frequencies comparing all the sites 1 through 11. Station 9 shows the low-frequency levels that occur annually over 365 days. Station 11 shows high-frequency levels that occur daily under 365 days. Station 7 and the others that follow its trend generally occur in areas with larger populations, so it is within reason to say that overconsumption of groundwater accounts for the lack of the annual cycle peak on the graphs.

Conclusion

As the groundwater levels fluctuate more frequently during less than the annual time it creates stress on the sediments and minerals at higher elevations by rapid vibration movements which then break apart these minerals leading to potential landslides. Not much research has been conducted like this experiment to study the effects that groundwater levels have on landslide occurrences. Past research has described the destruction caused to private properties due to landslides. There are various sites throughout Long Island's north shore containing no or unavailable groundwater data, which led to the reconstruction of new sites with available data that is used in this experiment. This study encourages the need for more data on groundwater levels around the areas of Long Island, especially where there are high elevations. This research can not only encourage Long Island researchers but also researchers from different states like Oregon, California, and Washington that experience major landslide impacts.

Credit Authorship Contribution Statement

Badger, T.: editing, literature, Rstudio coding, Figure 4, Figure 5, writing- Results, Discussion; Parag, A: Literature, editing, writing- Global Mapper, Google Earth, Abstract, Results- figure 1, Methods, Discussion; Pelletier, A.: references, literature, editing, writing - Introduction, Discussion; DeRocchis, S.: figures, editing, USGS Graphs, Global Mapper, writing - Methods, Discussion; Marsellos, A.E.: supervision, Rstudio coding, guidance, editing; Tsakiri, K.G.: Rstudio coding.

References
Barrett T, Dowle M, Srinivasan A, Gorecki J, Chirico M, Hocking T (2024). _data.table: Extension of `data.frame`_. R package version 1.15.2, https://CRAN.R-project.org/package=data.table.

Bischl B, Lang M, Bossek J, Horn D, Richter J, Surmann D (2022). _BBmisc: Miscellaneous Helper Functions for B. Bischl_. R package version 1.13, https://CRAN.R-project.org/package=BBmisc.

Cao, Ying. Yin, Kunlong Yin. Zhou, Chao. Ahmed, Bayes. Establishment of Landslide Groundwater Level Prediction Model Based on GA-SVM and Influencing Factor Analysis. PubMed Central. National Library of Medicine. February 5, 2020. Establishment of Landslide Groundwater Level Prediction Model Based on GA-SVM and Influencing Factor Analysis - PMC (nih.gov)

Chan K, Ripley B (2022). _TSA: Time Series Analysis_. R package version 1.3.1, <https://CRAN.R-project.org/package=TSA>.

Close B, Zurbenko I, Sun M (2020). _kza: Kolmogorov-Zurbenko Adaptive Filters_. R package version 4.1.0.1, https://CRAN.R-project.org/package=kza.

Desantis, Michael. Callahan's Beach Of Fort Salonga Reopens After Seawall Collapse. Kings Park, NY Patch. November 08, 2023. Callahan's Beach Of Fort Salonga Reopens After Seawall Collapse | Kings Park, NY Patch

Fallon, Kathleen M. Coastal Processes on Long Island: An Introduction to Erosion. Sea Grant. March 27, 2024. CoastalErosionOnLI-0318.pdf (sunysb.edu)

Garrett Grolemund, Hadley Wickham (2011). Dates and Times Made Easy with lubridate. Journal of Statistical Software, 40(3), 1-25. URL https://www.jstatsoft.org/v40/i03/

Good, R. E., & Good, N. F. Vegetation of the Sea Cliffs and Adjacent Uplands on the North Shore of Long Island, New York. 1970. Bulletin of the Torrey Botanical Club, 97(4), 204–208. Vegetation of the Sea Cliffs and Adjacent Uplands on the North Shore of Long Island, New York on JSTOR

Hester J, Bryan J (2024). _glue: Interpreted String Literals_. R package version 1.7.0, https://CRAN.R-project.org/package=glue.

Kozlowski, Dr. Andrew. Landslides in New York State | The New York State Museum. New York State Museum. March 25, 2024. Landslides in New York State | The New York State Museum (nysed.gov)

"Landslide Susceptibility." NYS Hazard Mitigation Plan. Oct. 2004. Microsoft Word - 3-Risk-6-NY-landslide.doc (nj.gov)

Tsakiri, K.G. & Marsellos, A.E., 2024. Signal detection in high-noise time series data using R. International conference on Time Series and Forecasting,ITISE2024, Spain, July 2024.

Moritz S, Bartz-Beielstein T (2017). "imputeTS: Time Series Missing Value Imputation in R." _The R Journal_, *9*(1), 207-218. doi:10.32614/RJ-2017-009 https://doi.org/10.32614/RJ-2017-009.

New York Water Science Topography. Long Island Topography. U.S. Geological Survey. March 27, 2024. Long Island Topography | U.S. Geological Survey (usgs.gov)

Ooms J (2024). _curl: A Modern and Flexible Web Client for R_. R package version 5.2.1, https://CRAN.R-project.org/package=curl.

Oregon Department of Transportation. FACT SHEET Climate Change Impacts and Landslides in Oregon. Oregon Department of Transportation. March 13, 2024. https://www.oregon.gov/odot/climate/Documents/Landslides.pdf

Pair, Donald L. Kappel, William M. Geomorphic studies of landslides in the Tully Valley, New York: implications for public policy and planning. Geomorphology. May 24, 2002. Geomorphic studies of landslides in the Tully Valley, New York: implications for public policy and planning - ScienceDirect

Petley, David. Global patterns of loss of life from landslides. Geology. GeoScienceWorld. October 01, 2012. Global patterns of loss of life from landslides | Geology | GeoScienceWorld

Precipitation. New York State Climate Impacts Assessment. 2024. Precipitation – New York State Climate Impacts Assessment (nysclimateimpacts.org)

Rienzo, A.*, Roscoe, S.L.*, Mahoney, L.*, Weinstein, P.*, Tsakiri, K.G.*, Petrocheilos, C.*, Marsellos, A.E., 2019. Time series analysis comparing climatic averages and the water levels of aquifers in Albany, NY and Queens, NY. 26th Conference on the Geology of Long Island and Metropolitan New York. April 13th 2019, p.1-8. url: https://pbisotopes.ess.sunysb.edu/lig/Conferences/abstracts19/abstracts%202019/Rienzo %20et%20al,%202019%20LIG.pdf

Scavetta, Alyssa. How Mudslides Contaminate Your Water Supply. aquasana.com. March 27, 2024. How Mudslides Contaminate Your Water Supply | Aquasana

Seidman, Alyssa. Bay Avenue home in Sea Cliff is barely hanging on. Herald Community Newspapers. March 29, 2018. Bay Avenue home in Sea Cliff is barely hanging on | Herald Community Newspapers | www.liherald.com

USGS. U.S. Landslide Inventory Web Application. ArcGIS Web Application. March 27, 2024. U.S. Landslide Inventory (arcgis.com)

USGS. Water Resources of the United States. USGS Water Data for the Nation. March 27, 2024. Water Resources of the United States—National Water Information System (NWIS) Mapper (usgs.gov)

Water Resources of the United States-National Water Information System (NWIS) Mapper. March 4, 2024. https://maps.waterdata.usgs.gov/mapper/index.html

Wickham H, François R, Henry L, Müller K, Vaughan D (2023). _dplyr: A Grammar of Data Manipulation_. R package version 1.1.4, https://CRAN.R-project.org/package=dplyr.

U-Pb Age of 448 Ma for Shelter Rock, a Large Glacial Erratic in Western Long Island, New York, Confirms its Source from a Late Ordovician Meta-Granodiorite Pluton Beneath Western Long Island Sound

J Bret Bennington[1], Steven Jaret[2],. Andrew Byrne[1], Brandon Bookbinder[1], and Sandra Guevara Sanchez[3]

[1]Department of Geology, Environment, and Sustainability, Hofstra University
[2]Department of Physical Sciences, Kingsborough Community College
[3]Freeport High School, Freeport, NY

Summary

Shelter Rock is a large, historically significant glacial erratic (one of the largest on Long Island) located on the property of the former Whitney Estate in Manhasset, NY. Shelter Rock is the highlight of field trips conducted as part of the Greentree Foundation Teachers Ecology Workshop and is of great interest to Long Island teachers and their students. A previous report described the location, historical background, lithology, and probable origin of Shelter Rock (Ciano et al., 2013). Here we amend the original lithologic description of Shelter Rock to a meta-granodiorite and report a U-Pb zircon crystallization age of 447.9±2.3 Ma for the bedrock pluton that Shelter Rock was derived from. This age ties Shelter Rock to a suite of granitic-dioritic orthogneiss plutons of Late Ordovician age located in southeastern New York and eastern Connecticut that were emplaced during subduction associated with the Paleozoic closure of the Iapetus (aka Proto-Atlantic) Ocean.

Methods

A large hand sample of Shelter Rock was obtained from a block that was dislodged from the main boulder by weathering along a joint fracture. Part of this block was used to produce polished hand samples and petrographic thin sections and the remainder was crushed to obtain zircon grains for dating analysis. Zircons were concentrated via magnetic and density separation and hand-picked from the 63-250 micron size fraction. Grains were annealed and then mounted in epoxy for CL and LA-ICP-MS analysis at Boise State University. Spot size for isotope measurements was 20 microns.

Results and Interpretation

Hands sample and thin section analysis of the petrology of Shelter Rock shows a moderately foliated orthogneiss composed primarily of plagioclase and biotite, with lesser amounts of hornblende, quartz, and accessory garnet (Figures 1 and 2). Zircon analysis shows a uniform texture to the zircons (Figure 3), consistent with an igneous source. Ages from 39 zircons (Figure 4) are consistent and yield a concordant age of 447.9±2.3. Based on the petrography and age, the most likely source of Shelter Rock is the Harrison gneiss. The Harrison gneiss in eastern NY and near Stamford, CT has been correlated with the Brookfield (and other) orthogneisses, whose age is 453 +/- 3 (Sevigny and Hanson, 1995). This age is within error of our new age on Shelter Rock. Geographically, Harrison gneiss outcrops 15-20 km due north of Shelter Rock making it a possible source for the glacial erratic (Figure 5). The direction of Late Wisconsin glacial flow (Figure 5) across southeastern NY obtained from bedrock striations and the

inferred short travel distance for glacial erratics of large size and angularity (Pacholik et al., 2001) suggest that there is a body of Harrison gneiss in the bedrock beneath western Long Island Sound.
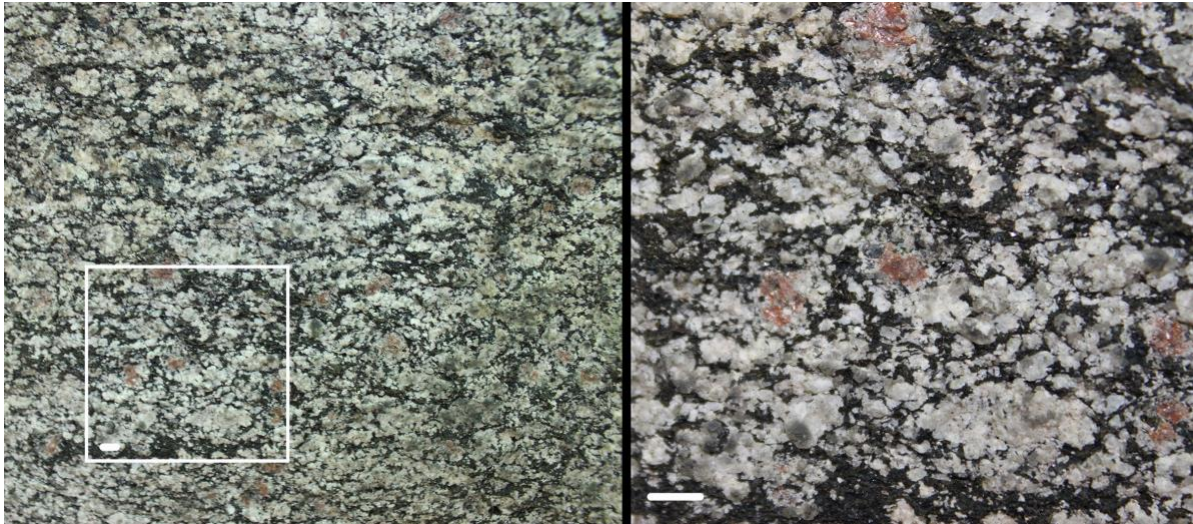

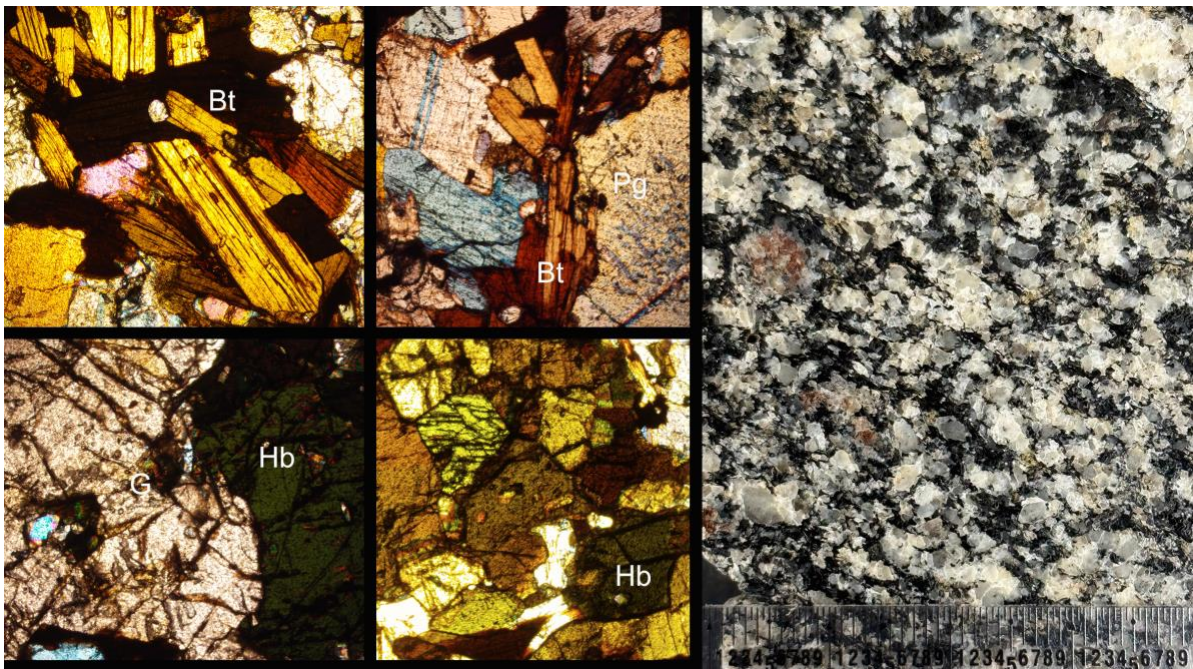Figure 1. Outcrop photo of Shelter Rock with detail. Scale bar = 5mm

Figure 2. Thin section and polished hand sample images showing mineral composition (G-garnet, Hb-hornblende, Bt-biotite, Pg-plagioclase). Ruler scale is mm, thin section images X40, cross polarized illumination.
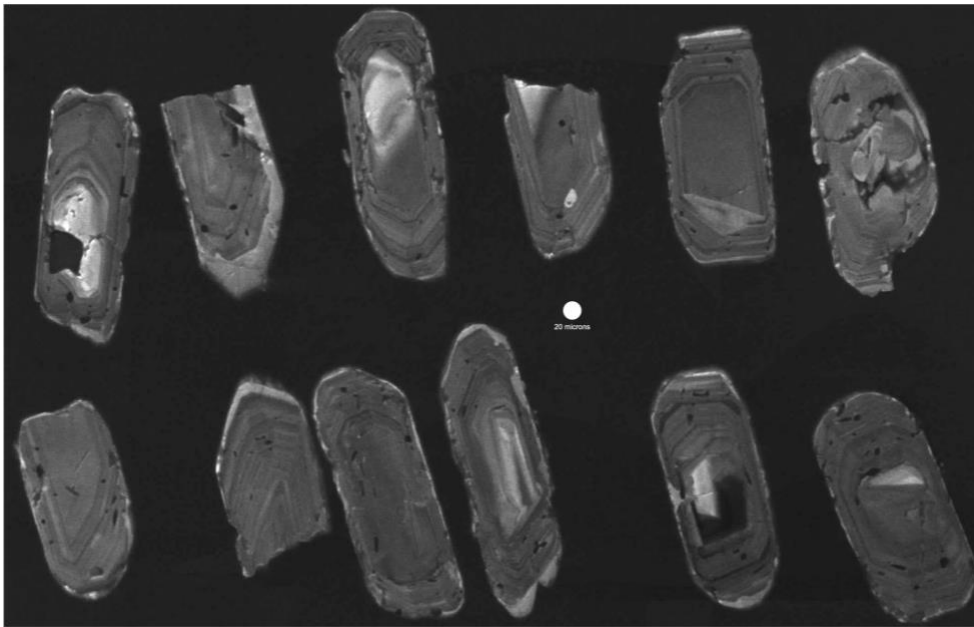
Figure 3. Cathodoluminescence image of Shelter Rock zircon grains.
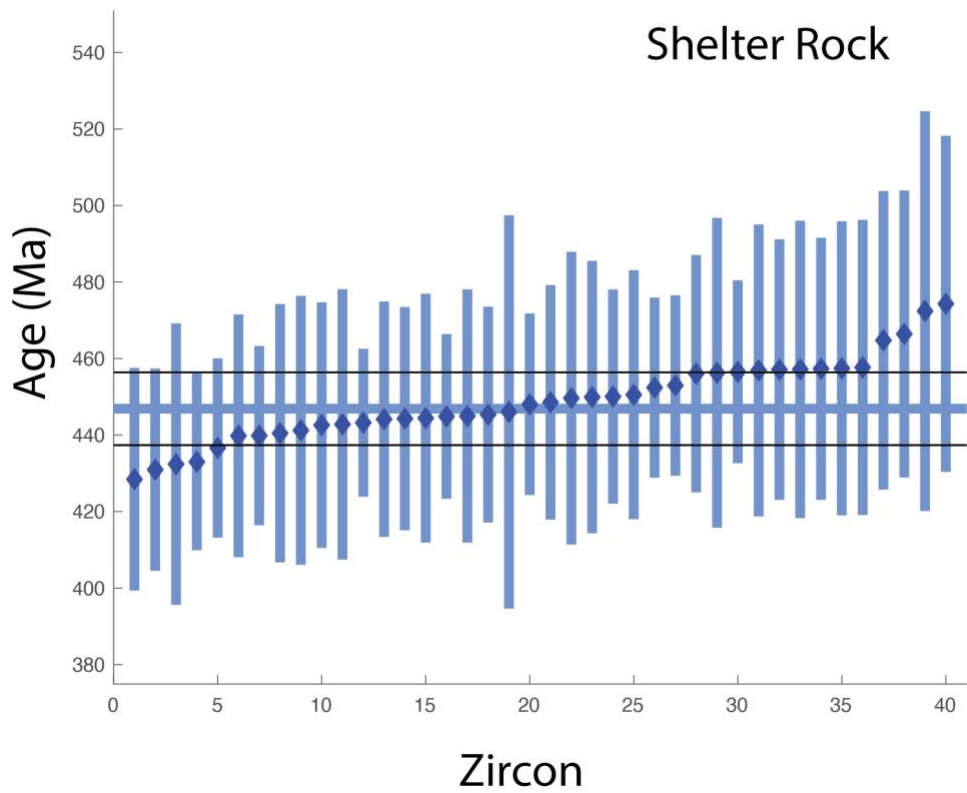
Figure 4. Individual zircon ages ranked by age. Thick horizontal bar indicates mean age with 2-sigma errors shown in black horizontal lines.
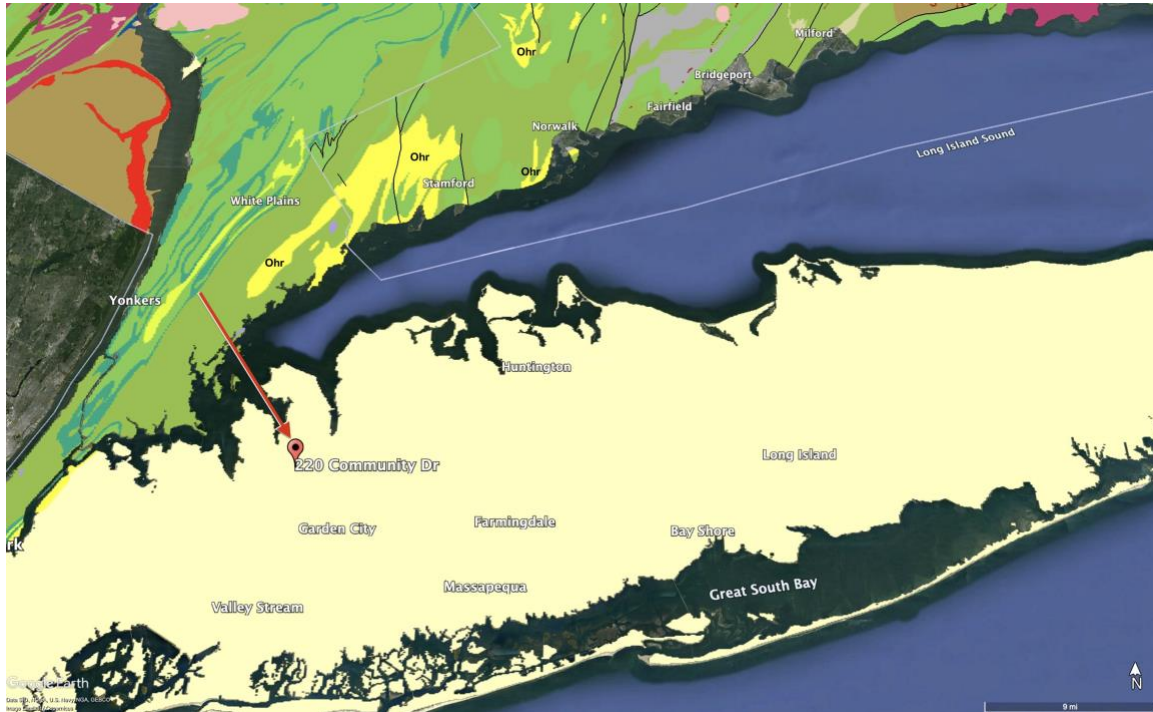

Figure 5. Overlay of the state geologic maps of NY and CT in Google Earth showing the location of Shelter Rock, direction of glacial flow, and the Harrison Gneiss (Ohr) in yellow.

References

Ciano, Carly, Julie Chu Cheong, Steven Leone, Charles Merguerian, and J Bret Bennington, 2013. Petrography and Bedrock Origin of Shelter Rock, a Large Glacial Erratic in Western Long Island, New York, Online: https://www.stonybrook.edu/commcms/geosciences/about/_LIG-Past-Conference-abstract-pdfs/Ciano.pdf

Pacholik, Waldemar and Gilbert N. Hanson, 2001, Boulders on Stony Brook Campus May Reveal Geology of Long Island Sound Basement, Online: http://www.geo.sunysb.edu/lig/Conferences/abstracts-01/Pacholik/Pacholik-GNH-abst.pdf

Sevigny, J. H. and G. N. Hanson, 1995, Late-Taconian and pre-Acadian history of the New England Appalachians of southwestern Connecticut. *GSA Bulletin*: 107 (4): 487–498. doi: https://doi.org/10.1130/0016-7606(1995)107<0487:LTAPAH>2.3.CO;2